VOLUME 85 NO. HY9
SEPTEMBER 1959

# JOURNAL of the

# Hydraulics Division

PROCEEDINGS OF THE
AMERICAN SOCIETY
OF CIVIL ENGINEERS

Journal of the

HYDRAULICS DIVISION

Proceedings of the American Society of Civil Engineers

HYDRAULICS DIVISION
EXECUTIVE COMMITTEE
Carl E. Kindsvater, Chairman; Arthur T. Ippen, Vice-Chairman;
Harold M. Martin; Maurice L. Dickinson; Joseph B. Tiffany, Jr., Secretary

COMMITTEE ON PUBLICATIONS
James W. Ball, Chairman; Haywood G. Dewey, Jr.; Eugene P. Fortson, Jr.;
Carl E. Kindsvater; Joseph B. Tiffany, Jr.

CONTENTS

September, 1959

Papers

| | Page |
|---|---|
| Flood Control Aspects of Cauca Valley Development by Phillip Z. Kirpich and Carlos S. Ospina | 1 |
| Friction Factors in Corrugated Metal Pipe by Marvin J. Webster and Laurence R. Metcalf | 35 |
| Revised Computation of a Velocity Head Weighted Value by Joe M. Lara and Kenneth B. Schroeder | 69 |
| Eddy Diffusion in Homogeneous Turbulence by Gerald T. Orlob | 75 |
| Discussion | 103 |

Copyright 1959 by the American Society of Civil Engineers.

Journal of the
HYDRAULICS DIVISION
Proceedings of the American Society of Civil Engineers

# FLOOD CONTROL ASPECTS OF CAUCA VALLEY DEVELOPMENT

Phillip Z. Kirpich,[1] F. ASCE and
Carlos S. Ospina,[2] F. ASCE

## SYNOPSIS

The Cauca Valley project applies two techniques relatively new in Latin America: integrated water-resource development and administration by a decentralized, TVA-type agency. The flood-control aspects are greatly affected by the other aspects, mainly power, irrigation and drainage.

Parallel matters discussed herein are the hydrology of the region, which is in the equatorial "doldrum belt," and the rate of development as affected by economic and political considerations.

## INTRODUCTION

Flanked by the two westernmost ranges of the Colombian Andes, the Cauca Valley is a flat, verdant strip of land 200 km long, an average of 20 km wide and almost 400,000 ha in extent; see Figs. 1 and 2. (Abbreviations and equivalents are listed at the end of this paper.)

As the elevation is 950 m above sea level, it enjoys a pleasant, balmy climate, despite the equatorial latitude. Long-term averages are: temperature 24°C, humidity 63%, and annual rainfall 1,200 mm.

Although well settled for over four centuries, only a third of the valley is cultivated at present. This low degree of development results from a complex of sociologic and technologic reasons, some of which are discussed in this paper.

The Corporación Autónoma Regional del Cauca (Autonomous Corporation of the Cauca Region) was established in 1954 by the government of Colombia.

Note: Discussion open until February 1, 1960. To extend the closing date one month, a written request must be filed with the Executive Secretary, ASCE. Paper 2147 is part of the copyrighted Journal of the Hydraulics Division, Proceedings of the American Society of Civil Engineers, Vol. 85, No. HY 9, September, 1959.

1. Associate, Tippetts-Abbett-McCarthy-Stratton and Chf. Engr., Corporación Autónoma Regional del Cauca, Cali, Colombia.
2. Partner, Olarte, Ospina, Arias y Payán, Ltda., Bogotá, Colombia.

FIGURE I. VICINITY MAP

David E. Lilienthal, former chairman of the TVA, assisted the government in preparing the basic legislation; for this reason, the Cauca Valley Development is often referred to locally as the "Plan Lilienthal." The area of interest of the Corporation was defined as comprising the upper Cauca River drainage basin (above Cartago) and the adjacent watershed of the Pacific. Water-resource developments are planned within three departamentos (provinces): Cauca, Valle and Caldas: Hence, the abbreviation "CVC" in common local usage. The CVC is charged with the integrated development of water resources including flood control, electric power, drainage, irrigation, pollution abatement and related uses. The CVC in 1955 engaged the consulting engineering firms of Olarte, Ospina, Arias & Payán, Ltda. of Bogotá, Colombia, and Gibbs & Hill, Inc., and Tippetts-Abbett-McCarthy, both

FIGURE 2. GENERAL MAP

of New York, to carry out the planning and engineering required for the Cauca Valley development. This paper is based on the studies made by these three firms, together with the technical staff of the CVC.

Within CVC's development area reside 2,600,000 persons. The center of the valley is Cali, a booming city of 400,000, with an annual population increase of 8%. A hundred kilometers to the west is the Pacific deepwater port of Buenaventura.

Almost a third of the valley is in the flood zone. The river overflows almost every year, in some years as many as three or four times. A major flood occurs once in 7 to 10 years when about 85,000 ha are inundated by the river (see Figs. 3 and 4), plus about 30,000 ha by tributary streams.

Because the banks of the Cauca River are higher than the adjoining land on each side, damages from Cauca River floods extend well beyond the 85,000-ha area subject to direct flooding in two ways: (1) Floodwater trapped behind the river banks causes high groundwater levels over extensive adjacent areas (a condition that would be materially relieved if there were adequate drainage outlets, even in the absence of general flood control). (2) Owing to unfavorable outlet conditions, flooding extends over a wide area at the mouths of many of the tributaries.

Despite the large area flooded, actual damage is small because the frequent flooding has discouraged significant developments within the extensive low-lying areas along the river. The early Spanish settlers placed their towns on high ground for sanitary reasons. The present use of land in the flood zone and adjacent areas is limited to cattle grazing; when floods occur the cattle are simply moved to higher ground and brought back after the land dries out. Thus most of the benefits from flood protection are those that will result in the future from intensification in use of the land (for agriculture, industrial sites and for urbanization) rather than from avoidance of damage to existing crops and improvements.

Natural valley storage is high because of the large area flooded. During the February 1950 flood, 31,000 ha upstream of Cali were submerged beneath 740 million $m^3$ of water, the average depth being 2.4 m. The resulting natural regulation caused the peak discharge at Cali to be considerably less than at the head of the valley (La Balsa), as follows:

| | Drainage area | Discharge |
|---|---|---|
| La Balsa | 5,480 $km^2$ | 1,225 $m^3/s$ |
| Cali | 9,060 $km^2$ | 1,000 $m^3/s$ |

It is evident that flood control in the upper portion (say above Cali), if limited to levees or to channel improvements, would cause substantially greater flooding downstream.

## Flood Characteristics

### Regional Meteorology

Table 1 gives average monthly rainfalls at three representative stations. Popayán and Piendamó are in the "upper basin" (that portion of the drainage area upstream of the Timba damsite at La Balsa), while La Manuelita is representative of the valley. The valley has two distinct dry seasons; the upper basin has a single dry season extending from June to September.

FIGURE 3. FLOOD ZONE, PART I

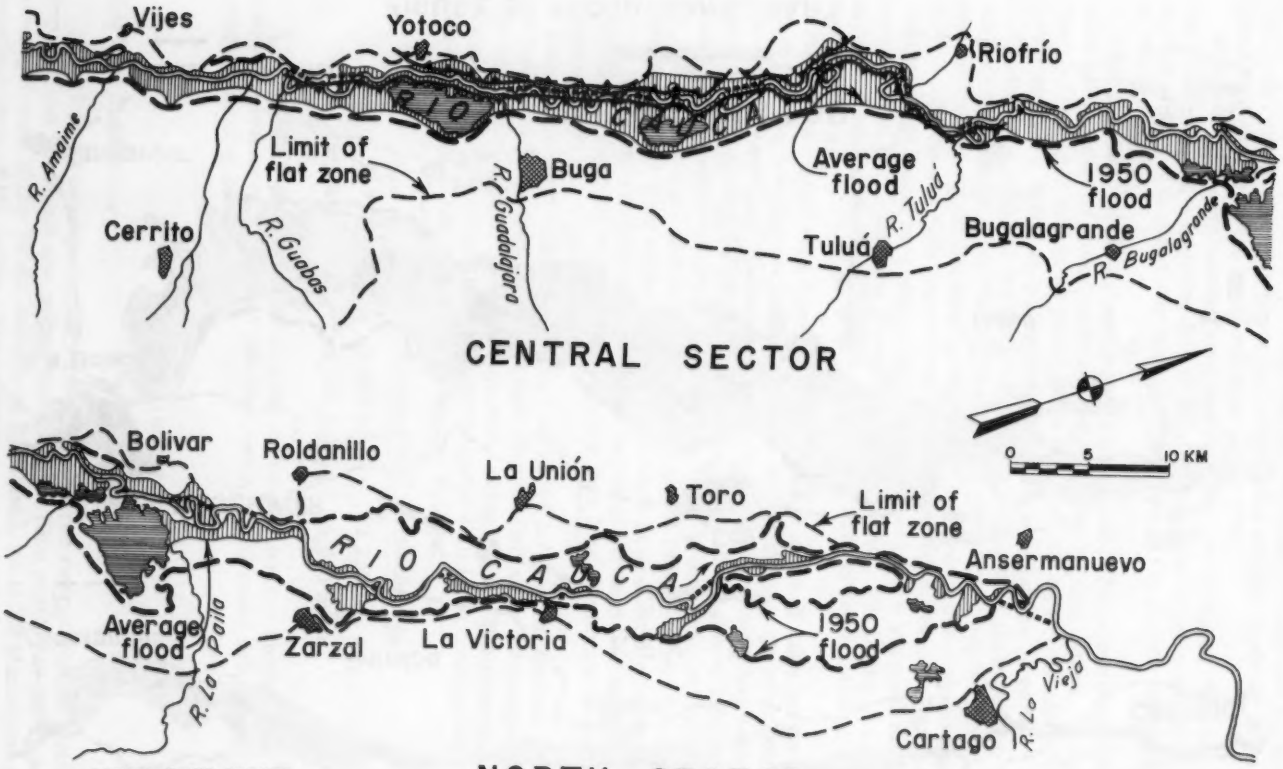


FIGURE 4. FLOOD ZONE, PART 2

TABLE 1

MEAN MONTHLY PRECIPITATION

(millimeters)

| Station | Popayán University | | Piendamó | | La Manuelita | |
|---|---|---|---|---|---|---|
| Period of record | 1929-35 1944-56 | | 1932-55 | | 1900-54 | |
| Month | Total | % | Total | % | Total | % |
| January | 179 | 9.7 | 216 | 10.2 | 72 | 6.4 |
| February | 172 | 9.3 | 221 | 10.4 | 79 | 7.1 |
| March | 146 | 7.9 | 178 | 8,4 | 111 | 9.9 |
| April | 145 | 7.8 | 194 | 9.1 | 145 | 12.9 |
| May | 132 | 7.1 | 207 | 9.8 | 131 | 11.7 |
| June | 86 | 4.6 | 102 | 4.8 | 71 | 6.3 |
| July | 49 | 2.7 | 39 | 1.8 | 37 | 3.3 |
| August | 34 | 1.8 | 34 | 1.6 | 43 | 3.9 |
| September | 98 | 5.3 | 103 | 4.9 | 70 | 6.3 |
| October | 262 | 14.2 | 284 | 13.4 | 142 | 12.7 |
| November | 314 | 16.9 | 313 | 14.8 | 128 | 11.4 |
| December | 236 | 12.7 | 230 | 10.8 | 91 | 8.1 |
| Annual | 1,853 | 100.0 | 2,121 | 100.0 | 1,120 | 100.0 |

Storm rainfall in the upper Cauca basin is spotty and erratic. There are sharp variations with respect to time and place even during short periods of less than a day. The precipitation records show that heavy rainfalls at the various stations seldom coincide.

Another characteristic of storm rainfall in the upper Cauca basin is its low depth as compared with the annual rainfall. Thus, for the 18 years of daily records at Popayán, the maximum 24-hr rainfall has never exceeded 6% of the average annual rainfall. This low percentage can be contrasted with the much higher percentages observed in other parts of the world, outside the latitudes of the equatorial trough (or "doldrums")in which the upper Cauca basin is located. In these latitudes, winds are mild and tropical hurricanes are unknown. (Tropical hurricanes universally originate at about 10° to 15° south latitude and move respectively northward and southward.) Moreover, cold fronts, such as those that cause major storms in the Canal Zone, do not reach these latitudes as they never penetrate further south than about 8°N latitude.(1)

The available records for the upper basin show that depths of storm rainfall are surprisingly low and do not increase with frequency as much as might be expected; see Table 2. The 10-year 24-hr rainfall at Popayán of 100 mm is about the same as at Washington, D. C. while the 100-year 24-hr rainfall at

TABLE 2

FREQUENCY OF STORM RAINFALL

(millimeters)

| | 1-year | 10-year | 100-year |
|---|---|---|---|
| 24-hr point rainfalls | | | |
| At Popayán | 64 | 100 | 136 |
| At Piendamó | 56 | 88 | 120 |
| Basin rainfall (5,480 km$^2$ above La Balsa) | | | |
| 24-hr | 28 | 40 | 56 |
| 5-day | 80 | 114 | 150 |

Popayán (estimated from an 18-year record) is about 10% less than at Washington; the corresponding basin rainfalls are only about 40% of the point rainfall at Popayan. Admittedly, the Popayán record is not long enough for a firm conclusion; on the other hand, that the infrequent, say 100-year, storms are not much worse than the 10-year storms is confirmed from the records of floods, described below, which indicate that since 1916 all major floods have been of about the same order of magnitude; nor is there evidence of any earlier and greater floods from the time of original settlement of the Cauca Valley in the sixteenth century.

A long-term record (1900 to date) for La Manuelita indicates a rough correlation between annual rainfall in the valley as against the upper basin; this record also indicates that there is a 6 to 7-year cycle of unusual wet and unusually dry years.

The apparent explanation for this cycle is a periodic shifting of the equatorial trough of low-pressure (inter-tropical convergence or "ITC") and of the accompanying pattern of atmospheric circulation off the Pacific coast of the northern part of South America. There is a parallel shifting of currents in the Pacific ocean off the coast of Colombia and Ecuador; this is the general area where the cold northern-flowing Humboldt current meets a warm current coming from Panamá; both currents then move westward to the Galápagos Islands. See Fig. 1.

Flood Frequency

On the basis of gage records (available only since September 1945), the frequency of the maximum recorded flood, that of 11 February 1950, is about once in 10 years. Preceding the beginning of gage records, there were four "historic floods": in 1916, 1932, 1934 and 1938. The available evidence indicates that at least three of these were about equal (in peak discharge) to the flood of February 1950, confirming that a flood of the magnitude of the

February 1950 has a frequency of about 10 years, at least with respect to peak discharge.

The worst flood of record at La Balsa had a discharge of 1,225 $m^3/s$ from a drainage area of 5,480 $km^2$. The corresponding Myers rating C, in the Jarvis-Myers formula $Q = C\sqrt{A}$, with Q and A in English units (cubic feet per second and square miles), is 1,050. The available records indicate that this value applies to the tributary streams as well.

Compared with values observed in the United States, C is low in the Cauca Valley region; the apparent reason is the absence of both tropical hurricanes and storms involving cold fronts. Moreover, as precipitation in the form of snow is practically non-existent in the Cauca drainage basin, floods produced by a combination of rain and snow-melt are unknown.

## Degree of Protection

When the protected area consists of cities or towns, a high degree of protection is justified to avoid catastrophic losses that may result from great floods occurring once in say 100 to 200 years. In the case of the Cauca Valley, however, and with the exception of the Aguablanca project described below, only agricultural land is involved. Following protection, the land in the flood zone will be devoted to crops (such as rice, corn, beans and cotton) and to intensive pasture, for which the average growing season (including harvesting) is only 5 to 6 months.

Sugarcane, for which the growing season is 15 to 18 months, is widely grown in the Cauca Valley; harvesting takes place the year round—an important advantage in that the refineries can operate almost continuously—and its cultivation will surely be extended. However, it is estimated that not more than 10 to 20 percent of the flood zone will be devoted to cane in the future: first, because the heavier soils located therein are better suited to other crops, mainly rice for which the high irrigation water-requirement will be relatively easy to supply in the flood zone; second, ample area, mostly free of flood risk, is available for cane cultivation outside the flood zone.

Thus, for the expected cropping pattern, 6 months may be assumed to be the average growing season. If protection is provided against a flood with average frequency of once in 10 years (once in 20 growing seasons), 19 crops out of 20 will be protected or 95% of the crops; if against a 20-year flood, 39 out of 40 or 97.5% of the crops. Thus, for a flood of half the frequency (with the corresponding expense of protection on the order of 50% greater), the benefit gain is only 2.5%.

The foregoing assumes that the area and consequently the crops damaged by the 20-year flood, would be about the same as by the 10-year flood. This is generally true for the largest part of the flooded area, located upstream of Buga.

Following the reasoning presented above, protection against a 5-year flood would constitute 90% protection so that the benefit gain of 10-year over 5-year protection is theoretically only 5%; however, it is necessary to consider what effect the degree of risk will have on the attitude of farmers. Conversations with them have indicated that 10-year protection corresponding to 5% risk (one in twenty) is sufficiently great so that they will not be discouraged from planting crops, but that 5-year protection providing 10% risk (one in ten) would have a discouraging effect. It has been concluded, considering the

various factors, that the desirable degree of protection of agricultural lands is that obtained by providing control of the 10-year flood.

There are no important towns or villages within the Cauca River flood zone. Some towns do suffer floods from tributary streams but these involve local projects generally requiring only minor works to achieve protection.

The city of Cali, although not suffering serious flood damage at present, has expanded into the flood plain to the extent that further expansion has been limited to narrow flood-free zones to the north and south; see Fig. 9. The Aguablanca project, described below, is being constructed to protect 5,000 ha of land adjacent to the city against a flood having an estimated frequency of 100 years, under present conditions. Following completion of the Timba reservoir and the Cauca River channel improvement, the degree of protection will be against a flood of at least 200-year frequency.

## Methods of Obtaining Flood Control

Upstream of the upper end of the valley at La Balsa, there are two reservoir sites: Timba and Salvajina. The drainage areas controlled are, respectively, 5,480 $km^2$ and 3,960 $km^2$. Other significant drainage areas are:

| | |
|---|---|
| At Juanchito bridge near Cali | 9,060 $km^2$ |
| At Buga | 12,930 " |
| At Cartago | 17,820 " |

The Timba reservoir is more valuable as a flood-control structure because it controls 38% more drainage area than Salvajina. Moreover, various additional factors, which cannot be discussed here because of space limitations, have required that, of the two reservoirs, Timba be given a higher priority.

The control of floods on the tributaries must be considered jointly with the drainage problem, as discussed in a later section.

### Optimum Combination

The desired degree of flood protection is obtainable by storage in the Timba reservoir and improvement of the channel of the Cauca River, the optimum combination being that giving the lowest overall cost, considering the value of salable electric energy lost because of storage reserved for flood control.

The channel capacity of the river is about 550 $m^3/s$ at La Balsa and about 650 $m^3/s$ at Cali. The amount of reservoir storage necessary to reduce past floods of record down to these limits was determined, and this study resulted in the development of a "rule curve," similar to that shown in Fig. 5, giving the reservoir level which may not be exceeded on a given calendar date. Other rule curves were developed for lesser degrees of flood reduction.

At the time that Timba is constructed, there will already be in existence two major hydroelectric stations (Anchicayá and Calima—See Fig. 2) and one coal-burning thermal station with an installed capacity of 53,000 kw located at Yumbo, a suburb of Cali. From a study of system power-output, using as basic data streamflow records from 1945 to date, it was determined that the firm power obtainable from Timba, if the rule curve in Fig. 5 is followed, will be 60,000 kw. The average annual generation will be 346,000,000 kwh.

Besides flood control and power, Timba will provide the means of diverting water to two principal irrigation canals, one on each side of the valley.

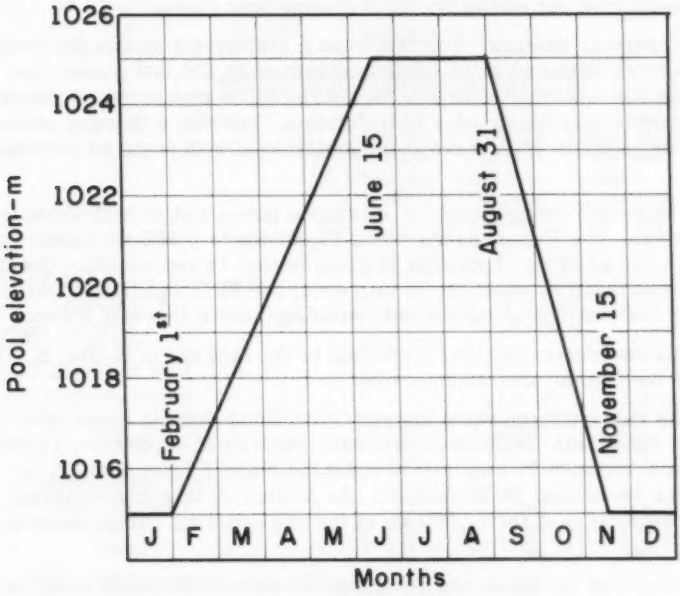


OPERATING RULES

| Reservoir level | Action required |
|---|---|
| 1. Higher than Rule Curve but lower than El. 1025.0 | Make the total outflow equal to the lowest of the following two quantities:<br>(a) 790 $m^3/s$<br>(b) 870 $m^3/s$ minus the tributary flow between La Balsa and Cali |
| 2. Higher than El. 1025.0 | Open all outlets to prevent a further rise in reservoir level |

FIGURE 5. RULE CURVE, TIMBA RESERVOIR

The total net irrigable area in the valley amounts to 280,000 ha, of which 113,000 will be irrigated by water diverted at the Timba damsite. The unregulated flow is sufficient at all times to meet irrigation water requirements.

Taking the power output corresponding to the rule-curve operation as a norm, the optimum combination of Timba reservoir storage and the channel improvement will be that giving the lowest overall cost of obtaining the following objectives:

10-year flood protection
Irrigation diversion
Firm capacity of 60,000 kw
Average annual generation of 346,000,000 kwh

Table 3 presents cost estimates for the following four cases:

1. No reservoir storage. For this case a low diversion dam for irrigation would be constructed at an estimated cost of 22,000,000 pesos. Because of the low head available and poor streamflow regulation, it would not be economical to construct a hydro station. Instead, a thermal station of 60,000 kw capacity would have to be constructed with costs as indicated in Table 3.

2. Timba reservoir operated for maximum power output with flood control incidental. The firm capacity being 67,000 kw or 7,000 kw higher than the norm, a credit of Ps 11 million is given in line 11 representing the cost of 7,000 kw of thermal capacity; in this case, the Ps 11 million actually represents cost savings at the already-existing Yumbo thermal station.

3. Timba reservoir operated according to the rule curve in Fig. 5. This case is for the "norm" described above.

4. Timba reservoir operated for maximum flood-control effect with firm power incidental. With the firm hydro capacity at 43,000 kw, 17,000 kw of thermal capacity is required to meet the norm. From line 11, Table 3, this would cost Ps 26 million. As in Case 2, this cost is taken as the incremental cost for 17,000 kw at the pre-existing Yumbo thermal station.

Peak discharges at La Balsa and Juanchito for these four cases would be as given in Table 4. Figure 7 presents the results of detailed computations of the effect of the Timba reservoir on the 1949-50 flood (Fig. 6) if operated according to the rule curve in Figure 5.

The capital cost of the channel improvements required for each of the four cases, with design capacities at La Balsa and at Cali as given, respectively, in the second and fourth columns of Table 4, are given in line 8 of Table 3.

The total capital cost (lines 12 or 23, Table 3) is increased in each case by the capitalized value of the annual cost of operation and maintenance, depreciation and fuel consumption. The overall cost thus obtained provides the basis for comparison. It is the lowest in Case 3, which therefore represents the optimum solution.

## Flood Control and Drainage

Groundwater levels are high during the wet season (and for a long period thereafter) within the 85,000-ha area subject to direct flooding from the Cauca River and in an additional area of about equal size immediately adjacent to the flood zone on each side; flood control of the Cauca River will thus benefit directly about 170,000 ha or over 40% of the valley. Drainage works, principally canals and pumping stations, will of course be necessary to supplement the main flood-control works (Timba reservoir and Cauca River improvement).

Flood control and supplementary drainage works within this 170,000-ha low zone will also benefit the remaining 230,000 ha in the valley but in an indirect way. Irrigation of these 230,000 ha is proceeding on a gradual basis. (The rate will be accelerated once the Timba dam and the main irrigation canals leading from it are completed.) A deterrent to more rapid development of irrigation has been lack of drainage outlets and high groundwater

TABLE 3

COST OF FOUR ALTERNATIVE SOLUTIONS

| | Case 1. Storage negligible | Case 2. Storage used for maximum power output | Case 3. Storage used according to rule curve | Case 4. Storage used for maximum flood-control effect |
|---|---|---|---|---|
| 1. Flood control storage (million $m^3$) | 0 | 73(a) | 378(b) | 690(b) (c) |
| POWER OUTPUTS | | | | |
| Firm Capacity (kw) | | | | |
| 2. Timba hydro | 0 | 67,000 | 60,000 | 43,000 |
| 3. Thermal | 60,000 | (-) 7,000 | — | 17,000 |
| 4. Total | 60,000 | 60,000 | 60,000 | 60,000 |
| Firm Generation (million kwh/yr) | | | | |
| 5. Timba hydro | 0 | 381 | 346 | 259 |
| 6. Thermal | 346 | (-) 35 | -- | 87 |
| 7. Total | 346 | 346 | 346 | 346 |
| CAPITAL COSTS (million pesos)(d) | | | | |
| 8. Channel improvements | 283 | 171 | 70 | 64 |
| 9. Diversion dam for irrigation | 22 | — | - | - |
| 10. Timba multipurpose project | - | 203 | 198 | 186 |
| 11. Thermal station | 92 | (-) 11 | - | 26 |
| 12. Total | 397 | 363 | 268 | 276 |
| ANNUAL COSTS (thousand pesos) | | | | |
| Operation & Maintenance | | | | |
| 13. Channel improvements | 6,000 | 3,500 | 2,000 | 2,000 |
| 14. Diversion dam | 90 | -- | -- | -- |
| 15. Timba multipurpose project | — | 590 | 560 | 460 |
| 16. Thermal station | 1,300 | (-) 150 | -- | 370 |
| 17. Total | 7,390 | 3,940 | 2,560 | 2,830 |
| Depreciation | | | | |
| 18. Diversion dam | 145 | — | -- | -- |
| 19. Timba multipurpose project | -- | 1,340 | 1,310 | 1,230 |
| 20. Thermal station | 2,210 | (-) 260 | -- | 620 |
| 21. Total | 2,355 | 1,080 | 1,310 | 1,850 |
| 22. Fuel (f) | 5,200 | (-) 520 | — | 1,310 |
| TOTAL COSTS (million pesos) | | | | |
| 23. Capital costs (line 12) | 397 | 363 | 268 | 276 |
| 24. O & M capitalized (g) | 92 | 48 | 32 | 35 |
| 25. Depreciation capitalized (g) | 37 | 17 | 21 | 29 |
| 26. Fuel capitalized (g) | 65 | (-) 7 | - | 16 |
| 27. Total | 591 | 421 | 321 | 356 |

TABLE 3 (Continued)

(a) Surcharge storage.

(b) Includes 73 million $m^3$ surcharge storage.

(c) Reservoir drawn down to El 1000.

(d) Include interest during construction. Foreign-currency costs converted to pesos at rate of 1 US dollar = 7 pesos.

(e) Depreciation assumed negligible for the channel improvements. Depreciation computed on sinking-fund basis with interest at 4%. Resulting annual rates are:

| | Life in years | Annual rate |
|---|---|---|
| Diversion dam and Timba multipurpose project | 50 | 0.66% |
| Thermal station | 25 | 2.40% |

(f) Coal consumption 0.5 kg per kwh; coal price 30 pesos per metric ton; results in cost of 1.5 centavos per kwh.

(g) The CVC can borrow local funds at an interest rate of 8% and foreign funds at 5½%. Operation and maintenance, and fuel costs are in local currency and are therefore capitalized at 8%. As 2/3 of the cost of the diversion dam and of the Timba multipurpose project are in foreign currency the weighted average interest rate is 6.33%. For thermal stations 4/5 of the cost is in foreign currency, giving a weighted average interest rate of 6.20%. As these rates are close to each other, for simplicity a uniform rate of 6.3% was used.

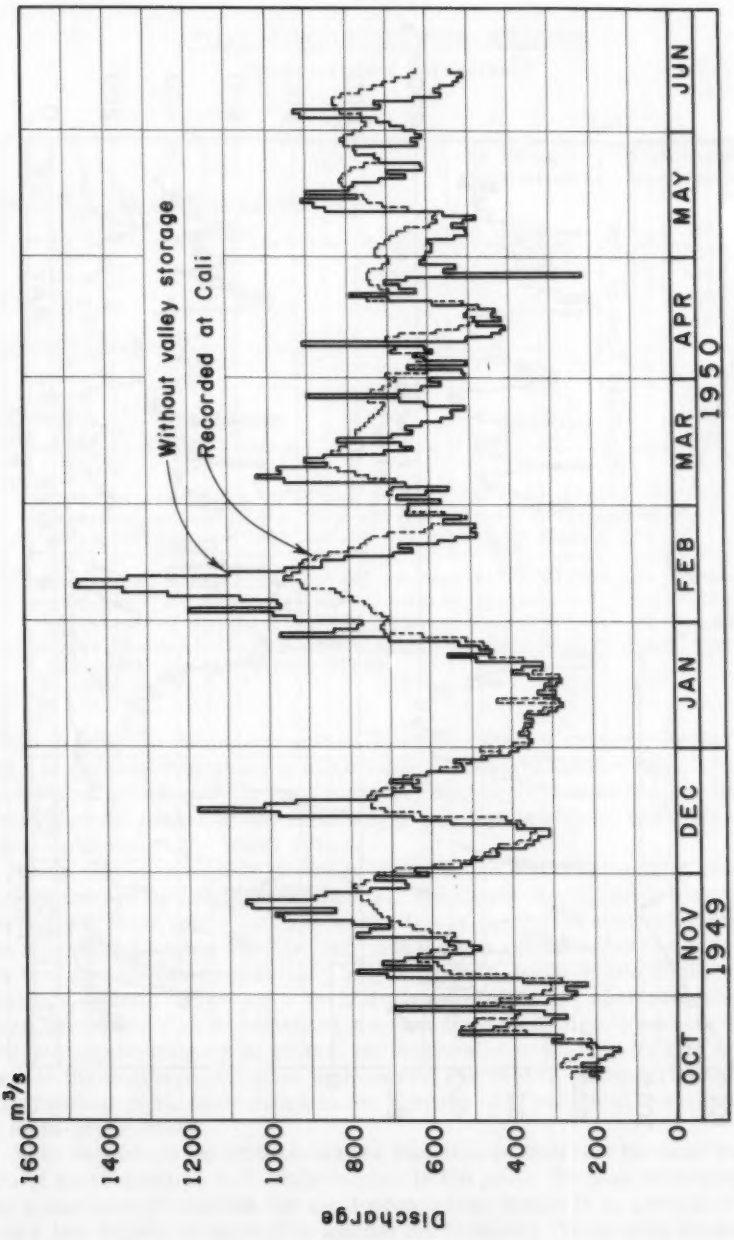


FIGURE 6. 1949-50 FLOOD, ACTUAL OCCURRENCE

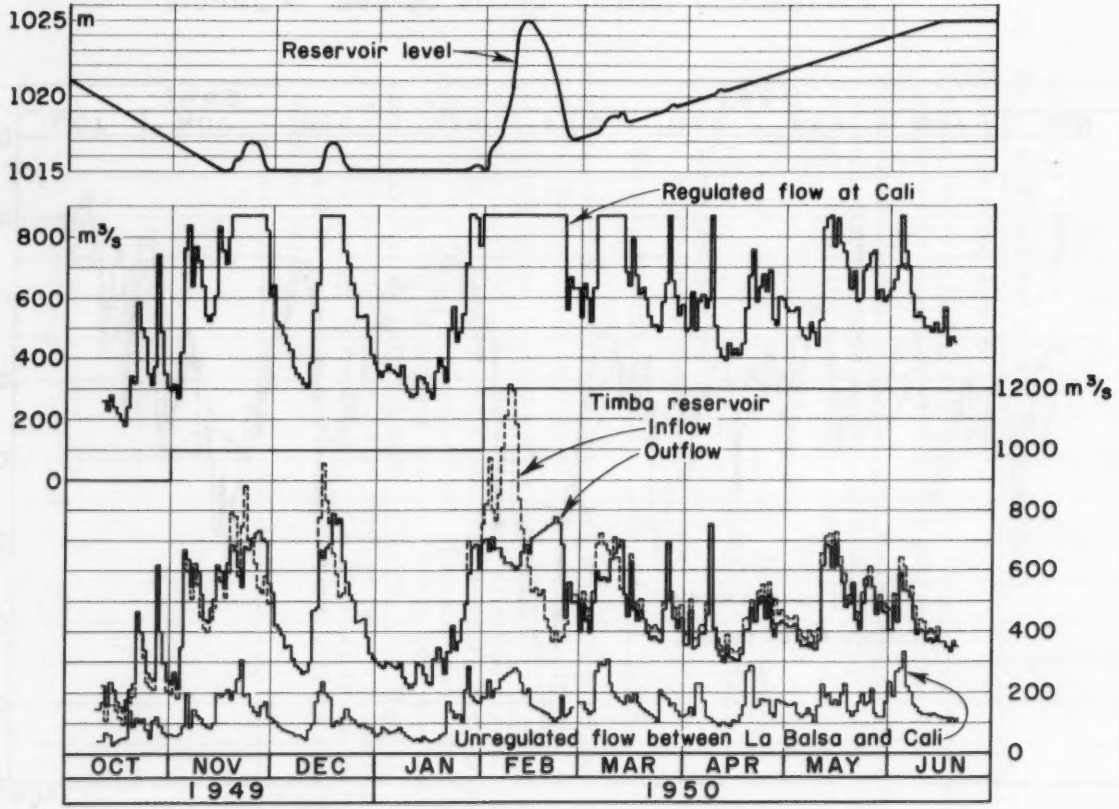


FIGURE 7. 1949-50 FLOOD, CONTROLLED

TABLE 4

FLOOD REDUCTIONS BY TIMBA RESERVOIR

(Cubic meters per second)

| | La Balsa | Cali | |
|---|---|---|---|
| | | No channel improvement | With channel improvement |
| **1949-50 Flood (Design Flood)** | | | |
| Case 1 | 1,300 | 1,000 | 1,500 |
| Case 2 | 950 | 1,200 | 1,210 |
| Case 3[x] | 790 | 870 | 870 |
| Case 4 | 620 | 700 | 700 |
| **Average Flood** | | | |
| Case 1 | 860 | 870 | 1,050 |
| Case 2 | 460 | 670 | 670 |
| Case 3[x] | 660[xx] | 870 | 870 |
| Case 4 | 300 | 510 | 510 |

(x) Reservoir operated according to rule curve in Fig.5. For reservoir levels at or above the rule curve, release from reservoir is such that discharge at Cali equals 870 $m^3/s$ (see Fig.7).

(xx) Controlled discharges for the average flood are higher for Case 3 than for Case 2 because of rule-curve operation whereby reservoir is evacuated in anticipation of possible occurrence of the design flood (that of 1949-50); but note that Case 3 provides greater reduction for the design flood.

FIGURE 7. 1949-50 FLOOD, CONTROLLED

levels in adjacent downslope areas. In many cases, a rather anarchic situation has developed in which upslope landowners have thrown their irrigation wastes on their downslope neighbors; or, drainage-ways have been constructed in the higher areas outletting to inadequate natural channels or permanent swamps in the lower areas.

It was stated above that drainage works alone would materially relieve damage caused by Cauca River floods. The Cauca River rarely remains above flood stage more than two weeks (many crops, if sufficiently mature, can withstand flooding for this long) but the low areas behind the riverbanks are now flooded for considerably longer periods, owing to the absence of drainage outlets. However, even if drainage outlets are constructed as a first stage (providing sizable benefits), general flood control will nevertheless soon become necessary to protect the high-value crops that will be grown, as well as the drainage facilities themselves. Moreover, most farmers will not risk planting of valuable crops in the absence of a sufficient degree of control of main-river floods.

With respect to the tributaries the situation is different because the floods are of short duration with little volume in the peak. Studies of several typical areas have shown that the most economical design is to provide a relatively low degree of protection against the tributary floods with occasional overflows (once in 4 or 5 years) removed by a system of drainage canals. A typical case (the Roldanillo-La Union-Toro project) is described below.

## The Timba Project

The Timba dam will feature an earth embankment 46 m high and 1,200 m long; three spillway gates, each 13 m wide by 11.5 m high; a 60,000-kw powerhouse; and miscellaneous facilities including a flood-control outlet and irrigation intakes. The discussion herein will be limited to the spillway capacity and the method used for determining the economic justification of the project.

### Spillway Design

A difficult problem has been establishment of a design flood for the spillway. On the one hand, it is known that the upper Cauca basin is in a region of mild climate, completely free of tropical hurricanes and storms involving cold polar air masses. On the other hand, the period of actual streamflow records is short even though the qualitative historic record since the sixteenth century indicates the absence of floods of the order of magnitude recorded in the United States. The hydrologic problem is further complicated in that it is practically impossible, owing to the paucity of data and the spotty and erratic character of storm rainfall, to apply methods now having standard acceptance involving "storm transposition" and the "unit hydrograph." Other methods were therefore applied described briefly as follows:

1. Correlation between basin rainfall and average daily discharge were attempted. The basin rainfall was determined by the Thiessen method; a more accurate method involving the plotting of isohyetal maps was not possible owing to lack of sufficient data. A correlation between the average daily flood flow at La Balsa and the daily basin rainfall was found to be unsatisfactory; however, a better correlation was found between the total basin rainfall for the preceding five consecutive days and the average daily flood flow. Considering all recorded daily flows higher than 300 $m^3/s$, the correlation plotted as shown in Fig. 8. It is thought that the envelope curve represents the maximum daily discharge that can be reasonably expected as a function of the 5-day rainfall.

2. The 1000-year 5-day precipitation was obtained by extrapolating the 18-year rainfall record up to a frequency of 1,000 years giving a 5-day basin precipitation of 186 mm (7.3 inches), or 62% more than the 10-year storm (see Table 2). It is believed that the upper Cauca basin, because of its location in the equatorial latitudes, can receive a probable maximum depth of rainfall of no greater order of magnitude than the 1000-year rainfall. Such a premise is considered sound based on the following reasoning: great floods in the United States have been caused by rare and fortuitous "meteorological accidents" in which, however, one or more of the following conditions are always involved: a tropical hurricane, a meeting between a cold polar air mass and a warm tropical air mass, or snow-melt. None of these conditions are possible in the Cauca Valley region.

3. The maximum average daily discharge for the spillway design flood was determined from the envelope curve in Fig. 8.

4. From study of the shapes of hydrographs for past isolated floods, which indicate the expected rate of rise and fall of floods, a hydrograph was sketched based on the maximum daily average discharge determined in Step 3.

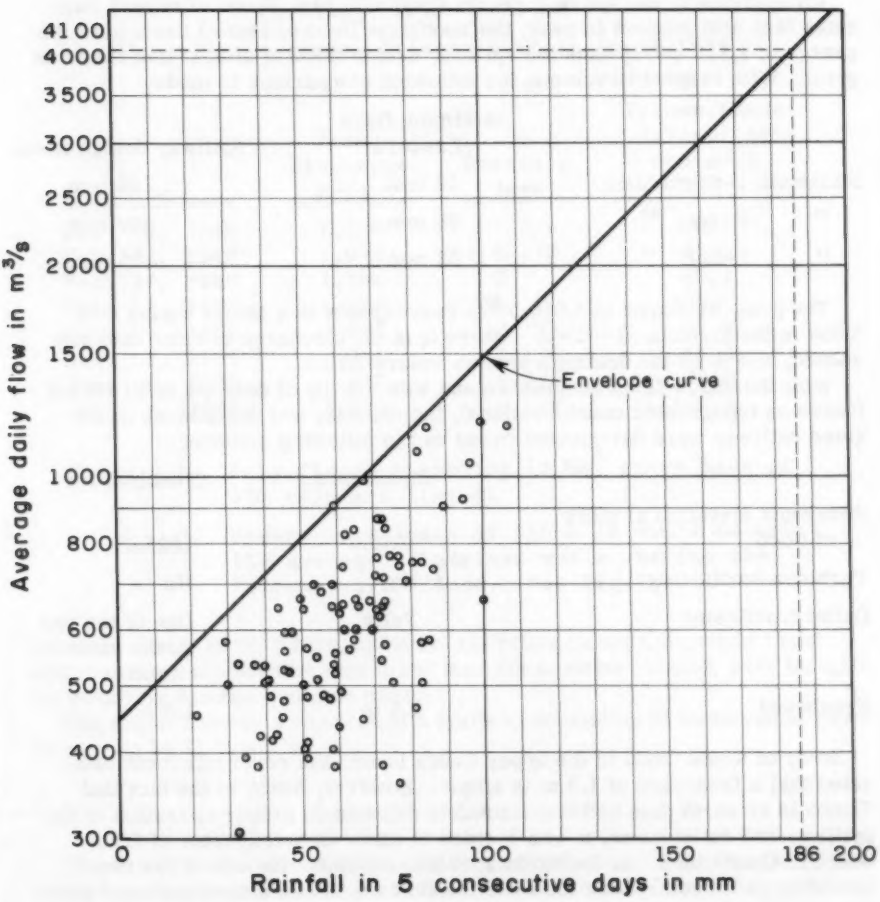


FIGURE 8. DAILY DISCHARGE VS. 5-DAY PRECIPITATION

5. The resulting hydrograph had the following characteristics:

| | |
|---|---|
| Peak | 6,000 $m^3/s$ |
| Width of base | 3 days |
| Base flow | 400 $m^3/s$ to 480 $m^3/s$ |
| Volume (in 3 days) | 685,000,000 $m^3$ or 125 mm |

Comparison of the spillway design flood with past floods of record indicates that with respect to peak, the maximum flood of record has a peak discharge of 1,225 $m^3/s$; thus the spillway design flood is almost five times as great. With respect to volume, the following comparison is made:

| | Maximum flood of record | Spillway design flood |
|---|---|---|
| Maximum 1-day volume | 19 mm | 65 mm |
| " 2-day " | 36 mm | 109 mm |
| " 3-day " | 53 mm | 125 mm |

The peak discharge of 6,000 $m^3/s$ corresponds to a Myers rating C of 4,550 in the formula $Q = C\sqrt{A}$ where Q is the discharge in cubic feet per second, and A is the drainage area in square miles.

With the inflow flood established and with the top of dam set at El 1029.0 (based on topographic considerations), the capacity and dimensions of the gated spillway were determined based on the following criteria:

| | Condition 1 | Condition 2 |
|---|---|---|
| Reservoir elevation at start of flood | 1025.0 | 1025.0 |
| Turbines functioning | No | No |
| Outlet functioning | Fully | One of the two intake gates closed |
| Freeboard | 2.5 m | 1.5 m |

Study of winds (mild in the upper Cauca basin) and reservoir fetch indicated that a freeboard of 1.5 m is ample. However, owing to the fact that Timba is an earth dam and that its safety depends on proper operation of the spillway and outlet gates, it was decided to allow an extra meter of freeboard in Condition 1. In Condition 2, it was assumed that one of the two operating gates controlling the outlet conduit would be stuck in a closed position; however, as this is only a remote possibility (the gates will be operated frequently) a reduced freeboard of 1.5 m was accepted for this case.

Conservatism is also involved in the adoption of an initial reservoir elevation of 1025.0, which is the level of the top of the spillway crest gates. The record of greatest floods, Table 5, indicates that floods of appreciable volume (more than 10% of the flood storage of 305 million $m^3$) have never succeeded each other within a short time; nor have such floods occurred from early March to mid-November. Thus, provided that the rule-curve operation is adhered to, the spillway design flood is not likely to occur on top of a full reservoir. On the other hand, it was felt that pressure from farmers along

TABLE 5

FLOOD VOLUMES ABOVE RESERVOIR RELEASE

Cauca River at La Balsa

(Drainage Area 5,480 $km^2$)

Streamflow records, October 1945 to April 1958

| Date | Peak Discharge $m^3/s$ | Duration days | Volume Above Release of 650 $m^3/s$ $Mm^3$ |
|---|---|---|---|
| May 3, 1949 | 1,225 | 3/4 | 20.1 |
| Nov. 22, 1949 | 1,075 | 6 1/2 | 49.0 |
| Dec. 16, 1949 | 1,000 | 3 | 45.1 |
| Feb. 10, 1950 | 1,225 | 12 | 243.7 |
| Nov. 27, 1953 | 885 | 4 | 32.0 |
| Dec. 1, 1954 | 931 | 5 1/2 | 67.6 |
| Jan. 5, 1955 | 950 | 2 1/2 | 36.0 |
| Jan. 1, 1956 | 1,225 | 9 1/2 | 132.5 |

Notes: 1. Only floods exceeding 15 $Mm^3$ above base of 650 $m^3/s$ are listed.

2. Reservoir release of 650 $m^3/s$ would be about the average maintained while storing the February 1950 flood. See Fig.7.

the river could, in the future, upset the operating rules; they might insist that reservoir releases be kept lower than the amounts planned, even though the resulting damage would be minor.

The adopted criteria resulted in a spillway consisting of three radial gates 13-m wide by 11.5-m high.

### Cauca River Improvement

The two principal elements of a balanced flood-control plan are the Timba reservoir combined with the Cauca River improvement (Case 3 described above). Planning and design are well advanced for the Timba reservoir but not for the Cauca River improvement. Preliminary design of the latter has, however, been completed as summarized in Table 6; in general, design capacities are 20% to 25% higher than existing channel capacities. Admittedly approximate, the preliminary design is still considered good enough for the making of economic comparisons, which are based on estimated annual costs of alternative long-range plans.

Final design of the Cauca River improvement (in common with all major river improvements) will be a highly complicated matter involving the following factors (among others):

TABLE 6

PROPOSED CAUCA RIVER CHANNEL IMPROVEMENTS

(kilometers)

| | La Balsa to Buga | Buga to Cartago | Total |
|---|---|---|---|
| Length of Cutoffs | 15 | 23 | 38 |
| Present River Length | 179 | 194 | 373 |
| Future River Length | 119 | 139 | 258 |
| River Shortening Due to Cutoffs | 60 | 55 | 115 |
| Length of Right-bank Levees | 26 | 37 | 63 |
| Length of Left-bank Levees | 18 | 17 | 35 |

1. Within the 400-km reach from La Balsa to Cartago, the Cauca is an alluvial river (as defined by Matthes.[3a]). The profile is parabolic; slopes are not great, varying from 40 to 15 cm per kilometer. The meanders are most prevalent in the upper 100 km where the slope is greatest; this is apparently explained by a higher proportion of bedload and higher erodibility of the riverbanks in this portion. The riverbanks, in general, consist of fine-grained silty sand having relatively low resistance to erosion; the river bed consists of sand and gravel.

2. Since records began at Cali (Juanchito Bridge) in 1945, the river has been degrading at an average rate of 5.8 cm per year. (This degradation may be due, in part, to dredging of the river for sand and gravel to supply the local construction industry which has been increasingly active in recent years. It is estimated that 350,000 $m^3$ are removed annually by hand, and about 100,000 $m^3$ by mechanical means, within a reach of river several hundred meters long just upstream of the Juanchito bridge near Cali.) Such degradation has not, however, been noticeable at points along the river other than Cali.

3. The Timba reservoir will have the effect of removing a major part of the sediment (suspended as well as bedload) now transported by the river, thereby increasing its erosive power; on the other hand, the reduction of flood peaks caused by Timba will have an opposite effect.

4. Sediments will continue to be carried to the main river by the tributaries. However, some of the largest tributaries, such as the Palo, Fraile, Bolo and Amaime, traverse the valley floor for a distance of about 25 km; typically, these tributaries overflow and deposit the bulk of their sediment

in alluvial fans on the valley floor before reaching the river.

5. The tributaries vary in their sediment-carrying characteristics owing largely to differing soil characteristics and vegetal cover. For example, the Rio Bugala-grande is a notorious silt carrier; a soil-conservation program within its watershed would produce benefits to local agriculture and, incidentally, would greatly reduce the quantity of sediment now reaching the Cauca River from this source.

6. At present, the river overflows frequently and deposits appreciable quantities of sediment on the flood plain. In the future, after construction of Timba and the channel improvement, the net sediment-load remaining will be confined to the channel instead of being deposited on the flood plain.

7. Below Cartago, the river changes from an alluvial to an erodible-bed stream, flowing for the greatest part of its length through relatively narrow canyons to its mouth at the Magdalena River. There is practically no settlement along the river below Cartago; therefore, any treatment of the river upstream can have no deleterious effects.

8. Excessive degrading of the river in the reach from Cali to Yumbo would create serious dislocations because of the existence of several important water intakes of which the most important are those for the municipal water supply of Cali, and for several important industries near Yumbo including a large steam-electric station.

9. A vast hydroelectric project (capacity about 1,500,000 kw), for which a reconnaissance study has been completed, involves diverting about 130 $m^3/s$ continuously from the Cauca River to the Pacific slope by means of a tunnel through the Cordillera Occidental. This diversion would require a barrier dam near Vijes. Such a barrier could be designed to prevent the degradation mentioned above.

10. Some channel degradation in other reaches of the river would be beneficial as there would result savings in the cost of levee construction and improved drainage conditions for land both within and adjacent to the flood zone.

11. For excavation of the river cutoffs the "pilot cut" method is planned (used most notably on the lower Mississippi where the original river length of 680 miles from Memphis, Tennessee to Baton Rouge, Louisiana, was shortened 25% through use of cutoffs). Techniques to be followed in applying this method have been described by Matthes.(2a, 3b)

12. The estimated average height of the levees (Table 6) is 2 m from La Balsa to Buga and 1.5 m from Buga to Cartago. Levees will generally be set back from the river-bank a distance of 25 to 50 m in order to provide a margin of safety against bank erosion and to carry out erosion-preventive measures within the 25 to 50-m belt, to consist mainly of various types of local vegetation with deep root systems.

## Economic Justification

As described in the introduction, the primary flood control benefit will be that resulting from more intensive use of the land rather than from prevention

of damage to existing crops and improvements; this benefit should be measured as the difference in its productive capacity under conditions expected with and without flood control.(4) To estimate the difference in productive capacity it would be necessary to determine the net income expected from the land and from associated resources with and without the project. However, because of time limitations and lack of specialized personnel, an alternative method was used based on estimates of the increased market value of the affected land areas. Checks on these market values were obtained by analyzing the productivity of the land for typical crops with and without flood control.

As a first step, net farm income per hectare for various land classes was estimated in Table 7 on the basis of rental value plus added value produced by management. Rental values were taken at 10% of the selling prices for land in the Cauca Valley, for which conservative values, somewhat lower than currently prevailing prices, were used. (The rate of 10% is the current interest rate in Colombia for relatively large private enterprises.)

Added value produced by management was taken at 30% of rental value. Entrepreneurs customarily pay landowners a rental equal to a third of the gross profit. The remaining two-thirds is for entrepreneur's gross profit including bank-interest charges, management services, income taxes and net profit. The latter two items are conservatively estimated at 10% and 5%, respectively, of the entrepreneur's gross profit; this is equivalent to 20% and 10% respectively of the rental value; see note 2, Table 7, Income taxes, while not a part of net farm income from the entrepreneur's point of view, are wealth produced by the project and should therefore be included in evaluating benefits.

A check on the assumed selling price for Class G land is provided by considering current values and production costs for rice and soybeams, typical crops, as follows:

1. The present average price of unmilled rice per sack of 150 pounds (avoirdupois) is Ps 55; for soybeans, the price per sack of 125 pounds is Ps 46.25.

2. In a 3-year cycle, at least four harvests of rice and two of beans can be obtained. The yields per plaza (0.64 ha) are 47.5 sacks per harvest of rice and 16 sacks per harvest of beans. The resulting gross annual crop value is Ps 4,000 per plaza.

3. Production costs per harvest per plaza are Ps 620 for rice and Ps 250 for beans, which gives an average production cost of Ps 1,000 per plaza annually. All production costs are included except entrepreneur's bank-interest charges, the value of his management services and income taxes; these are considered part of entrepreneur's gross profit (see item 5). Gross profit is therefore Ps 3,000 per plaza.

4. Allowing 10% for area occupied by roads and irrigation canals, the foregoing figure reduces to Ps 2,700 per plaza.

5. The annual rent (see above) is a third of the gross profit or Ps 900. (The remaining Ps 1,800 is entrepreneur's gross profit.)

6. As use of money in Colombia now costs about 10% per annum, Class G land is worth Ps 9,000 per plaza. To be conservative, a value of Ps 7,500 per plaza was assumed.

TABLE 7

NET ANNUAL FARM INCOME PER HECTARE

(pesos)

| Land Class | Sale Price Per Plaza (b) | Rental Value Per Plaza | Added Value Per Plaza (see note 2) | Net Farm Income "A" Per Plaza | Net Farm Income "B" Per Plaza | Net Farm Income "B" Per Ha |
|---|---|---|---|---|---|---|
| A. Permanently flooded | 500 | 0 | 0 | 0 | 0 | 0 |
| B. Flooded 3 to 6 months during most years | 1200 | 120 | - | 120 | 120 | 190 |
| C. Flooded once in 2 to 5 years; without drainage and irrigation works | 2400 | 240 | 70 | 310 | 310 | 480 |
| D. Flooded once in 7 to 10 years; without drainage and irrigation works | 3500 | 350 | 100 | 450 | 450 | 700 |
| E. Flood-free; without drainage and irrigation works | 4000 | 400 | 120 | 520 | 520 | 810 |
| F. Flooded once in 7 to 10 years; with drainage and irrigation works | 6500 | 650 | 200 | 850 | 700 | 1100<br>990(a) |
| G. Flood-free; with drainage and irrigation works | 7500 | 750 | 220 | 970 | 820 | 1280<br>1150(a) |

Notes:

1. Rental value taken at 10% of sale price.
2. Added Value Produced by Management taken at 30% of rental value (see text).
3. Net Farm Income "B" equals Net Farm Income "A" less annual cost of irrigation and drainage works, taken at Ps 150 per plaza (applies only to Classes F and G). The latter cost is (i) 10% of the estimated construction cost of Ps 850 per plaza of these works limited, however, to lateral canals and drainage ditches (main canals and pumping stations and the Timba project allocation to irrigation are not included) plus (ii) operation and maintenance charge of Ps 65 per plaza.

(a) Reduced 10% to allow for land occupied by irrigation and drainage canals.

(b) One plaza equals 0.64 ha.

There are 85,000 ha in the flood zone of which 80,000 ha will be devoted to agriculture. The latter area is subdivided into land classes, with corresponding benefits per hectare, in Table 8. Also indicated in this table are the benefits in the areas adjacent to the flood zone due to lowered groundwater conditions. The ultimate direct flood-control benefit, in Part I of Table 8, is Ps 26 million from La Balsa to Buga and Ps 12 million from Buga to Cartago or a total of about Ps 38 million. Following construction of Timba and the river improvement, the completion of the bulk of which will take 4 years, full cultivation of the benefited lands will require additional time: this has been assumed to be 5 years. The ultimate direct flood-control benefit has therefore been discounted from Ps 38 million to Ps 32 million as shown in Part II of Table 8.

Additional indirect flood-control benefits will include: value added through processing of increased agricultural production; reduction in loss of human life; improved sanitary conditions; reduction of loss of livestock by drowning; savings in cost of highway and airport construction and maintenance resulting from improved flood and drainage conditions; and elimination of flood damage caused by interruptions to commerce and to industrial production. Although exact data are not available, it is believed that these benefits are worth at least half of the direct benefit. The total flood-control benefit then is 1.5 times 32 or Ps 48 million.

The annual cost of flood control was determined by adding the capital cost of the river improvement to that part of the Timba project capital cost allocated to flood control, as estimated on the basis of the "justifiable-alternative-expenditure method." It was assumed that the foreign-currency part of the resulting total capital cost will be amortized in 20 years and that interest on the local-currency part will be paid indefinitely. Allowances were then made for depreciation and for operation and maintenance. The resulting annual costs were:

| | |
|---|---|
| Timba project | Ps 4,250,000 |
| Cauca River improvement | 6,890,000 |
| Total | Ps 11,140,000 |

As the annual benefit of Ps 48 million is about 4.3 times the annual cost of Ps 11.1 million, the two projects are clearly justified.

## Pilot Projects

For planning purposes it has been assumed that complete development (including irrigation and drainage, as well as flood control) of the entire valley floor of 395,000 ha will be accomplished during a 30-year period. The key structure in the program is the Timba dam. Owing to its cost and multipurpose nature, several years are required to arrange for its financing. However, in the meantime, it is possible to proceed with the reclamation of certain areas that are not greatly affected by floods from the Cauca River nor dependent on the Timba reservoir for irrigation water. Moreover, these initial projects may be regarded as "pilot projects" as they will point the way toward efficient development of the bulk of the area in later years.

Three such pilot projects are Roldanillo-La Unión-Toro (11,200 ha), Aguablanca (5,000 ha) and Bugalagrande-Zarzal (16,000 ha). Their selection

TABLE 8

DIRECT FLOOD-CONTROL BENEFIT

(thousands of pesos annually)

I - Ultimate Direct Benefit

| Present Land Class | Benefit per Hectare (a) | La Balsa to Buga | | Buga to Cartago | |
|---|---|---|---|---|---|
| | | Farming Area (ha) | Benefit | Farming Area (ha) | Benefit |
| 1. Flood Zone | | | | | |
| A | 0.81 | 8,000 | 6,500 | 4,000 | 3,200 |
| B | 0.62 | 8,000 | 5,000 | 3,000 | 1,900 |
| C | 0.33 | 23,000 | 7,600 | 8,000 | 2,600 |
| D | 0.11 | 6,000 | 700 | 20,000 | 2,200 |
| Subtotals | | 45,000 | 19,800 | 35,000 | 9,900 |
| 2. Areas Adjacent to Flood Zone | | | | | |
| C | 0.22 (b) | 28,000 | 6,200 | 9,000 | 2,000 |
| Totals | | 73,000 | 26,000 | 44,000 | 11,900 |

Total Ultimate Direct Benefit Ps 37,900,000

(a) Difference in net farm income between Class E and present class. See Table 7.

(b) Estimated benefit due to lowered groundwater in area adjacent to flood zone.

II - Discounted Direct Benefit

Assume 5 years will be required to achieve the ultimate direct benefit. Use interest rate of 8%. Determine present value of the benefit for the 50 years following project completion.

| Year | % developed | Present Value | Product |
|---|---|---|---|
| 1 | 20 | .926 | .185 |
| 2 | 40 | .856 | .342 |
| 3 | 60 | .794 | .476 |
| 4 | 80 | .736 | .589 |
| 5 | 100 | .681 | .681 |
| 6 to 50 | 100 | 8.247 (a) | 8.247 |
| | | | 10.520 |

Present value of an Annuity Certain for 50 years is 12.23

Discount is therefore: $\frac{10.52}{12.23} = 86\%$

Direct Flood Control Benefit is therefore 0.86 x Ps 37,900,000 or Ps32,000,000

(a) Present value of an Annuity Certain for 45 years is 12.11;
12.11 x .681 = 8.247

was based mainly on: extent of local interest, technical feasibility and economic return. The first two projects are under construction while the third is being designed.

### Aguablanca Project

As the land reclaimed by this project will ultimately be devoted to urban use (see Fig. 9), the degree of protection will be much higher than that adopted elsewhere in the valley. The river levee on the east is being built to a profile 2.5 m higher than the highest recorded—during the flood of February 1950. The frequency of a flood 1.5 m higher (allowing 1.0 m freeboard) is estimated to be 100 years initially; and 200 years ultimately, after completion of the Timba reservoir.

Elimination of flooding within the Aguablanca project area will eliminate 55 million $m^3$ of natural valley storage or 7.5% of the 740 million $m^3$ between La Balsa and Cali. The peak discharge of the 1950 flood was 1,000 $m^3/s$. The eliminated valley storage would cause an increase to 1,032 $m^3/s$, for which the river level would be only 15 cm higher than under present conditions.

Although, as described above, diking of the entire flood zone in the valley is not feasible, it was decided nevertheless to make an exception in the case of Aguablanca for the following reasons: (a) The valley storage eliminated by this one project has a negligible effect on river levels. (b) Benefits will be much higher in the case of the Aguablanca project, per hectare of reclaimed land, than elsewhere in the valley. (c) Further urban encroachments on the flood plain are not visualized, at least for the next generation or two. (The remaining towns are all located well outside the flood zone.)

The interior drainage system includes (1) a pumping station to remove interior drainage water during flood stages in the river and to lower the presently excessively high groundwater level; and (2) a dredged storage pond to reduce pumping requirements and, at the same time, provide a permanent pond as a nucleus for a park development.

#### Pumping station

Design data with respect to the pumping station are as follows:

| | |
|---|---|
| Interior drainage area | 56 $km^2$ |
| Portion of drainage area urbanized, initially | 20% |
| **Design Storm** | |
| Frequency | 3 years |
| Sump level, minimum | El 949.5 |
| Sump level, maximum | El 952.1 |
| Peak inflow | 18.0 $m^3/s$ |
| Pondage | 770,000 $m^3$ |
| Peak outflow | 7.8 $m^3/s$ |
| **Cauca River Levels** | |
| Minimum level requiring pumping | El 950.3 |
| Average | 950.6 |
| 3-year flood (Design Flood) | 953.8 |
| 100-year flood | 956.0 |

FIGURE 9. AGUABLANCA PROJECT

Pumps

| | |
|---|---|
| Number of units, initially | 3 |
| Number of units, ultimatelly | 5 |
| Rated capacity (each unit) | 27,000 gpm |
| Rated head (static) | 3.0 m |

The design conditions assume coincidence of a 3-year storm on the interior area with a 3-year flood in the Cauca River. The available data indicate that these two events, if not entirely independent, are almost so and that the probability of their coincidence is about once in 7 years.

Variable-blade pumps

For design conditions with river level at 953.8, static heads will be 4.3 m maximum and 1.9 m minimum. However, pumping will be required also for river levels equal to the sump level or as high as 956.0. The minimum static head is thus zero and the maximum is 6.5 m.

Because of the largely independent nature of the two hydrologic factors (river level and rainstorm on the interior area) the normal occurrence will be high rainstorm with low flood-stage and vice versa. It is therefore desirable, as a second requirement, to have a pump with a characteristic curve of head vs. discharge in approximately inverse relation.

To best meet these two requirements, vertical propellor pumps with variable blades are being specified. This type has the further advantage of low starting current, which is important at the Roldanillo-La Unión-Toro project where pumps identical to that at Aguablanca will be used and where electric power is limited.

Although unavailable until recently in the United States except in large sizes and on special order, variable-blade pumps in relatively small sizes (the 27,000-gpm pumps will be about 42 inches in diameter) are now being manufactured in the United States and Europe by several well-known firms. Bids recently received have confirmed that the variable-blade type provides the most economical solution.

Artificial storage pond

The pondage of 770,000 $m^3$ will be composed of 600,000 $m^3$ in a storage pond and 170,000 $m^3$ in the drainage canals. If the drainage canals are later replaced by conduits or lined channels, thus increasing velocities and reducing storage-in-transit, the storage pond can be enlarged.

To obtain the 600,000 $m^3$ of usable storage in the storage pond, 840,000 $m^3$ of soil will be removed by means of a hydraulic pipeline dredge at an estimated cost of Ps 1,430,000. This expenditure is justified for the following reasons:

1. Without the storage pond, the capacity of the pumping station would have to be doubled at a cost approximately equal to that of excavating the pond. If the capitalized cost of depreciation and electric energy consumption, as applied to the required additional pumping equipment, is added, the economic comparison is clearly in favor of the storage pond.

2. As the interior drainage area becomes urbanized over the course of the years with storm sewers and streets constructed, runoff characteristics will become progressively worse in the sense that the volume and especially the peak will progressively increase. The peak inflow could easily

increase four times, that is, up to 36 to 54 $m^3/s$, as compared with 18 $m^3/s$ under initial conditions. With the storage pond, little if any increase in the pumping capacity will be required to meet the needs of increased urbanization. However, to be safe, space is being provided at the pumping station for two additional pumping units, when and if needed, which would raise the rated capacity from 81,000 to 135,000 gpm.

3. The value of the general area in which the pond will be located will be greatly enhanced. This area is now a swamp, 62 ha in extent. The completed pond will occupy only 46 ha of which the water area will be 31 ha and 15 ha will be in islands. Moreover, the area surrounding the storage pond is being reserved for parks and housing developments. The excavation is planned so that the shores of the pond will be well defined, without flat shallow places. A minimum depth of 80 cm is being provided to permit pleasure boating, and to prevent mosquito breeding and undesirable aquatic growths.

Project repayment

A law adopted by the National Government in April 1958 provides that the landowners benefited by the Aguablanca project shall repay the project cost to CVC in the form of an assessment which can be paid within optional periods of either 5 or 10 years. For the shorter term, interest of 8% will be charged and, for the latter, 10%. (The usual interest rate in Colombia for commercial credits is 10%.) In addition, landowners must pay CVC 10% of the enhanced value of the land benefited by the project, as determined by a committee of three assessors chosen jointly by CVC and the landowners.

Although many landowners are opposed to this formula, they should have no difficulty in paying the assessment it calls for. Unimproved flood-free land near the project area has a market value of 15,000 to as high as Ps 50,000 per ha with an average of about 20,000. In comparison, the average value of the land in the flood zone is about Ps 7,500 per ha.

To assist those landowners claiming hardship, the law of April 1958 contains a provision whereby landowners may elect to pay a part of their assessment in the form of land.

The project benefits, as measured by the enhancement value averages Ps 12,500 per ha or Ps 72,350,000 for the project area of 5,800 ha (5,000 ha within the project proper plus 800 ha outside that will benefit because of improved drainage). The estimated project cost including rights-of-way is Ps 15,060,000 giving a benefit-cost ratio of 4.8 to 1.

Roldanillo-La Unión-Toro Project

An interesting aspect of this project, Fig. 10, is the dual-purpose nature of two of its features: the La Unión Pumping Station and the intercepting canal.

The La Unión Pumping Station will contain three 27,000-gpm units to pump drainage water to the Cauca River during flood stages; also, to pump water from the principal drain to irrigation canals located on the high bank of the river. As static lifts are similar to that at the Aguablanca project, it has been possible to adopt identical requirements for the pumping units at both stations.

The intercepting canal will be of relatively large capacity in order to handle flood flows from streams draining the east slope of the Cordillera

FIGURE 10. ROLDANILLO-LA UNIÓN-TORO PROJECT

Occidental; this canal will also serve as the main irrigation-supply canal for the western half of the area. To accomplish this second purpose, the canal will be provided with check structures each including a tainter gate operated automatically to maintain water levels sufficient for irrigation; during floods, the gates will open completely so as to provide unobstructed passages.

The natural levee along the left bank of the Cauca River provides protection against floods up to an estimated frequency of once in 5 years. When the irrigation canals on the Cauca River bank are constructed, the excavated material will be placed to form a levee 1 to 2 m high; the protection then available will be against about a 7-year flood. This degree of protection is considered adequate in view of the low degree of present land use and intense desires of the small landowners in the area to cultivate their land. The future Cauca River improvement will increase the degree of protection to about 10 years.

FIGURE 10. ROLDANILLO-LA UNIÓN-TORO PROJECT

## REFERENCES

1. "Maximum Possible Precipitation over the Panama Canal Basin"; Hydrometeorological Report No. 4; U. S. Weather Bureau in cooperation with Corps of Engineers; Vicksburg, Miss., 1943.

2. "The Unified Development of Power and Water Resources in the Cauca Valley." An engineering report prepared by Olarte, Ospina, Arias & Payán, Ltda., Bogotá; Gibbs & Hill, Inc., New York; and Tippetts-Abbett-McCarthy-Stratton, New York, for the Corporación Autónoma Regional del Cauca, Cali, Colombia; January 1956.

   a) Appendix H "Analysis of Cauca River Improvements by Means of Cutoffs," Gerard H. Matthes, Hom. M. ASCE.

3. "American Civil Engineering Practice," Robert W. Abbett; Section 15, "River Engineering," Gerard H. Matthes; John Wiley & Sons, New York, 1956.

   a) pp. 15-52 to 15-59

   b) p. 15-122

4. "Proposed Practices for Economic Analysis of River Basin Projects"; report to the Federal Inter-Agency River Basin Committee; Washington, D. C.; May 1950; page 42.

### Abbreviations and Equivalents

| | |
|---|---|
| cm | centimeters = 0.394 inches |
| °C | degrees Centigrade |
| El | elevation in meters |
| gpm | U. S. gallons per minute |
| ha | hectare = 2.47 acres |
| km | kilometers = 0.621 miles |

| | |
|---|---|
| $km^2$ | square kilometers = 0.386 square miles |
| kw | kilowatts |
| m | meters = 3.28 feet |
| $m^3$ | cubic meters |
| mm | millimeters (100 mm = 3.94 inches) |
| $Mm^3$ | million cubic meters = 811 acre-feet |
| $m^3/s$ | cubic meters per second = 35.3 cubic feet per second |
| plaza | 0.64 ha |
| Ps | Colombian pesos |

Journal of the
HYDRAULICS DIVISION
Proceedings of the American Society of Civil Engineers

# FRICTION FACTORS IN CORRUGATED METAL PIPE

Marvin J. Webster,[1] F. ASCE, and
Laurence R. Metcalf,[2] M. ASCE

## SYNOPSIS

A study made to determine friction coefficients for flow in large corrugated metal pipe by measurement of head losses in pipes 3, 5, and 7 ft in diameter and to determine velocity distribution for several discharges in each test pipe so that the results could be generalized to show the relationship between friction coefficients and absolute roughness is discussed in this paper. Data taken during the study are presented together with recommended values of friction and roughness coefficients.

## INTRODUCTION

Numerous laboratory and field tests have been made to determine friction factors for various types and sizes of pipes and conduits. However, comparatively few tests had been made prior to 1950 on corrugated metal pipe of the larger sizes commonly used in engineering practice. For this reason, the Office, Chief of Engineers, U. S. Army, authorized tests on 3-, 5-, and 7-ft-diam corrugated metal pipe to be conducted at the Bonneville Hydraulic Laboratory.

In 1926, Yarnell, Nagler, and Woodward published results of hydraulic tests(1) at the State University of Iowa on 12-, 18-, 24-, and 30-in.-diam corrugated metal pipe that varied in length from 24 to 36 ft. The results of these tests are applicable to similar installations of short pipes and culverts, such as those under highway and railroad fills. However, they are not directly applicable to long pipelines because entrance, transition, and exit losses cannot

Note: Discussion open until February 1, 1960. To extend the closing date one month, a written request must be filed with the Executive Secretary, ASCE. Paper 2148 is part of the copyrighted Journal of the Hydraulics Division, Proceedings of the American Society of Civil Engineers, Vol. 85, No. HY 9, September, 1959.

1. Chf. Hydr. Design and Lab. Section, U. S. Army Engr. Dist., Portland, Corps of Engrs., Portland, Ore.
2. Hydr. Engr., U. S. Army Engr. Dist., Portland, Corps of Engrs., Portland, Ore.

be isolated from the pipe friction losses when the test pipes are of such short length in relation to their diameter. Keulegan[2] used velocity distribution data from the foregoing tests to compute friction factors for long pipelines and for pipes of larger diameter.

In 1950, Straub and Morris published results on studies[3] conducted at the St. Anthony Falls Hydraulic Laboratory, University of Minnesota, of flow through 18-, 24-, and 36-in.-diam circular and arched corrugated metal pipe 193 ft in length and laid on a slope of 0.002. These studies showed a definite systematic increase in the values of the friction and roughness coefficients "f" and "n" with increased Reynolds numbers ($R_e$) over the entire range of discharges tested. These findings were contrary to expectations because most "f" vs $R_e$ curves for both smooth and rough commercial pipe have shown constant or slightly decreasing characteristics throughout the experimental range. Values of "n" from 0.0216 to 0.0252 were obtained for corrugated metal pipe flowing full and from 0.0228 to 0.0258 for open-channel flow. Values recommended for use in design were 0.025 and 0.0235 for full-pipe and open-channel flow, respectively.

The purpose of the tests at the Bonneville Hydraulic Laboratory was to determine friction factors for 3-, 5-, and 7-ft-diam corrugated metal pipe as indicated by head-loss measurements for a range of velocities up to approximately 10 fps for 5- and 7-ft-diam pipe and 16 fps for 3-ft-diam pipe. Tests were made with both full-pipe and open-channel flow in the 3- and 5-ft-diam pipe and with full-pipe flow in the 7-ft-diam pipe. The initial test schedule was expanded to include studies on the 5- and 7-ft-diam pipe with 25 per cent of the periphery (at the invert) smooth paved and on the 5-ft-diam pipe with 50 per cent of the periphery smooth paved.

## Description of Project

The tests were conducted at a site located on the Washington shore of the Columbia River at the north end of Bonneville Dam. This site was selected because sufficient space was available for the test and metering sections and because sufficient head and water supply were available to produce the discharges and velocities required for the tests. The layout for the 7-ft-diam pipe, typical for the three sizes of pipe tested, is shown in Fig. 1. The 3-ft-diam pipe in the test section is shown in Fig. 2. Water for the study was taken from one of the fingerling by-pass channels through the main dam. From the fingerling by-pass, the water flowed through a 6-ft-diam, smooth-wall pipe to the test section. From the test section, the flow passed through a 7-ft-diam, smooth-wall pipe and then dropped 11 ft to the metering section where it was measured by a system of flat-plate orifices and then returned to the river through gate valves and short outlets. The 11-ft difference in elevation between the test and metering sections was sufficient to provide adequate head on the meters for the tests with open-channel flow.

The corrugated metal test pipes were of standard commercial manufacture and arrived at the test site in 20-ft-long pieces composed of a series of 2-ft-long overlapping sections. The sections were riveted together and each contained lapped and riveted longitudinal joints that were staggered so that no two were in line in adjacent sections. Before installation, the riveted joints were sealed against leakage by welding on the outside of the pipe. The 20-ft sections were then butt-welded together to form a pipeline that was set to

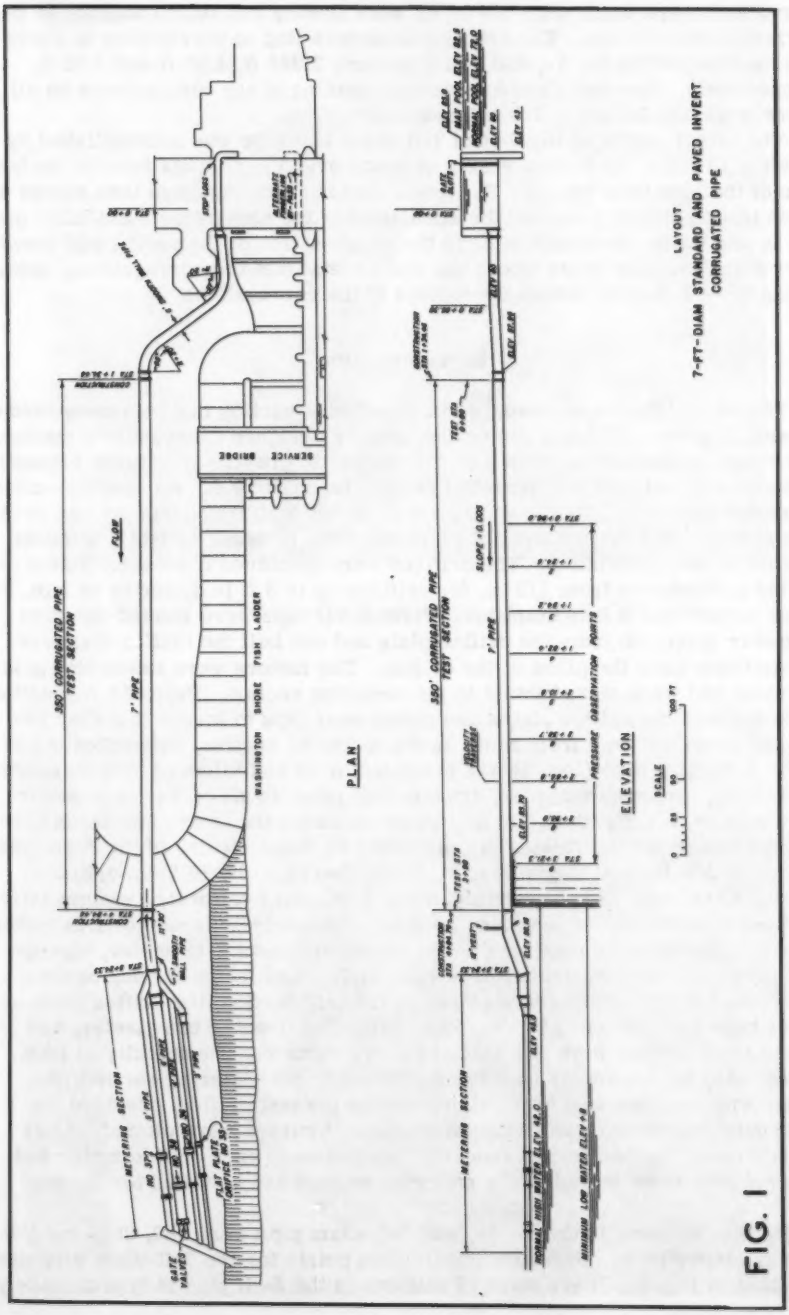
LAYOUT
7-FT-DIAM STANDARD AND PAVED INVERT
CORRUGATED PIPE
PLAN
ELEVATION
SCALE
0
50
100 FT
FLOW
350' CORRUGATED PIPE TEST SECTION
7' PIPE
WASHINGTON SHORE FISH LADDER
BRIDGE
METERING SECTION
GATE VALVES
PRESSURE OBSERVATION POINTS
SLOPE = 0.005
MINIMUM LOW WATER ELEV +9

FIG. 1

grade and alignment along a continuous footing between concrete saddles. Observations were made when the pipes were flowing full but no sagging or deformation was visible. The average diameters (top of corrugation to top of corrugation) of the 3-, 5-, and 7-ft pipe were 2.996 ft, 4.95 ft and 7.05 ft, respectively. The depth and longitudinal spacing of the corrugations on all pipes were 1/2 in. and 2-2/3 in., respectively.

The invert paving of the 5- and 7-ft-diam test pipe was accomplished by welding 18-gage, 10-ft-long sheets of metal over the corrugations on the bottom of the pipe (see Fig. 3). The lower sector of the pipe was then coated with bituminous paint to complete the simulation of the conventional asphaltic paving in use today. A compromise in the reproduction of the paving was necessary along the side joints where the sheet metal met the corrugations; these joints were left open across the valleys of the corrugations.

## Instrumentation

The rate of flow was measured in a metering section that was composed of a parallel system of flat-plate orifice meters designed to measure a continuous range of discharges from 8 to 385 cfs and to provide an overlap between meters operated with a differential head of from 1 to 9 ft. An aperture-plate diameter ratio of 0.7 to 1.0 was selected for all orifices except the one in the 5-ft section; this orifice had a 0.66-to-1.0 ratio to secure slightly different discharge characteristics. The orifices were machined from steel plates that varied in thickness from 1/2 in. for orifices up to 3 ft in diameter to 1 in. for those larger than 5 ft in diameter. Piezometer taps were located one pipe diameter upstream from the orifice plate and one half the orifice diameter downstream from the plane of the orifice. The meters were assembled prior to rating and were moved intact to the metering section. Periodic inspections were made of the orifice plates and piezometer taps to insure that they remained clean and free from rust. In the metering section, the orifice meter in the 6-ft-diam pipe (Fig. 1) was preceded by 19 and followed by 6 diameters of straight, constant-diameter, smooth-wall pipe; in all of the other meter installations, the approach and exit pipes exceeded the length standards prescribed by the Special Research Committee on Fluid Meters of the American Society of Mechanical Engineers.[4] First, two 24.0- by 16.2-in. orifice meters were calibrated separately, using a standard calibrated venturi meter, and then installed in the metering section. Successively larger orifice meters were calibrated as follows: the entire length of constant-diameter, smooth-wall pipe to be used upstream from each orifice and the 20-ft-long section that contained the orifice were placed in the test section, the orifice piezometer taps were attached to a standard differential water manometer, and varied rates of flow were introduced into the system. The quantity of flow, as indicated by previously calibrated orifices in the metering section, together with the observed head differential on the test orifice, provided the basic data from which experimental coefficient curves were plotted. After all data were checked for accuracy and consistency, each orifice meter and adjacent pipe were moved to the metering section and installed for further use.

The test sections in the 3-, 5-, and 7-ft-diam pipe were 180, 251, and 350 ft long, respectively. Pressure observation points for the 7-ft-diam pipe are indicated in Fig. 1. There were 12 stations in the 3- ft pipe at approximately

Fig. 2 Three-Ft-Diam Pipe In Test Section

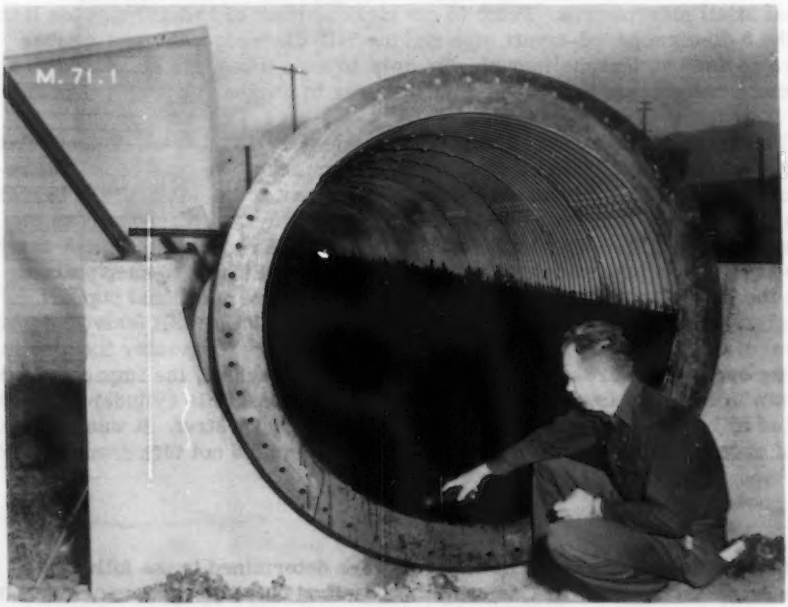


Fig. 3 Five-Ft-Diam Pipe With 50% Paving

15-ft spacings and 10 stations in the 5-ft pipe at approximately 20-ft spacings. Each pressure observation point consisted of two 1/8-in.-diam piezometers that were drilled into the valleys of the corrugations 45 degrees above the pipe invert on each side. The two piezometers were interconnected by a common lead to a single manometer in the bank shown in Fig. 4. Individual pressure fluctuations at each piezometer varied from 0.005 ft at low discharges to 0.015 or 0.02 ft at high discharges, however, it was found that consistent results could be obtained from a series of 5, 10, or 20 consecutive visual observations.

It was determined in a preliminary study on 3-ft pipe (Fig. 5) that these piezometers were influenced by the partial recovery of velocity head in the corrugations and therefore indicated pressures higher than the true static pressure as taken at a point 6 in. within the pipe. However, they were considered sufficiently accurate to determine the differential pressure between successive stations along the pipe axis. The data in Fig. 5 are qualitative in nature and are included to show that the uniformity of pressures measured along the corrugations depends on exact placement of piezometers. It is believed that the nonuniform points shown on some of the grade lines presented in Fig. 7 were caused either by abnormal velocity distribution or by imperfections within the pipe that affected localized velocities and pressure adjacent to the piezometers.

Static pressures during the velocity distribution studies and free water-surface levels for open-channel flow were measured by means of tubes that were the equivalent of the static leg of a conventional pitot tube (Fig. 6). The static tubes were checked to determine the effect of local flow acceleration. At first these tubes contained four piezometers that were connected to individual water manometers, and the instrument was aligned with the flow by rotating the tube until the pressure, as reflected by the manometers, was equal at all piezometers. Prior to the measurement of hydraulic grade lines in the 5-ft-diam paved-invert pipe and the 7-ft-diam pipe, the static tubes were revised so that the four piezometers in each tube were connected to a common manometer that reacted much faster to pressure changes than did the instrument of original design.

Two types of impact tubes were used to measure local velocity heads from which velocity distribution curves were determined. The type used first resembled a pitot tube but lacked the static openings on the sides of the barrel. The tube was mounted in a bracket that slid along a strut placed across the pipe diameter. The impact tube was satisfactory during tests on the 3-ft pipe, although at high test velocities it vibrated and was difficult to keep pointed into the flow. It was found that the tube would require additional support brackets when velocity heads were measured in the lower half (extended positions) of the 5-ft pipe. Because it would be necessary to unwater the pipeline during each run in order to install the additional brackets, the impact cylinder (shown in Fig. 6) was substituted for the impact tube. This cylinder was supported by brackets mounted 12 in. apart on the support strut. It was found to be of excellent accuracy as a measuring device and did not turn from the flow.

## Procedure

Friction losses for pipes flowing full were determined in the following manner: after the flow was adjusted to a desired rate through one or more of

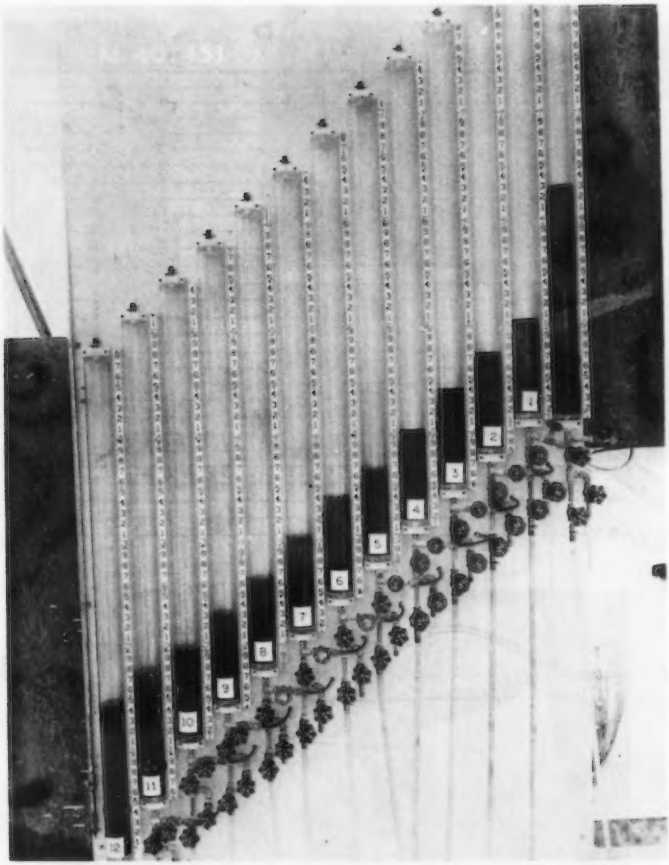

Fig. 4 Differential Manometer

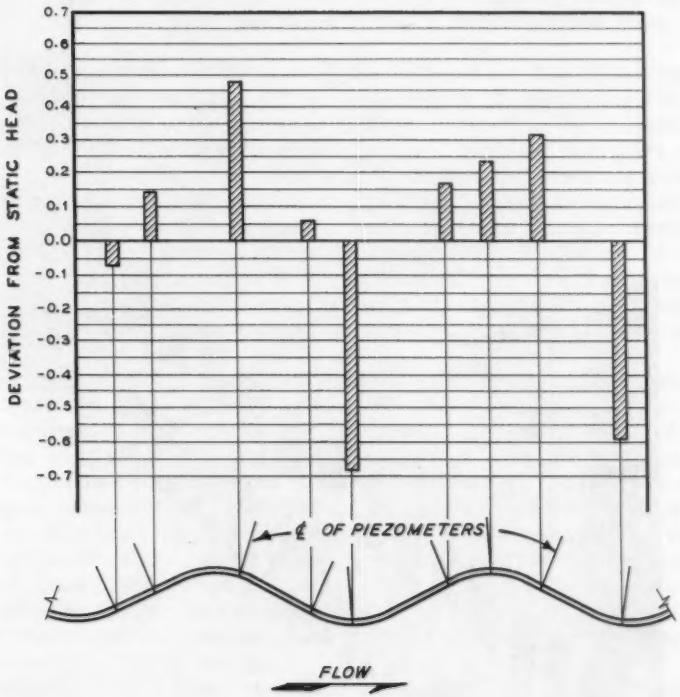


NOTES

1. READINGS TAKEN AT STA 1+50.
2. VELOCITY IN THE PIPE 10 FPS.
3. ZERO EQUALS STATIC PRESSURE (6 IN. INSIDE PIPE).
4. PIEZOMETERS $\frac{1}{8}$ IN. DIAMETER, PLACED 45 DEG ABOVE PIPE INVERT.
5. DEPTH OF CORRUGATION $\frac{1}{2}$ IN.; CYCLE LENGTH $2\frac{2}{3}$ IN.

PRESSURE DISTRIBUTION ALONG CORRUGATIONS

3-FT-DIAM PIPE

FIG. 5

Pitot Tube

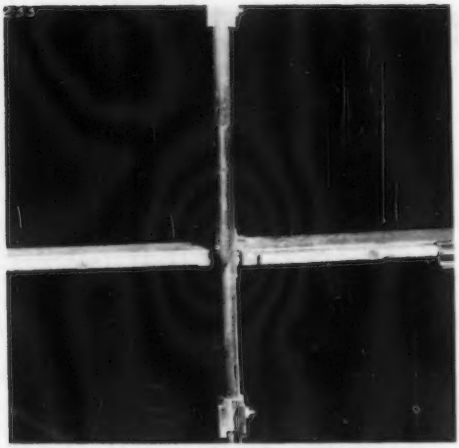

Impact Cylinder

Pressure Tube

Fig. 6 Velocity and Pressure Instruments

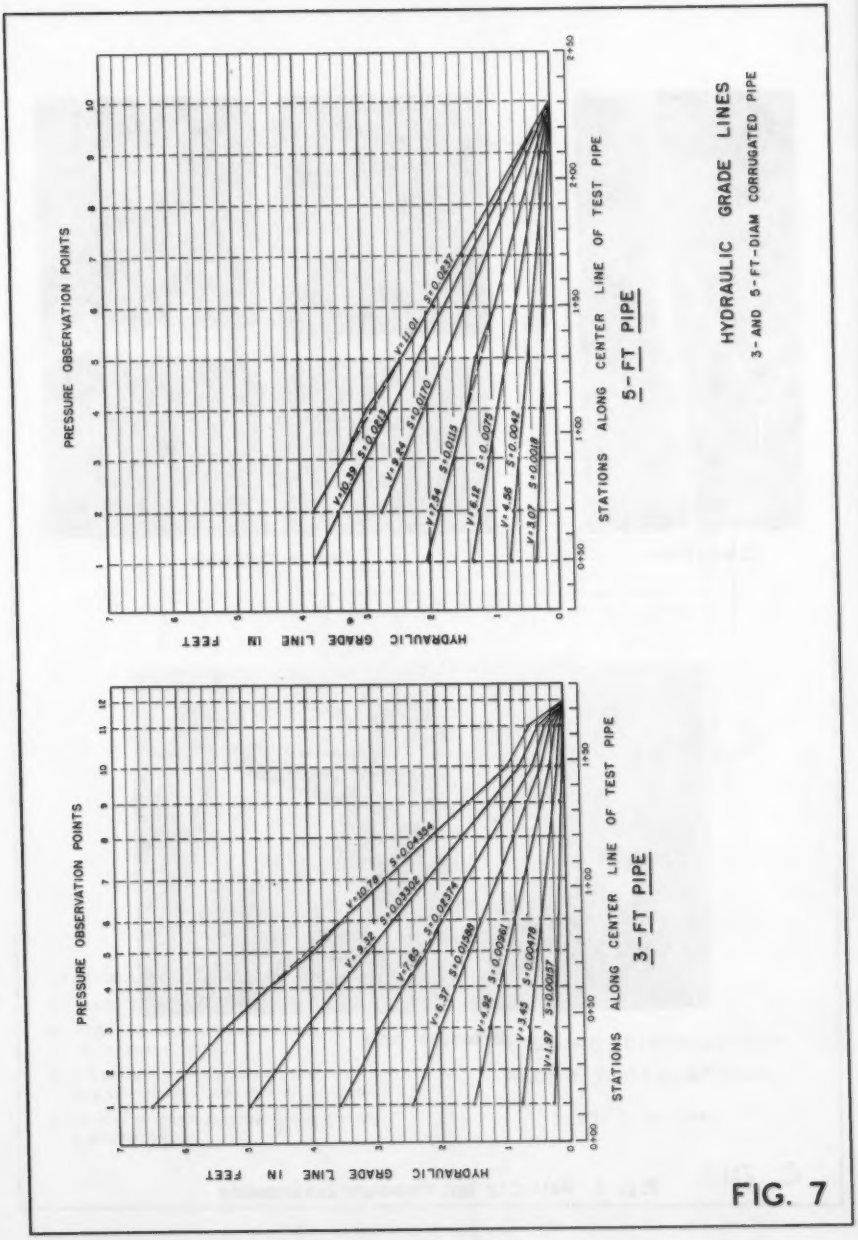
HYDRAULIC GRADE LINES
3- AND 5-FT-DIAM CORRUGATED PIPE
5-FT PIPE
PRESSURE OBSERVATION POINTS
HYDRAULIC GRADE LINE IN FEET
STATIONS ALONG CENTER LINE OF TEST PIPE
V=10.39 S=0.0213
V=11.01 S=0.0237
V=9.24 S=0.0170
V=7.54 S=0.0113
V=6.18 S=0.0075
V=4.56 S=0.0044
V=3.07 S=0.0018
3-FT PIPE
PRESSURE OBSERVATION POINTS
HYDRAULIC GRADE LINE IN FEET
STATIONS ALONG CENTER LINE OF TEST PIPE
V=10.78 S=0.04584
V=8.32 S=0.03302
V=7.89 S=0.02374
V=6.37 S=0.01580
V=4.82 S=0.00961
V=3.45 S=0.00478
V=1.87 S=0.00157

FIG. 7

the orifice meters and respective gate valves, and the average differential heads on the meters were derived from a series of 10 readings, the two observers proceeded to the test section and measured the hydraulic grade line within the test pipe by means of 10 consecutive readings of the water-surface elevations within the manometer tubes. Then the observers returned to the metering section and checked the meter readings. In all tests, if the average differential head on the meters at the beginning and end of a test run agreed within 1 per cent, the average of the two heads was used to compute the rate of flow; otherwise the entire run was discarded.

Velocity distribution in the 3-ft-diam pipe was measured by means of a combination of one of the previously described static tubes and two impact tubes at each observation station. Leads from the three tubes were connected to a 3-leg differential manometer where velocity heads were recorded in groups of 10 simultaneous readings. The static tube was mounted 6 in. within the pipe and 45 degrees above the invert, whereas the two impact tubes were traversed through the horizontal and vertical diameters on separate struts. In order that the proximity of the horizontal strut might not affect the accuracy of observations, the horizontal strut was removed while the vertical traverses were being made. The velocity distribution in the standard 5-ft-diam pipe was measured by means of three impact tubes and one static tube that were used simultaneously at each station. One impact tube was used on each half of the horizontal traverse and the other on the vertical traverse. Instrumental data were observed 20 times in succession to determine the average velocity for each position of the tubes. Two impact cylinders and a static tube were used to measure velocities in the 5-ft-diam pipe with a paved invert and in the 7-ft-diam pipe.

For tests of open-channel flow in the 3- and 5-ft-diam pipes, the approximate rate of flow was regulated at the intake gate; and the depth in the test pipe was balanced by adjusting the valves in the metering section until the hydraulic grade line, as recorded by the same piezometers or static tubes used for the studies of full-pipe flow, was nearly parallel to the pipe invert slope. Then the depth of flow was measured by means of a static tube located near the longitudinal center of the test section and the rate of flow was determined in the metering section. It was difficult to maintain a constant slope of the water surface in the test pipes, and continuous fluctuations of the forebay level made it impossible to conduct tests of open-channel flow during certain periods when Bonneville Dam was used to absorb peaks in the regional power demand. Tranquil flow was required to avoid the occurrence of standing waves in the test section; therefore, it was necessary to decrease the slope of the 5-ft-diam, paved-invert pipe from 0.005 to 0.002. The same change and possibly revisions of the intake structure would have been required to permit tests of open-channel flow in the 7-ft-diam pipe.

## Computations

### Full-Pipe Flow

The average velocity of flow for both standard and paved pipes flowing full was based on the measured discharge and on the area corresponding to pipe diameters of 3.00, 4.95, and 7.05 ft. In the case of the paved pipe, the area reductions effected by the paving are reflected in the values of "f" and "n." The values of "S" were then determined from straight-line portions of the

hydraulic grade line, typical examples of which are shown in Figs. 7 to 9. It will be noted that the grade lines for all tests are fairly straight with the exception of the 3-ft pipe tests shown in Fig. 7. In this case, only the straight portions of the grade lines between measuring points 3 and 10 were used to compute the slope. The other points, near the ends of the test section, were apparently affected by entrance and exit conditions. Values of "S" obtained from these grade lines were plotted against measured discharges to form the rating curves shown in Fig. 10 and were used to derive numerical equivalents for "f," "n," and $R_e$ that are shown in Figs. 11 and 12. The friction factor "f" was computed from the Darcy formula, in which

$$H_f = f \frac{L}{D} \frac{V^2}{2g} \quad ;$$

the roughness coefficient "n" for the Manning formula,

$$V = \frac{1.486}{n} R^{2/3} S^{1/2}$$

was computed from the friction factor "f" by the relationship

$$n = \frac{R^{1/6} \sqrt{f}}{10.8} \quad ;$$

and $R_e$ was determined from the formula

$$R_e = \frac{VD}{\nu}$$

Typical curves of velocity distribution within the test pipes are shown in Figs. 13 and 14. Local velocities were computed from the formula $V_1 = \sqrt{2gh}$, where "h" was the mean difference between readings obtained from the previously described impact and static tubes. In the vertical traverse in the 3-ft-diam pipe, where the impact tube was displaced downstream from the static tube, a correction of

$$H_f = f \frac{L}{D} \frac{V^2}{2g}$$

(where L equals the horizontal displacement)

was applied to the value of "h" before the local velocity was computed. Also shown in Figs. 13 and 14 are curves of the relationship $V_1/V_*$, as computed from the formula: $V_* = \sqrt{RSg} = V\sqrt{f/8}$. This relationship was one of the means used to analyze the adequacy and consistency of the velocity data.

## Open-Channel Flow

The first step toward determination of "n" values for open-channel flow in the 3- and 5-ft-diam pipes was the computation of cross-sectional areas and hydraulic radii for observed depths and rates of flow in the test pipes. Then slopes were determined from straight-line portions of plotted hydraulic grade lines, and values of "n" were computed from the Manning formula. The curves presented in Fig. 15 show the variation of the roughness coefficient with the depth of flow. In order to plot rating curves for open-channel flow, the observed measurements were reduced to equivalent values for a slope of

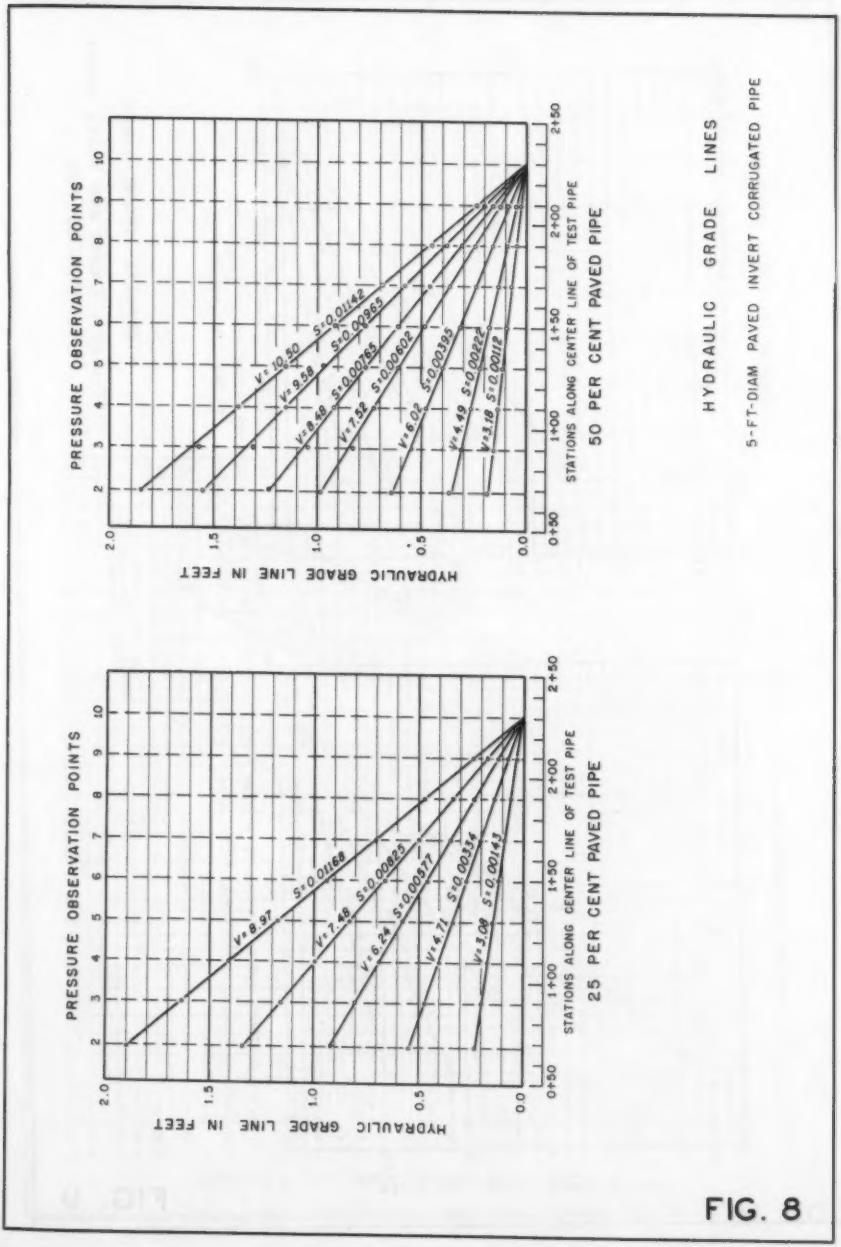
HYDRAULIC GRADE LINES
5-FT-DIAM PAVED INVERT CORRUGATED PIPE
50 PER CENT PAVED PIPE
25 PER CENT PAVED PIPE
PRESSURE OBSERVATION POINTS
HYDRAULIC GRADE LINE IN FEET
STATIONS ALONG CENTER LINE OF TEST PIPE
V=10.80 S=0.01142
V=9.58 S=0.00965
V=8.48 S=0.00765
V=7.52 S=0.00602
V=6.62 S=0.00395
V=4.49 S=0.00222
V=3.18 S=0.00118
V=8.97 S=0.01168
V=7.48 S=0.00829
V=6.24 S=0.00577
V=4.71 S=0.00334
V=3.08 S=0.00141

FIG. 8

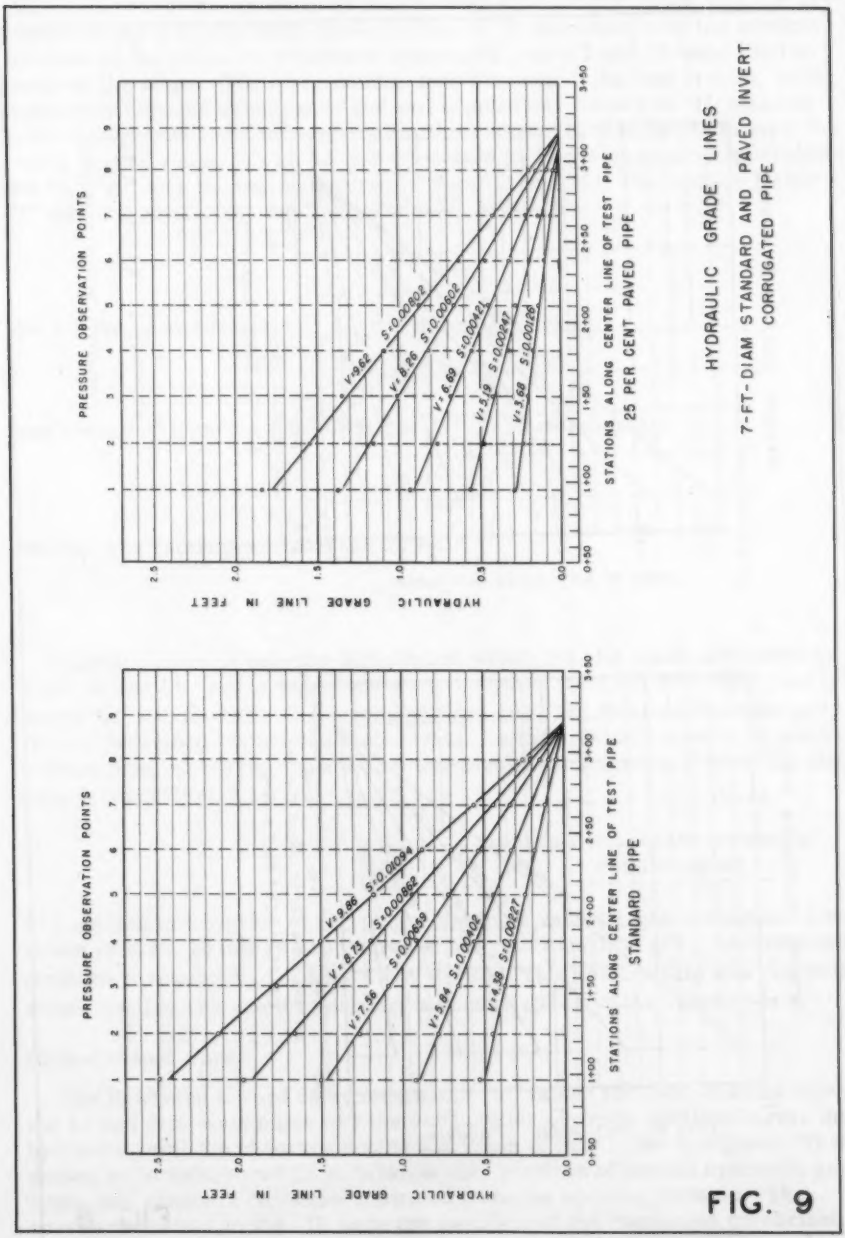
HYDRAULIC GRADE LINES
7-FT-DIAM STANDARD AND PAVED INVERT CORRUGATED PIPE
25 PER CENT PAVED PIPE
V=9.62 S=0.01902
V=8.26 S=0.01902
V=6.69 S=0.00421
V=5.38 S=0.00247
V=3.69 S=0.00126
STATIONS ALONG CENTER LINE OF TEST PIPE
PRESSURE OBSERVATION POINTS
HYDRAULIC GRADE LINE IN FEET
STANDARD PIPE
V=9.85 S=0.0094
V=8.73 S=0.00662
V=7.56 S=0.00459
V=5.84 S=0.00208
V=4.38 S=0.00221
STATIONS ALONG CENTER LINE OF TEST PIPE
PRESSURE OBSERVATION POINTS
HYDRAULIC GRADE LINE IN FEET

FIG. 9

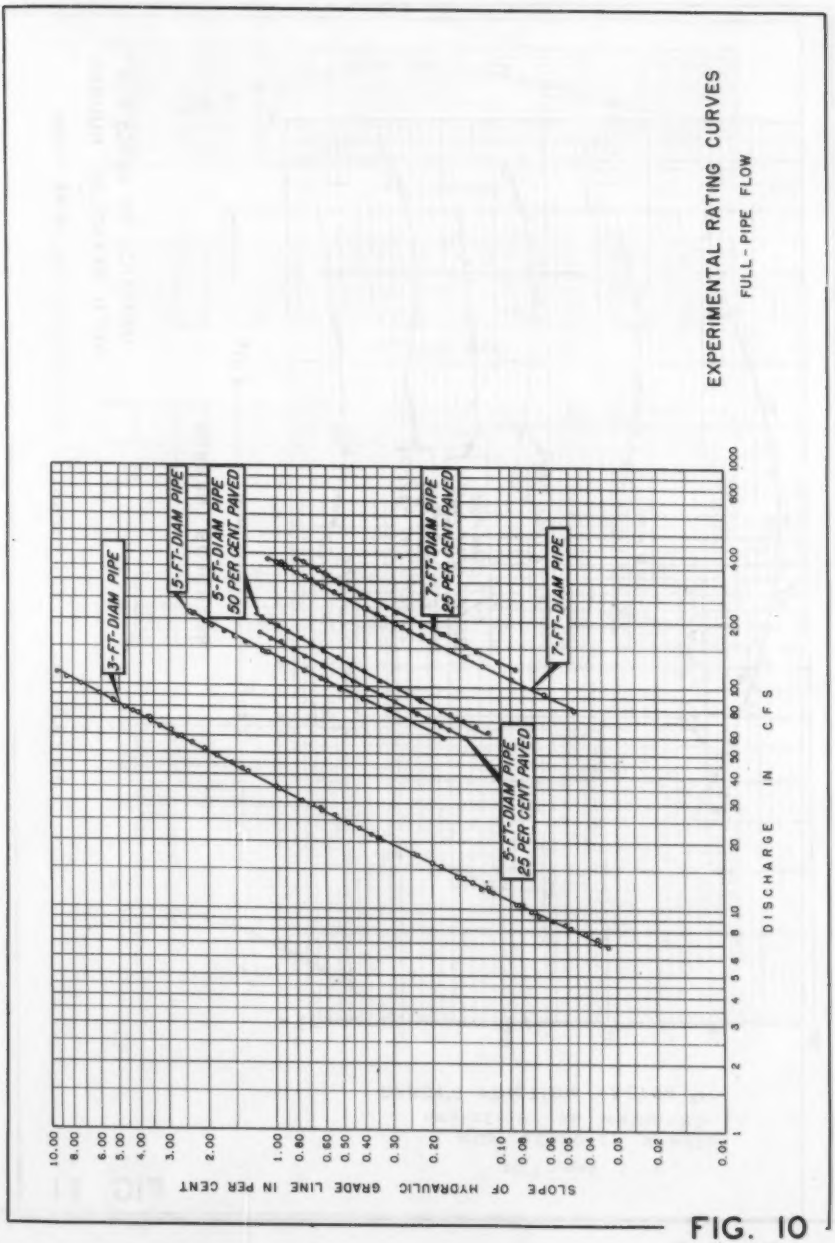
EXPERIMENTAL RATING CURVES
FULL-PIPE FLOW
SLOPE OF HYDRAULIC GRADE LINE IN PER CENT
DISCHARGE IN CFS
5-FT-DIAM PIPE
5-FT-DIAM PIPE
5-FT-DIAM PIPE 50 PER CENT PAVED
7-FT-DIAM PIPE 25 PER CENT PAVED
7-FT-DIAM PIPE
5-FT-DIAM PIPE 25 PER CENT PAVED

FIG. 10

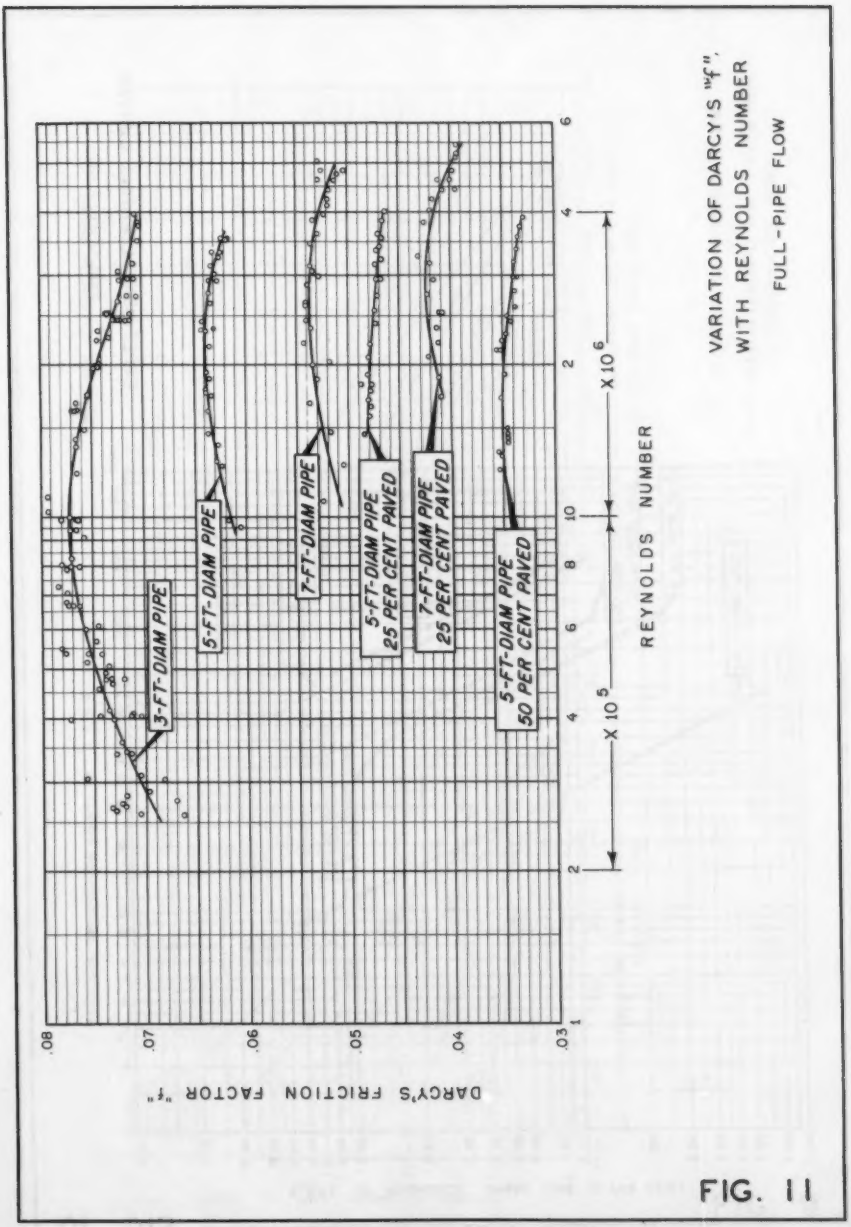
VARIATION OF DARCY'S "f",
WITH REYNOLDS NUMBER
FULL-PIPE FLOW
DARCY'S FRICTION FACTOR "f"
REYNOLDS NUMBER
X 10^5
X 10^6
3-FT-DIAM PIPE
5-FT-DIAM PIPE
7-FT-DIAM PIPE
5-FT-DIAM PIPE 25 PER CENT PAVED
7-FT-DIAM PIPE 25 PER CENT PAVED
5-FT-DIAM PIPE 50 PER CENT PAVED
.08
.07
.06
.05
.04
.03
2
4
6
8
10
1
2
4
6

FIG. 11

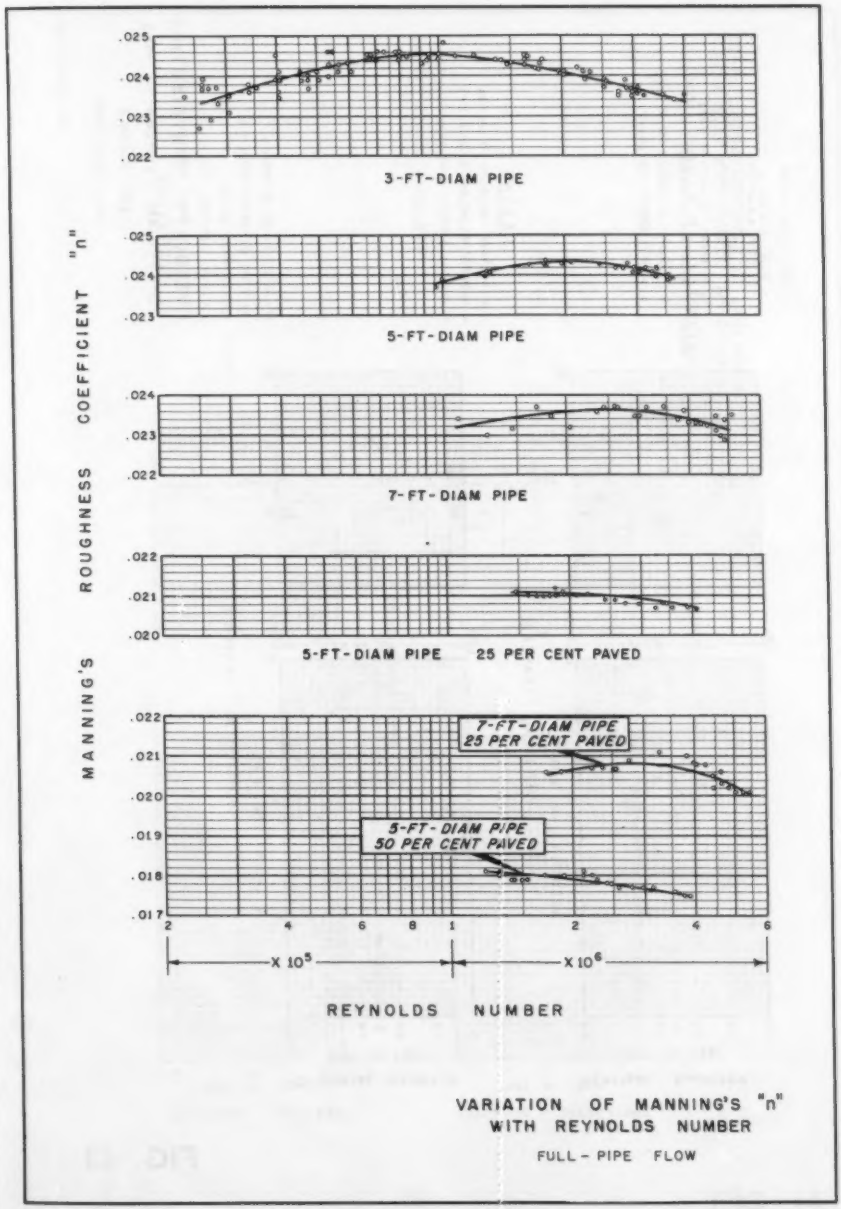


VARIATION OF MANNING'S "n"
WITH REYNOLDS NUMBER
FULL-PIPE FLOW

FIG. 12

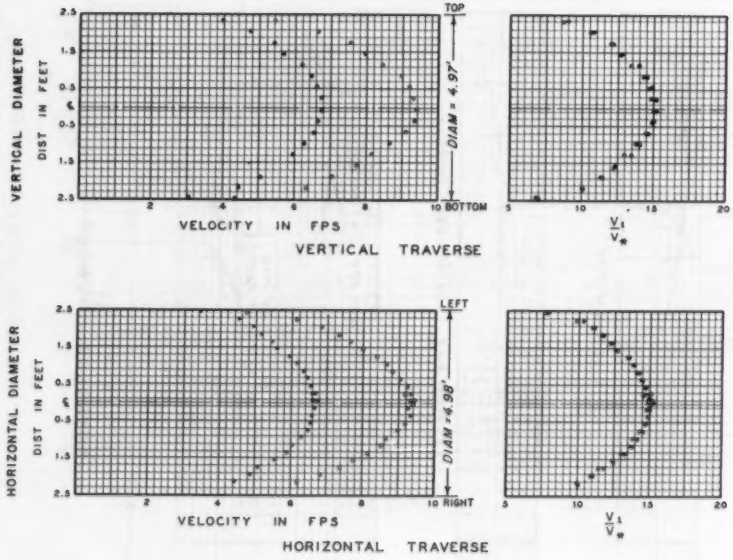


FIG. 13

VELOCITY DISTRIBUTION
5-FT- DIAM CORRUGATED PIPE
STA 2 + 46.3
FULL - PIPE FLOW

FILE M 40.2-11.1

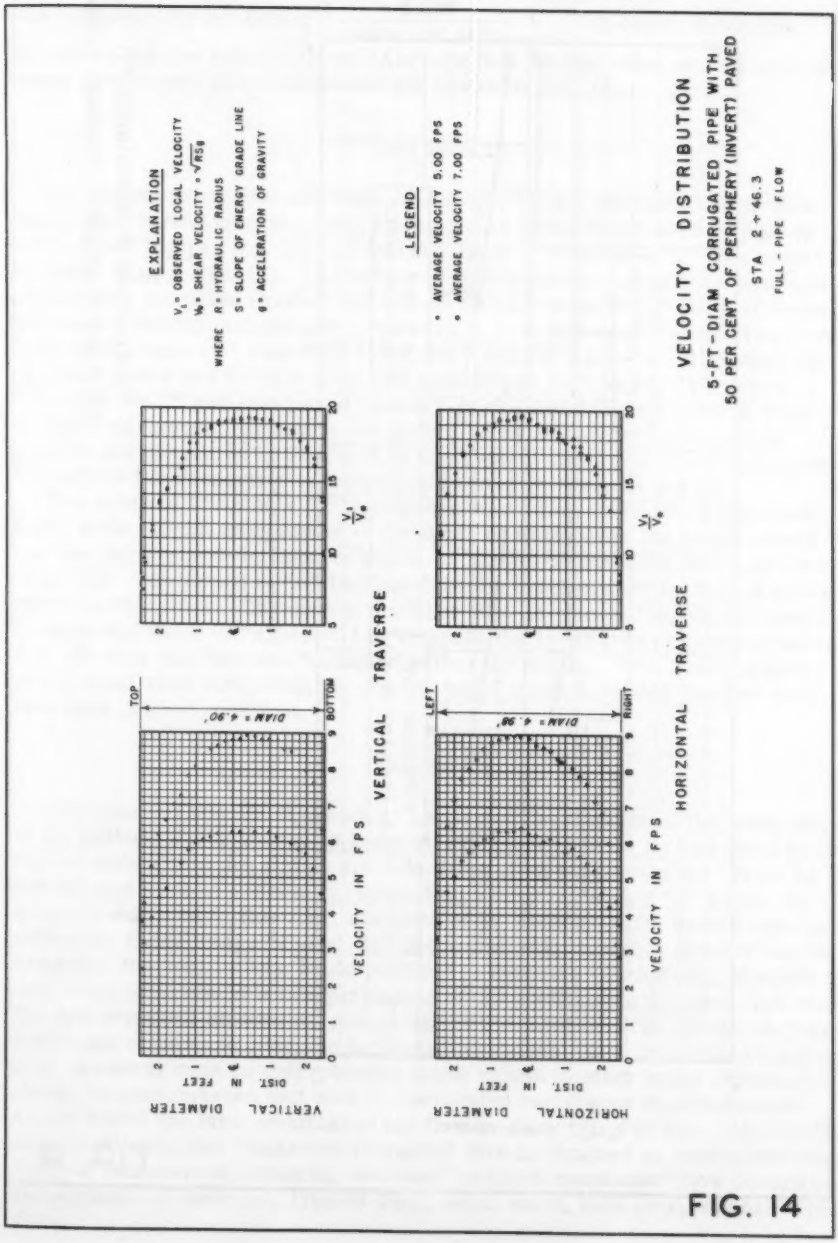
VELOCITY DISTRIBUTION
5-FT-DIAM CORRUGATED PIPE WITH
50 PER CENT OF PERIPHERY (INVERT) PAVED
STA 2+46.3
FULL-PIPE FLOW
EXPLANATION
$V_i$ = OBSERVED LOCAL VELOCITY
$V_*$ = SHEAR VELOCITY = $\sqrt{RSg}$
WHERE R = HYDRAULIC RADIUS
S = SLOPE OF ENERGY GRADE LINE
g = ACCELERATION OF GRAVITY
LEGEND
• AVERAGE VELOCITY 5.00 FPS
• AVERAGE VELOCITY 7.00 FPS
VERTICAL TRAVERSE
HORIZONTAL TRAVERSE
VELOCITY IN FPS
VERTICAL DIAMETER
HORIZONTAL DIAMETER
DIST. IN FEET
TOP
BOTTOM
LEFT
RIGHT
DIAM = 4.90'
$\frac{V_i}{V_*}$

FIG. 14

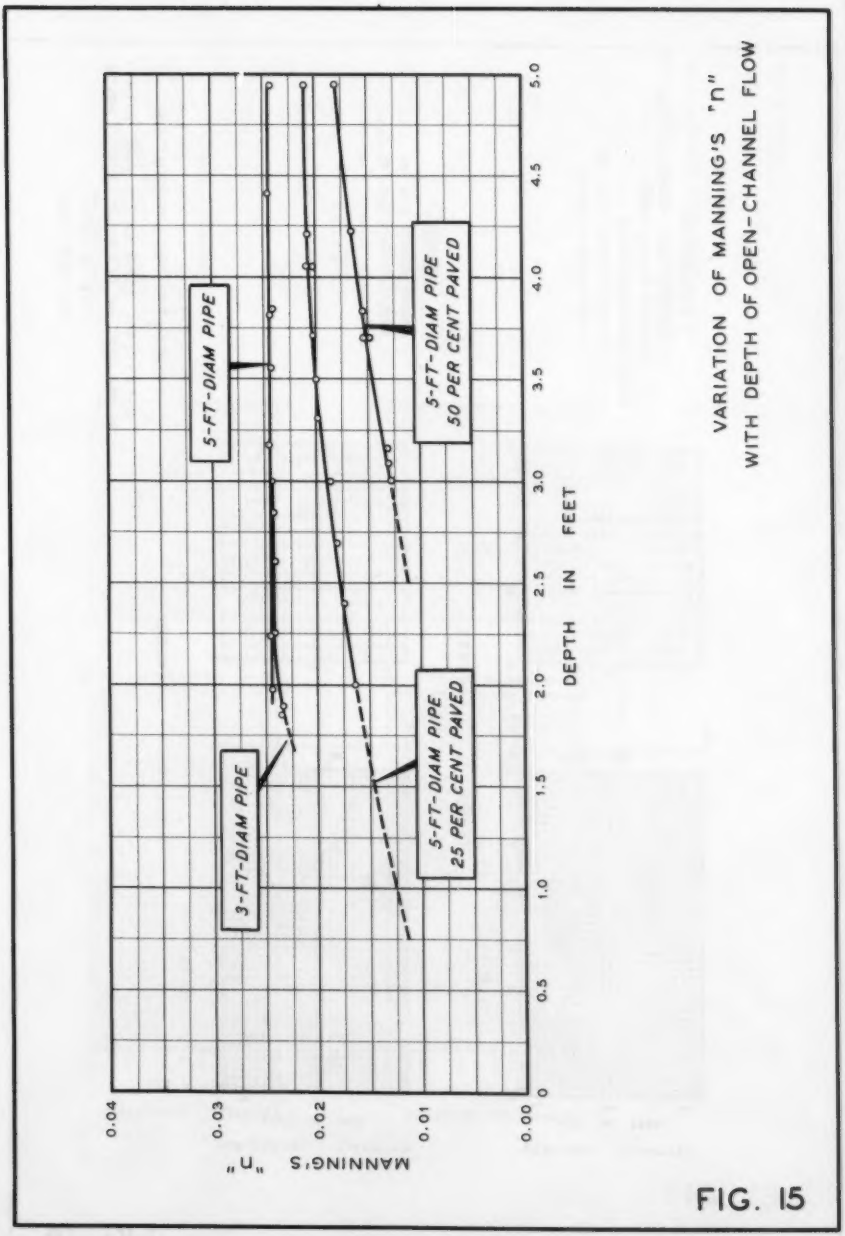
VARIATION OF MANNING'S "n"
WITH DEPTH OF OPEN-CHANNEL FLOW
MANNING'S "n"
0.04
0.03
0.02
0.01
0.00
DEPTH IN FEET
0
0.5
1.0
1.5
2.0
2.5
3.0
3.5
4.0
4.5
5.0
3-FT-DIAM PIPE
5-FT-DIAM PIPE
5-FT-DIAM PIPE
25 PER CENT PAVED
5-FT-DIAM PIPE
50 PER CENT PAVED

FIG. 15

0.005. The discharge quantities, as derived from the Manning formula, are proportional to the square root of the slope; therefore, measured discharges were adjusted by the factor $\left(\frac{0.005}{\text{measured slope}}\right)^{1/2}$ to obtain discharge quantities for the rating curves. Average flow depths, when plotted against these discharges, provided the curves shown in Fig. 16.

## Test Results

The tests showed that the value of Darcy's "f" for standard corrugated metal pipe varied inversely with the pipe size (from 0.077 for 3-ft pipe to 0.054 for 7-ft pipe; Fig. 11) and that the value of Manning's "n" was nearly constant (0.024; Fig. 12). The values of both coefficients for each pipe size varied with Reynolds number and reached a maximum within the test range. The invert paving reduced the resistance to flow and caused lower values for both coefficients ("f" values of 0.048 and 0.042 for the 5- and 7-ft pipes 25 per cent paved and 0.035 for the 5-ft pipe 50 per cent paved; "n" values of 0.021 for the 25 per cent paved 5- and 7-ft pipes and 0.018 for the 5-ft pipe 50 per cent paved). Values of the plotted points shown on the foregoing figures are presented in Tables A to G. Typical curves of velocity distribution within the respective test pipes are shown in Figs. 13 and 14.

The value of Manning's "n" for open-channel flow in standard pipe was found to be almost independent of the depth of water over the range tested and was approximately equal to the value (0.024) obtained for full-pipe flow (Fig. 15). The values of "n" increased as the depth of flow increased in the paved-invert pipes. The curves shown in Fig. 15 were extrapolated down to an assumed value of "n" = 0.011 to compute the lower parts of the curves in Fig. 16 when the flow was contained within the paving. This value is commonly used when computing the flow of water through welded steel or cast iron pipe in good condition.

## Discussion

The over-all results of the study confirmed the findings of the tests made at St. Anthony Falls Hydraulic Laboratory(3) that friction factors for a given size of corrugated metal pipe are a function of Reynolds number (Figs. 11 and 12) and were in general agreement on values of "f" and "n" within the scope of that study. However, the tests at St. Anthony Falls were concluded within the range where "f" and "n" increased with Reynolds number and implied that the coefficients would continue to increase indefinitely, whereas this study determined maximum values of the coefficients for each pipe size. From a practical standpoint, and except in the most critical situations, these maximum values are adequate for design purposes. In a theoretical application, however, such as extrapolating these values to other sizes of pipe, it should be remembered that flow in corrugated metal pipe does not necessarily follow the laws established for flow in other types of pipe. Morris(5) has established that "wake-interference" flow is obtained on corrugated surfaces of commercial conduits, whereas "isolated-roughness" flow occurs over the surfaces of concrete, riveted steel, wood-stave, cast-iron, and brick conduits.

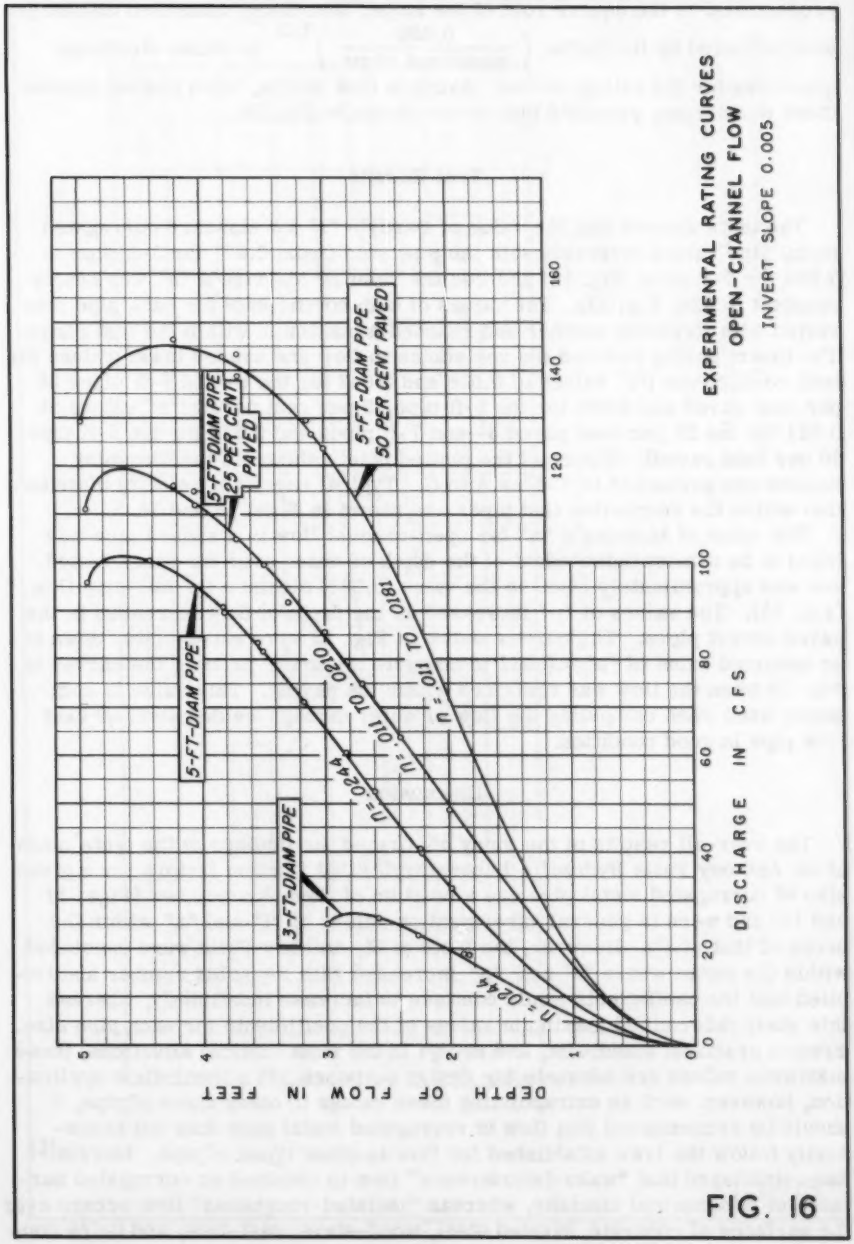
EXPERIMENTAL RATING CURVES
OPEN-CHANNEL FLOW
INVERT SLOPE 0.005
DISCHARGE IN CFS
DEPTH OF FLOW IN FEET
0
20
40
60
80
100
120
140
160
1
2
3
4
5
5-FT-DIAM PIPE
50 PER CENT PAVED
5-FT-DIAM PIPE
25 PER CENT PAVED
5-FT-DIAM PIPE
3-FT-DIAM PIPE
n = .011 TO .0181
n = .010 TO .0120
n = .020 TO .024
n = .024

FIG. 16

TABLE A

SUMMARY OF TEST RESULTS
FULL-PIPE FLOW

3-FT-DIAM CORRUGATED PIPE

| V (FPS) (1) | Q (CFS) (2) | S (%) (3) | Water Temp (Deg. Fah) (4) | Re $X10^{-3}$ (5) | f (6) | n (7) |
|---|---|---|---|---|---|---|
| 0.95 | 6.72 | 0.0331 | 66.1 | 258 | 0.0706 | 0.0235 |
| 0.96 | 6.81 | .0351 | 66.1 | 261 | .0730 | .0238 |
| 0.97 | 6.89 | .0360 | 66.1 | 264 | .0732 | .0239 |
| 0.98 | 6.95 | .0360 | 70.3 | 281 | .0720 | .0237 |
| 0.98 | 6.95 | .0360 | 66.1 | 267 | .0720 | .0237 |
| 0.99 | 7.05 | .0370 | 68.2 | 270 | .0723 | .0237 |
| 1.04 | 7.33 | .0370 | 60.1 | 257 | .0663 | .0227 |
| 1.10 | 7.75 | .0419 | 60.4 | 273 | .0671 | .0229 |
| 1.16 | 8.20 | .0487 | 59.5 | 285 | .0698 | .0233 |
| 1.21 | 8.54 | .0516 | 60.4 | 301 | .0682 | .0231 |
| 1.24 | 8.75 | .0560 | 59.8 | 305 | .0706 | .0235 |
| 1.26 | 8.88 | .0584 | 66.4 | 340 | .0715 | .0236 |
| 1.31 | 9.26 | .0672 | 55.0 | 301 | .0758 | .0243 |
| 1.36 | 9.63 | .0701 | 60.4 | 339 | .0729 | .0238 |
| 1.38 | 9.75 | .0711 | 59.8 | 341 | .0720 | .0237 |
| 1.48 | 10.45 | .0818 | 58.3 | 357 | .0723 | .0237 |
| 1.48 | 10.45 | .0799 | 66.1 | 401 | .0705 | .0235 |
| 1.48 | 10.45 | .0847 | 66.1 | 401 | .0747 | .0241 |
| 1.48 | 10.45 | .0808 | 66.1 | 401 | .0713 | .0236 |
| 1.48 | 10.45 | .0828 | 66.5 | 399 | .0731 | .0239 |
| 1.48 | 10.45 | .0808 | 66.7 | 402 | .0713 | .0236 |
| 1.69 | 11.96 | .1091 | 59.0 | 413 | .0735 | .0239 |
| 1.73 | 12.26 | .1208 | 55.0 | 399 | .0774 | .0245 |
| 1.73 | 12.20 | .1130 | 66.7 | 469 | .0732 | .0239 |
| 1.75 | 12.35 | .1169 | 66.2 | 475 | .0739 | .0240 |
| 1.75 | 12.35 | .1159 | 66.4 | 475 | .0733 | .0239 |
| 1.77 | 12.51 | .1169 | 66.4 | 479 | .0720 | .0237 |
| 1.86 | 13.14 | .1334 | 59.1 | 454 | .0746 | .0241 |
| 1.95 | 13.78 | .1461 | 67.0 | 532 | .0742 | .0240 |
| 1.97 | 13.93 | .1568 | 68.5 | 549 | .0790 | .0246 |
| 1.97 | 13.94 | .1568 | 66.1 | 535 | .0778 | .0246 |
| 1.97 | 13.94 | .1519 | 66.1 | 533 | .0754 | .0243 |
| 1.97 | 13.96 | .1509 | 70.3 | 564 | .0748 | .0241 |
| 2.20 | 15.52 | .1840 | 55.0 | 505 | .0736 | .0239 |
| 2.27 | 16.02 | .2016 | 60.1 | 562 | .0758 | .0243 |
| 2.44 | 17.22 | .2347 | 66.3 | 662 | .0763 | .0244 |
| 2.46 | 17.42 | .2435 | 66.2 | 666 | .0774 | .0245 |
| 2.47 | 17.44 | .2444 | 66.7 | 671 | .0775 | .0245 |
| 2.47 | 17.44 | .2405 | 66.5 | 670 | .0762 | .0244 |
| 2.47 | 17.49 | .2405 | 58.3 | 598 | .0758 | .0243 |

TABLE A - CONTINUED

| (1) | (2) | (3) | (4) | (5) | (6) | (7) |
|---|---|---|---|---|---|---|
| 2.51 | 17.72 | .2425 | 58.6 | 609 | .0745 | .0241 |
| 2.95 | 20.84 | .3515 | 66.2 | 800 | .0780 | .0246 |
| 2.95 | 20.84 | .3476 | 66.2 | 797 | .0772 | .0245 |
| 2.95 | 20.82 | .3467 | 68.5 | 821 | .0771 | .0245 |
| 2.96 | 20.93 | .3525 | 57.2 | 703 | .0776 | .0246 |
| 3.05 | 21.57 | .3778 | 57.0 | 724 | .0783 | .0246 |
| 3.26 | 23.07 | .4217 | 59.0 | 796 | .0764 | .0244 |
| 3.26 | 23.03 | .4275 | 58.3 | 788 | .0777 | .0246 |
| 3.45 | 24.42 | .4752 | 66.2 | 933 | .0768 | .0244 |
| 3.45 | 24.42 | .4781 | 66.2 | 937 | .0773 | .0245 |
| 3.72 | 26.32 | .5453 | 59.0 | 908 | .0759 | .0243 |
| 3.94 | 27.88 | .6213 | 68.5 | 1099 | .0771 | .0245 |
| 4.01 | 28.31 | .6388 | 68.5 | 987 | .0768 | .0244 |
| 4.12 | 29.15 | .6817 | 58.5 | 999 | .0773 | .0245 |
| 4.31 | 30.46 | .7654 | 57.2 | 1024 | .0794 | .0248 |
| 4.92 | 34.77 | .9611 | 68.5 | 1371 | .0766 | .0244 |
| 4.98 | 35.24 | .9932 | 59.0 | 1216 | .0771 | .0245 |
| 5.86 | 41.41 | 1.365 | 58.8 | 1427 | .0767 | .0244 |
| 5.87 | 41.48 | 1.369 | 70.3 | 1673 | .0767 | .0244 |
| 6.01 | 42.44 | 1.418 | 60.4 | 1495 | .0759 | .0243 |
| 6.37 | 45.04 | 1.589 | 66.2 | 1728 | .0755 | .0242 |
| 6.37 | 45.04 | 1.588 | 68.2 | 1730 | .0755 | .0242 |
| 6.81 | 48.16 | 1.845 | 57.2 | 1618 | .0770 | .0245 |
| 6.82 | 48.19 | 1.853 | 57.0 | 1617 | .0769 | .0245 |
| 6.82 | 48.24 | 1.851 | 57.0 | 1618 | .0767 | .0244 |
| 6.86 | 48.49 | 1.826 | 70.2 | 1956 | .0749 | .0241 |
| 7.36 | 52.03 | 2.095 | 66.2 | 1998 | .0746 | .0241 |
| 7.36 | 52.03 | 2.092 | 67.1 | 1989 | .0745 | .0241 |
| 7.85 | 55.49 | 2.374 | 70.3 | 2239 | .0743 | .0241 |
| 8.35 | 59.03 | 2.646 | 67.0 | 2281 | .0732 | .0239 |
| 8.41 | 59.44 | 2.725 | 57.3 | 2002 | .0744 | .0241 |
| 8.41 | 59.48 | 2.722 | 57.3 | 2003 | .0742 | .0240 |
| 8.81 | 62.28 | 2.961 | 70.5 | 2522 | .0736 | .0239 |
| 9.32 | 65.87 | 3.307 | 66.2 | 2530 | .0735 | .0239 |
| 9.32 | 65.86 | 3.302 | 66.2 | 2518 | .0734 | .0239 |
| 9.78 | 69.17 | 3.637 | 70.4 | 2816 | .0733 | .0239 |
| 9.81 | 69.37 | 3.616 | 67.1 | 2680 | .0725 | .0238 |
| 9.98 | 70.52 | 3.732 | 59.7 | 2459 | .0724 | .0237 |
| 10.51 | 74.33 | 4.128 | 57.6 | 2513 | .0721 | .0237 |
| 10.78 | 76.20 | 4.354 | 70.3 | 3074 | .0723 | .0237 |
| 10.82 | 76.23 | 4.360 | 67.1 | 2952 | .0723 | .0237 |
| 11.01 | 77.84 | 4.494 | 60.4 | 2741 | .0715 | .0236 |
| 11.10 | 78.44 | 4.736 | 49.1 | 2336 | .0742 | .0241 |
| 11.95 | 84.48 | 5.229 | 54.8 | 2741 | .0707 | .0235 |
| 11.99 | 84.72 | 5.318 | 60.3 | 2982 | .0714 | .0236 |
| 12.10 | 85.52 | 5.381 | 59.5 | 2975 | .0709 | .0235 |
| 12.88 | 91.04 | 6.095 | 60.0 | 3188 | .0709 | .0235 |
| 14.25 | 100.73 | 7.419 | 59.6 | 3507 | .0705 | .0235 |
| 15.37 | 108.68 | 8.607 | 60.3 | 3822 | .0703 | .0234 |
| 15.39 | 108.78 | 8.610 | 59.6 | 3874 | .0702 | .0234 |
| 16.13 | 114.00 | 9.513 | 60.0 | 3998 | .0706 | .0235 |

TABLE B

SUMMARY OF TEST RESULTS
FULL-PIPE FLOW

5-FT-DIAM CORRUGATED PIPE

| V (FPS) | Q (CFS) | S (%) | Water Temp (Deg. Fah) | Re $X10^{-3}$ | f | n |
|---|---|---|---|---|---|---|
| 3.07 | 59.1 | 0.18 | 44.0 | 978 | 0.0618 | 0.0239 |
| 4.06 | 78.1 | .32 | 44.0 | 1291 | .0628 | .0241 |
| 4.56 | 87.8 | .42 | 44.0 | 1452 | .0638 | .0243 |
| 5.08 | 97.8 | .52 | 44.0 | 1618 | .0637 | .0243 |
| 5.46 | 105.1 | .60 | 44.4 | 1753 | .0638 | .0243 |
| 5.61 | 108.0 | .63 | 44.0 | 1786 | .0639 | .0243 |
| 6.12 | 117.9 | .75 | 44.0 | 1949 | .0638 | .0243 |
| 6.81 | 131.0 | .93 | 44.5 | 2181 | .0636 | .0242 |
| 7.39 | 142.2 | 1.08 | 44.5 | 2368 | .0631 | .0241 |
| 7.54 | 145.2 | 1.15 | 44.5 | 2416 | .0642 | .0243 |
| 7.40 | 142.4 | 1.11 | 44.0 | 2356 | .0644 | .0244 |
| 8.28 | 159.4 | 1.37 | 44.0 | 2636 | .0635 | .0242 |
| 8.76 | 168.6 | 1.53 | 44.0 | 2788 | .0636 | .0242 |
| 9.24 | 177.8 | 1.70 | 44.0 | 2942 | .0635 | .0242 |
| 9.86 | 189.8 | 1.93 | 44.0 | 3139 | .0633 | .0242 |
| 10.28 | 197.7 | 2.10 | 45.0 | 3324 | .0632 | .0242 |
| 10.28 | 197.7 | 2.07* | 45.0 | 3324 | .0625 | .0240 |
| 11.01 | 211.9 | 2.37 | 45.0 | 3562 | .0622 | .0240 |
| 11.01 | 211.9 | 2.35* | 45.0 | 3562 | .0617 | .0239 |
| 3.02 | 58.0 | .17* | 43.5 | 953 | .0606 | .0237 |
| 3.96 | 76.2 | .31* | 43.5 | 1252 | .0625 | .0240 |
| 4.40 | 84.7 | .38* | 43.5 | 1390 | .0628 | .0241 |
| 5.52 | 106.2 | .61* | 43.5 | 1743 | .0634 | .0242 |
| 5.91 | 113.8 | .70* | 43.5 | 1868 | .0636 | .0242 |
| 7.40 | 142.3 | 1.10* | 43.5 | 2336 | .0640 | .0243 |
| 9.30 | 178.9 | 1.70* | 43.5 | 2936 | .0628 | .0241 |
| 9.53 | 183.3 | 1.80* | 43.5 | 3009 | .0630 | .0241 |
| 10.39 | 199.9 | 2.13* | 43.5 | 3282 | .0627 | .0241 |
| 11.15 | 214.5 | 2.42* | 43.5 | 3521 | .0619 | .0239 |

* Head loss measured with static tubes.

TABLE C

SUMMARY OF TEST RESULTS
FULL-PIPE FLOW

5-FT-DIAM CORRUGATED PIPE
WITH 25 PER CENT OF PERIPHERY (INVERT) PAVED

| V (FPS) | Q (CFS) | S (%) | Water Temp (Deg. Fah) | $Re_{X10^{-3}}$ | f | n |
|---|---|---|---|---|---|---|
| 3.08 | 59.3 | 0.143 | 71.0 | 1464 | 0.0482 | 0.0211 |
| 3.32 | 63.9 | .166 | 70.5 | 1570 | .0479 | .0210 |
| 3.47 | 66.8 | .180 | 71.0 | 1651 | .0478 | .0210 |
| 3.59 | 69.1 | .194 | 71.0 | 1709 | .0480 | .0210 |
| 3.73 | 71.8 | .209 | 71.0 | 1770 | .0479 | .0210 |
| 3.89 | 74.9 | .232 | 71.0 | 1842 | .0489 | .0212 |
| 3.91 | 75.2 | .231 | 71.0 | 1843 | .0477 | .0210 |
| 4.00 | 77.0 | .242 | 71.0 | 1904 | .0481 | .0211 |
| 4.40 | 84.7 | .292 | 70.5 | 2074 | .0480 | .0210 |
| 4.71 | 90.6 | .334 | 70.5 | 2200 | .0479 | .0210 |
| 5.08 | 97.8 | .387 | 71.0 | 2413 | .0473 | .0209 |
| 5.47 | 105.3 | .446 | 70.5 | 2579 | .0474 | .0209 |
| 5.80 | 111.6 | .498 | 70.0 | 2726 | .0471 | .0208 |
| 6.24 | 120.1 | .572 | 71.0 | 2967 | .0468 | .0208 |
| 6.38 | 122.8 | .603 | 70.0 | 2984 | .0472 | .0208 |
| 6.91 | 133.0 | .698 | 70.0 | 3233 | .0466 | .0207 |
| 7.00 | 134.7 | .727 | 68.0 | 3193 | .0472 | .0209 |
| 7.06 | 135.9 | .737 | 72.0 | 3393 | .0471 | .0208 |
| 7.41 | 142.6 | .804 | 72.0 | 3561 | .0466 | .0207 |
| 7.48 | 143.9 | .825 | 68.0 | 3412 | .0469 | .0208 |
| 7.98 | 153.6 | .940 | 68.0 | 3640 | .0470 | .0208 |
| 8.46 | 162.9 | 1.048 | 68.0 | 3859 | .0466 | .0207 |
| 8.97 | 172.6 | 1.168 | 68.0 | 4090 | .0463 | .0207 |

A summary of recommended values of friction and roughness coefficients for use with corrugated metal pipes flowing full is presented in Fig. 17, in which the "n" curve for unpaved pipe was extrapolated to include pipes of from 1 to 10 ft in diameter, and values for the "f" curve were computed from values of "n." Points from the tests at St. Anthony Falls (1.5-, 2-, and 3-ft pipes) are included to show the validity of the curves for pipes of smaller diameter than those tested during the present study. The values for "n" show a slight decrease for pipes of large diameter — the over-all change between 1- and 10-ft diameters is from 0.025 to 0.023, whereas "f" values decline sharply from 0.117 for 1-ft-diam pipe to 0.046 for 10-ft-diam pipe. Parallel curves for the 25 per cent paved pipe are shown, in which "n" equals approximately 0.021 and "f" varies from 0.053 to 0.038 for pipes 4 and 8 ft in diameter, respectively. No curves are shown for 50 per cent paved pipe because

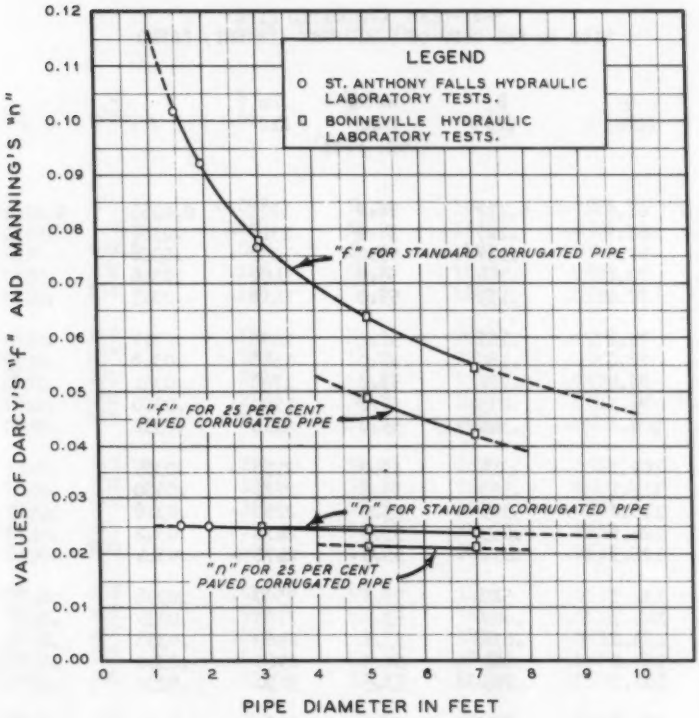


Variation of Darcy's "f" and Manning's "n" with pipe diameter for corrugated metal pipes flowing full (maximum values are shown)

FIG. 17

TABLE D

SUMMARY OF TEST RESULTS
FULL-PIPE FLOW

5-FT-DIAM CORRUGATED PIPE
WITH 50 PER CENT OF PERIPHERY (INVERT) PAVED

| V (FPS) | Q (CFS) | S (%) | Water Temp (Deg. Fah) | Re $X10^{-3}$ | f | n |
|---|---|---|---|---|---|---|
| 3.18 | 61.2 | 0.112 | 56.0 | 1224 | 0.0354 | 0.0181 |
| 3.42 | 65.9 | .129 | 56.0 | 1318 | .0351 | .0180 |
| 3.51 | 67.6 | .137 | 55.0 | 1332 | .0356 | .0181 |
| 3.64 | 70.0 | .144 | 56.0 | 1402 | .0346 | .0179 |
| 3.74 | 72.0 | .153 | 55.0 | 1418 | .0347 | .0179 |
| 3.88 | 74.6 | .165 | 56.0 | 1495 | .0349 | .0179 |
| 4.06 | 78.0 | .180 | 55.0 | 1540 | .0348 | .0179 |
| 4.49 | 86.4 | .222 | 55.0 | 1700 | .0351 | .0180 |
| 5.00 | 96.1 | .275 | 55.0 | 1900 | .0350 | .0180 |
| 5.55 | 106.8 | .340 | 55.0 | 2110 | .0352 | .0180 |
| 5.56 | 107.1 | .344 | 55.0 | 2110 | .0355 | .0181 |
| 5.98 | 115.1 | .393 | 53.5 | 2220 | .0350 | .0180 |
| 6.02 | 115.8 | .395 | 55.0 | 2280 | .0348 | .0179 |
| 6.49 | 124.9 | .453 | 53.5 | 2410 | .0342 | .0178 |
| 6.51 | 125.3 | .457 | 55.0 | 2470 | .0344 | .0178 |
| 6.99 | 134.5 | .520 | 53.5 | 2590 | .0338 | .0177 |
| 7.52 | 144.7 | .602 | 53.5 | 2790 | .0339 | .0177 |
| 7.98 | 153.6 | .675 | 53.5 | 2960 | .0338 | .0177 |
| 8.00 | 154.0 | .684 | 54.0 | 2960 | .0340 | .0177 |
| 8.48 | 163.1 | .765 | 53.5 | 3140 | .0339 | .0177 |
| 9.07 | 174.6 | .869 | 53.5 | 3360 | .0336 | .0176 |
| 9.58 | 184.3 | .965 | 53.5 | 3550 | .0335 | .0176 |
| 10.07 | 193.9 | 1.057 | 53.5 | 3740 | .0332 | .0175 |
| 10.50 | 202.1 | 1.142 | 53.5 | 3880 | .0330 | .0175 |

only one size was tested; for 5-ft pipe the values of "n" = 0.018 and "f" = 0.035 are recommended.

It was recognized that several factors might have affected the accuracy of the test results. Perhaps the most important of these factors involved the practice of calibrating successively larger orifice meters against several smaller ones. However, every known precaution was taken to ensure that all orifices were rated and used correctly and that they were kept in perfect condition throughout the course of the study. In addition, the random nature of the test pipes prevented an exact study of flow characteristics. For example, a 6-ft-long straight-edge laid along the inside of the respective pipes often revealed that one or two adjacent corrugations extended as much as 3/4 in. farther into the pipes than did the rest. Such inequalities within the test pipes probably had no significant effect on friction or roughness coefficients,

TABLE E

SUMMARY OF TEST RESULTS
FULL-PIPE FLOW

7-FT-DIAM CORRUGATED PIPE

| V (FPS) | Q (CFS) | S (%) | Water Temp (Deg. Fah) | Re $X10^{-3}$ | f | n |
|---|---|---|---|---|---|---|
| 2.01 | 78.5 | 0.047 | 54.0 | 1071 | 0.0526 | 0.0234 |
| 2.39 | 93.5 | .064 | 54.0 | 1275 | .0507 | .0230 |
| 2.79 | 109.0 | .089 | 54.0 | 1487 | .0519 | .0232 |
| 3.18 | 124 | .120 | 54.0 | 1691 | .0539 | .0237 |
| 3.53 | 138 | .146 | 54.0 | 1882 | .0531 | .0235 |
| 3.82 | 149 | .167 | 54.0 | 2032 | .0519 | .0232 |
| 4.15 | 162 | .207 | 54.0 | 2210 | .0545 | .0238 |
| 4.38 | 171 | .227 | 55.5 | 2386 | .0537 | .0236 |
| 4.61 | 180 | .253 | 54.0 | 2455 | .0541 | .0237 |
| 4.82 | 188 | .277 | 55.5 | 2624 | .0541 | .0237 |
| 4.94 | 193 | .291 | 54.0 | 2632 | .0541 | .0237 |
| 5.30 | 207 | .335 | 55.5 | 2889 | .0540 | .0237 |
| 5.51 | 215 | .354 | 55.5 | 3000 | .0529 | .0235 |
| 5.76 | 225 | .394 | 55.5 | 3140 | .0538 | .0237 |
| 5.84 | 228 | .402 | 53.5 | 3084 | .0535 | .0236 |
| 6.61 | 258 | .517 | 53.5 | 3490 | .0537 | .0237 |
| 6.86 | 268 | .550 | 53.5 | 3625 | .0530 | .0235 |
| 7.30 | 285 | .626 | 53.5 | 3855 | .0533 | .0236 |
| 7.56 | 295 | .659 | 53.3 | 3990 | .0523 | .0233 |
| 7.81 | 304 | .699 | 53.5 | 4125 | .0520 | .0233 |
| 8.07 | 315 | .748 | 53.5 | 4261 | .0520 | .0233 |
| 8.40 | 328 | .808 | 53.5 | 4437 | .0519 | .0232 |
| 8.73 | 341 | .862 | 53.5 | 4612 | .0513 | .0231 |
| 8.81 | 344 | .905 | 53.0 | 4622 | .0529 | .0235 |
| 9.04 | 353 | .919 | 53.5 | 4775 | .0510 | .0230 |
| 9.25 | 361 | .950 | 53.5 | 4883 | .0503 | .0229 |
| 9.27 | 362 | .997 | 53.0 | 4864 | .0526 | .0234 |
| 9.68 | 378 | 1.094 | 53.0 | 5079 | .0529 | .0235 |

TABLE F

SUMMARY OF TEST RESULTS
FULL-PIPE FLOW

7-FT-DIAM CORRUGATED PIPE
WITH 25 PER CENT OF PERIPHERY (INVERT) PAVED

| V (FPS) | Q (CFS) | S (%) | Water Temp (Deg. Fah) | Re $X10^{-3}$ | f | n |
|---|---|---|---|---|---|---|
| 3.06 | 120 | 0.085 | 57.5 | 1727 | 0.0410 | 0.0206 |
| 3.35 | 131 | .102 | 57.5 | 1885 | .0411 | .0206 |
| 3.68 | 144 | .126 | 57.5 | 2072 | .0421 | .0209 |
| 3.94 | 154 | .141 | 57.5 | 2216 | .0412 | .0207 |
| 4.17 | 163 | .158 | 58.5 | 2374 | .0413 | .0207 |
| 4.44 | 173 | .178 | 58.5 | 2519 | .0410 | .0206 |
| 4.48 | 175 | .181 | 57.5 | 2518 | .0409 | .0206 |
| 4.87 | 190 | .222 | 58.5 | 2767 | .0424 | .0209 |
| 5.19 | 202 | .247 | 58.5 | 2942 | .0416 | .0208 |
| 5.60 | 219 | .291 | 58.5 | 3189 | .0420 | .0208 |
| 5.79 | 226 | .318 | 58.5 | 3291 | .0431 | .0211 |
| 6.69 | 261 | .421 | 58.5 | 3801 | .0426 | .0210 |
| 7.10 | 277 | .467 | 58.5 | 4034 | .0420 | .0208 |
| 7.52 | 293 | .521 | 58.5 | 4267 | .0418 | .0208 |
| 7.75 | 303 | .540 | 58.5 | 4413 | .0408 | .0205 |
| 7.86 | 307 | .540 | 57.5 | 4417 | .0396 | .0202 |
| 8.11 | 317 | .596 | 58.5 | 4616 | .0411 | .0206 |
| 8.26 | 323 | .602 | 57.5 | 4648 | .0400 | .0203 |
| 8.58 | 335 | .644 | 57.5 | 4820 | .0397 | .0202 |
| 8.93 | 349 | .693 | 57.5 | 5016 | .0394 | .0201 |
| 9.30 | 363 | .750 | 57.5 | 5223 | .0393 | .0201 |
| 9.62 | 376 | .802 | 57.5 | 5410 | .0393 | .0201 |

but their presence would explain the nonuniform distribution of flow that sometimes was evident in the velocity traverses.

## CONCLUSIONS

The results of the study indicate that a closed correlation existed between Reynolds number and both Darcy's friction coefficient "f" and Manning's roughness coefficient "n" throughout the range of experimental discharges reproduced for study. The following values of Manning's coefficient "n" were obtained from tests on standard and paved-invert corrugated metal pipes flowing full:

TABLE G

SUMMARY OF TEST RESULTS
OPEN-CHANNEL FLOW

| Q (CFS) | D (FT) | R (FT) | A (SQ FT) | V (FPS) | S (%) | Water Temp (Deg. Fah) | Re $X10^{-3}$ | n |
|---|---|---|---|---|---|---|---|---|
| **3-FT-DIAM CORRUGATED PIPE** | | | | | | | | |
| 18.26 | 1.86 | 0.846 | 4.61 | 3.96 | 0.490 | 68.8 | 1251 | .0235 |
| 19.50 | 1.90 | 0.852 | 4.71 | 4.14 | 0.526 | 63.7 | 1229 | .0234 |
| 23.01 | 2.25 | 0.903 | 5.67 | 4.06 | 0.510 | 61.2 | 1229 | .0244 |
| 25.93 | 2.59 | 0.907 | 6.49 | 4.00 | 0.491 | 66.3 | 1310 | .0244 |
| 25.00* | 3.00* | 0.750* | 7.07* | 3.54* | 0.500* | 62.0* | 925* | .0244* |
| **5-FT-DIAM CORRUGATED PIPE** | | | | | | | | |
| 32.7 | 1.98 | 1.06 | 7.2 | 4.54 | 0.513 | 48.0 | 1365 | .0244 |
| 39.9 | 2.24 | 1.16 | 8.5 | 4.69 | 0.500 | 48.0 | 1552 | .0245 |
| 41.4 | 2.25 | 1.16 | 8.5 | 4.87 | 0.519 | 48.0 | 1602 | .0244 |
| 52.5 | 2.61 | 1.28 | 10.3 | 5.10 | 0.500 | 48.0 | 1849 | .0242 |
| 60.2 | 2.85 | 1.34 | 11.4 | 5.28 | 0.500 | 49.0 | 2006 | .0243 |
| 71.2 | 3.18 | 1.42 | 13.1 | 5.44 | 0.504 | 50.0 | 2193 | .0245 |
| 83.2 | 3.56 | 1.48 | 14.8 | 5.62 | 0.500 | 50.0 | 2360 | .0243 |
| 91.0 | 3.82 | 1.50 | 16.0 | 5.69 | 0.513 | 50.0 | 2427 | .0244 |
| 90.9 | 3.84 | 1.50 | 16.0 | 5.68 | 0.500 | 53.0 | 2414 | .0243 |
| 100.4 | 4.42 | 1.48 | 18.1 | 5.55 | 0.500 | 53.0 | 2324 | .0246 |
| 96.2* | 4.95* | 1.24* | 19.2* | 5.01* | 0.500* | 44.0* | 1630* | .0243* |
| **5-FT-DIAM CORRUGATED PIPE WITH 25 PER CENT OF PERIPHERY (INVERT) PAVED** | | | | | | | | |
| 30.64 | 2.00 | 1.07 | 7.29 | 4.20 | 0.200 | 63.0 | 1547 | .0165 |
| 40.15 | 2.40 | 1.21 | 9.25 | 4.34 | 0.200 | 63.0 | 1808 | .0174 |
| 47.24 | 2.70 | 1.31 | 10.73 | 4.40 | 0.200 | 63.0 | 1984 | .0180 |
| 53.80 | 3.00 | 1.38 | 12.20 | 4.41 | 0.200 | 64.0 | 2095 | .0187 |
| 58.46 | 3.31 | 1.45 | 13.67 | 4.48 | 0.200 | 64.0 | 2236 | .0198 |
| 62.84 | 3.50 | 1.47 | 14.53 | 4.33 | 0.200 | 64.5 | 2191 | .0199 |
| 66.35 | 3.72 | 1.50 | 15.53 | 4.27 | 0.200 | 64.5 | 2205 | .0203 |
| 70.65 | 4.06 | 1.51 | 16.88 | 4.19 | 0.200 | 65.0 | 2178 | .0208 |
| 72.61 | 4.06 | 1.51 | 16.88 | 4.30 | 0.200 | 65.5 | 2235 | .0203 |
| 73.40 | 4.22 | 1.50 | 17.49 | 4.20 | 0.200 | 64.0 | 2169 | .0207 |
| 70.2* | 4.95* | 1.24* | 19.24* | 3.65* | 0.200* | 71.0* | 1555* | .0210* |
| **5-FT-DIAM CORRUGATED PIPE WITH 50 PER CENT OF PERIPHERY (INVERT) PAVED** | | | | | | | | |
| 76.8 | 3.01 | 1.38 | 12.25 | 6.27 | 0.192 | 48.0 | 2380 | .0128 |
| 78.0 | 3.17 | 1.42 | 13.00 | 6.07 | 0.180 | 49.0 | 2380 | .0131 |
| 78.2 | 3.09 | 1.40 | 12.63 | 6.19 | 0.190 | 48.0 | 2360 | .0131 |
| 87.1 | 3.71 | 1.50 | 15.50 | 5.62 | 0.185 | 49.0 | 2340 | .0148 |
| 87.9 | 3.71 | 1.50 | 15.50 | 5.67 | 0.200 | 49.0 | 2360 | .0153 |
| 88.1 | 3.84 | 1.51 | 16.00 | 5.50 | 0.190 | 49.0 | 2300 | .0155 |
| 91.3 | 4.23 | 1.50 | 17.50 | 5.21 | 0.194 | 50.0 | 2220 | .0165 |
| 81.8* | 4.95* | 1.24* | 19.24* | 4.25* | 0.200* | 55.0* | 2000* | .0180 |

* Estimated from full-pipe data.

| Type of Pipe | Nominal Pipe Diameter in Feet | Coefficient "n" |
|---|---|---|
| Standard | 3, 5, 7 | 0.024 |
| 25 Per Cent Paved | 5, 7 | 0.021 |
| 50 Per Cent Paved | 5 | 0.018 |

## ACKNOWLEDGMENT

The authors wish to acknowledge the use of material from the U. S. Army Engineer District, Portland, Corps of Engineers, in the preparation of this paper. Particular acknowledgment is given Mr. R. B. Hatch, Assoc. M., ASCE, who directly supervised the tests and analyzed the data.

## List of Symbols

| | |
|---|---|
| A | cross-section area of flow, sq ft |
| D | pipe diameter or equivalent diameter, ft |
| f | Darcy friction factor |
| g | acceleration of gravity 32.2 ft/sec/sec |
| h | mean difference between readings from impact and static tubes |
| $H_f$ | head loss due to pipe friction, ft |
| L | Length of conduit reach, ft |
| n | Manning roughness coefficient |
| Q | rate of flow, cfs |
| R | hydraulic radius, ft |
| $R_e$ | Reynolds number |
| S | slope of hydraulic grade line |
| V | average velocity of flow, fps |
| $V_1$ | local velocity of flow, fps |
| $V_*$ | shear velocity, fps |
| $\upsilon$ | kinematic viscosity, sq ft/sec |

## REFERENCES

1. "The Flow of Water Through Culverts" by D. L. Yarnell, F. A. Nagler, and S. M. Woodward, State University of Iowa Studies in Engineering, Bulletin 1, 1926.
2. "Friction Losses in Short Pipes and Culverts Flowing Full" by G. H. Keulegan, U. S. Bureau of Standards, 1948.

3. "Hydraulic Tests on Corrugated Metal Culvert Pipes" by L. G. Straub and H. M. Morris, St. Anthony Falls Hydraulic Laboratory, Technical Paper No. 5, Series B, 1950.

4. "Piping Arrangements for Acceptable Flowmeter Accuracy" by R. E. Sprenkle, Transaction of American Society of Mechanical Engineers, Vol. 67, 1945.

5. "Flow in Rough Conduits" by Henry M. Morris, Jr., Transactions, American Society of Civil Engineers, Vol. 120, 1955.

Journal of the
HYDRAULICS DIVISION
Proceedings of the American Society of Civil Engineers

# REVISED COMPUTATION OF A VELOCITY HEAD WEIGHTED VALUE

Joe M. Lara,[1] M. ASCE and Kenneth B. Schroeder,[2] M. ASCE

## ABSTRACT

A revised computational procedure is proposed on the determination of a weighted value of the velocity head. An example of the procedure is illustrated by a hydraulic computation of the discharge of a stream using the slope-area method.

## Procedure

This paper presents a suggested change in the computational procedure now used by hydrographers to determine the discharge of a stream by the slope-area method. A simpler way of computing the weighted value of the velocity head in channels conveying overbank or subsectional flow is shown by example.

The usual method for determining the weighted value of velocity head is by use of a velocity head correction factor, $\alpha$, computed by the following laborious formula:

$$\alpha = \frac{K_1^3/A_1^2 + K_2^3/A_2^2 + \cdots K_n^3/A_n^2}{\Sigma\,(K)^3/\Sigma\,(A)^2}$$

where $K_1$, $K_2$, and $K_n$ are the conveyances for each of the component sections of Areas $A_1$, $A_2$, and $A_n$, respectively.

Note: Discussion open until February 1, 1960. To extend the closing date one month, a written request must be filed with the Executive Secretary, ASCE. Paper 2149 is part of the copyrighted Journal of the Hydraulics Division, Proceedings of the American Society of Civil Engineers, Vol. 85, No. HY 9, September, 1959.

1. Hydr. Engr., Commissioner's Office, Bureau of Reclamation, Denver, Colo.
2. Hydr. Engr., Commissioner's Office, Bureau of Reclamation, Denver, Colo.

$$\Sigma (K) = K_1, + K_2 + \cdots K_n$$

$$\Sigma (A) = A_1, + A_2 + \cdots A_n$$

Conveyance or K is defined in terms of Manning's formula as:

$$K = \frac{1.486}{n} AR^{2/3}$$

where R is the hydraulic radius,

A is the cross-sectional area,

and n is the roughness coefficient.

The above method assumes that the velocity within each subsection 1, 2, or n is constant and that the discharge of each subsection is proportional to its relative conveyance.

The equation for $\alpha$ reveals that astronomical values can result in the computation of K. As an example, for K = 230,000, $K^3$ = 12,200,000,000,000,000, or $12.2 \times 10^{15}$.

The following procedure is proposed for computing the weighted value of the velocity head by a more convenient method. The proposed procedure is similar in principle to that used by the Corps of Engineers in backwater computations.(1) This procedure can be best illustrated by an example using the slope-area data collected at Sections 2 and 3 of a stream. A table of the sample computations and the descriptions of the determination of the value in each column are shown on the following pages:

| Column Number | Description |
|---|---|
| 1. | Section designation. Sections 2 and 3 are the downstream and upstream cross sections, respectively. |
| 2. | Observed water surface elevations at each section. |
| 3. | Subdivisions of cross-sectional areas; square feet. |
| 4. | Distance between cross sections; feet. |
| 5. | Assumed discharge of 10,800 cfs. (trial discharge.) |
| 6. | Subdivisional conveyances of each cross section. |
| 7. | Subdivisional discharges computed as follows: $Q_p = \frac{(K_{d_p})\ (Q)}{\Sigma\ K_d}$ for example on line 1 $Q_p = \frac{175{,}000 \times 10{,}800}{179{,}605} = 10{,}520$ cfs. |

SAMPLE COMPUTATIONS
Standard English Units

| Col. 1 | 2 | 3 | 4 | 5 | 6 | 7 | 8 | 9 | 10 | 11 | 12 | 13 | 14 | 15 | 16 | 17 |
|---|---|---|---|---|---|---|---|---|---|---|---|---|---|---|---|---|
| Section | MS el | A | L | Assumed Q | $K_d$ | $Q_p$ | V | $V^2Q$ | $h_v$ | $h_{v_1}-h_{v_2}$ | f | $h_f$ | s | $s^{1/2}$ | $K_{ave}$ | $Q=K_{ave}S^{1/2}$ |
| 3 | 104.3 | 1895 | | 10,800 | 175,000 | 10,520 | 5.55 | 324,000 | | | | | | | | |
| | | 176 | | | 3,670 | 220 | 1.25 | 344 | | | | | | | | |
| | | 82.4 | | | 935 | 60 | 0.73 | 32 | | | | | | | | |
| | | | 1110 | | 179,605 | 10,800 | | 324,376 | .466 | | | | | | | |
| 2 | 100.0 | 893 | | | 66,400 | 4,350 | 4.87 | 103,000 | | | | | | | | |
| | | 589 | | | 67,000 | 4,390 | 7.46 | 245,000 | | | | | | | | |
| | | 150 | | | 5,240 | 340 | 2.27 | 1,750 | | | | | | | | |
| | | 594 | | | 26,300 | 1,720 | 2.90 | 14,500 | | | | | | | | |
| | | | | | 164,940 | 10,800 | | 364,250 | .524 | -.058 | 4.30 | 4.25 | .00383 | .0619 | 172272 | 10,700 |

3

| Column Number | Description |
|---|---|
| 8. | Subdivisional velocities from the formula: $V_p = \frac{Q_p}{A_p}$ — Column 7 divided by Column 3 for line 1 $V_p = \frac{10,520}{1,895} = 5.55$ feet per second |
| 9. | Column 8 squared times the corresponding values in Column 7. |
| 10. | This is the weighted velocity head value computed by dividing the sum of Column 9 by the product of the total discharge and twice the gravitational acceleration—illustrated algebraically as follows: $h_v = \frac{\Sigma (v^2 Q)}{Q \times 2 g}$ for Section 3 $h_v = \frac{324,376}{10,800 \times 2 \times 32.2} = 0.466$ feet. |
| 11. | Difference in velocity heads. The algebraic sign should be retained. |
| 12. | Observed fall of the water surface—the difference in the values of Column 2; feet. |
| 13. | Friction loss computed by the following formulas*: If Column 11 is negative, as in the example, $h_f = f + 0.9 (h_{v_1} - h_{v_2})$ of Column 12 plus 0.9 of Column 11. If Column 11 is positive, $h_f = f + 0.5 (h_{v_1} - h_{v_2})$ or Column 12 plus 0.5 of Column 11. Either formula accounts for an eddy loss correction. |
| 14. | Energy gradient computed by dividing Column 13 by Column 4. |
| 15. | The square root of Column 14. |
| 16. | Arithmetic average of the total conveyances of Column 6. (Sometimes the geometric mean is used.) |

*Refer to Appendix.

| Column Number | Description |
|---|---|
| 17. | Discharge resulting from the product of Columns 15 and 16. When this value agrees reasonably with the assumed discharge (Column 5), the computations are completed. If the results are too extreme, another discharge is assumed and a new set of computations is made. |

To compare this suggested procedure with the usual one, the following calculation shows how $\alpha$ would be derived for Section 3 in the example:

$$\alpha = \frac{\frac{(175{,}000)^3}{(1{,}895)^2} + \frac{(3{,}670)^3}{(176)^2} + \frac{(935)^3}{(82.4)^2}}{\frac{(179{,}605)^3}{(2{,}153.4)^2}}$$

$$= \frac{1{,}490{,}000{,}000 + 1{,}600{,}000 + 121{,}000}{1{,}250{,}000{,}000}$$

$$= 1.19$$

This value multiplied by $\frac{(10{,}800 / 2{,}153.4)^2}{64.4}$ results in 0.466, the weighted velocity head for Section 3, the same answer as obtained in the example. In addition, another like computation must be made for Section 2.

The above suggested procedure provides additional information not readily available from the usual method and that is—the velocities and discharges occurring in each subdivision are readily computed. True, they may be theoretical, but they indicate how much of the flow is conveyed by each segment. This information is particularly useful for the computations of backwater profiles.

## APPENDIX

### Bernoulli Theorem

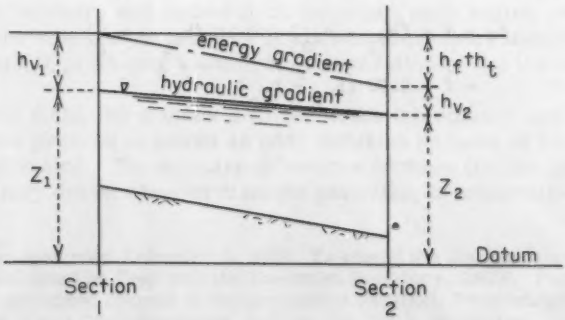

$h_{v_1}$ and $h_{v_2}$ = velocity heads at Sections 1 and 2, respectively

$Z_1$ and $Z_2$ = water surface elevations at Sections 1 and 2, respectively

$h_f$ = friction head loss

$h_t$ = eddy loss; considered as a percentage, m, of the change in velocity heads = $m (h_{v_1} - h_{v_2})$

Writing the energy equation:

$$Z_1 + h_{v_1} = Z_2 + h_{v_2} + h_f + h_t$$

Substituting and transposing

$$h_f = Z_1 - Z_2 + h_{v_1} - h_{v_2} - m (h_{v_1} - h_{v_2})$$

Let f = fall in water surface = $Z_1 - Z_2$

$$h_f = f + h_{v_1} - h_{v_2} - m (h_{v_1} - h_{v_2})$$

For an expanding reach

$$h_{v_1} > h_{v_2} \therefore h_{v_1} - h_{v_2} \text{ is positive}$$

m = .50 for positive values

Substituting

$$h_f = f + (h_{v_1} - h_{v_2}) - 0.50 (h_{v_1} - h_{v_2})$$

$$= f + 0.50 (h_{v_1} - h_{v_2})$$

For a contracting reach

$$h_{v_1} < h_{v_2} \therefore h_{v_1} - h_{v_2} \text{ is negative}$$

m = .10 for negative values

Substituting

$$h_f = f + (h_{v_1} - h_{v_2}) - 0.10 (h_{v_1} - h_{v_2})$$

$$= f + 0.90 (h_{v_1} - h_{v_2})$$

Journal of the
HYDRAULICS DIVISION
Proceedings of the American Society of Civil Engineers

# EDDY DIFFUSION IN HOMOGENEOUS TURBULENCE

Gerald T. Orlob,[1] A.M. ASCE

## SYNOPSIS

Taylor's theory of diffusion by continuous movements and the Einstein equation of diffusion were applied to eddy diffusion of particles in a two dimensional field of homogeneous turbulence produced by broad shallow channel with extreme bottom roughness. A simple method of determining the Lagrangian eddy size, eddy diffusivity, turbulence intensity, and mixing length was devised. Application of this technique provided experimental verification of the Kolmogoroff similarity principle which relates eddy diffusion, the rate of energy dissipation, and the Lagrangian eddy scale.

## INTRODUCTION

An interchange of fluid between two neighboring zones in a turbulent field necessarily results in the simultaneous interchange of every characteristic of the fluid masses involved. For example, if a fluid mass labeled with a tracer, say fluorescein dye, is transported laterally across an imaginary boundary into a zone which is free of contamination, it must, in order to satisfy continuity, be replaced by a fluid mass which contains no fluorescein. The immediate result is to increase the average concentration of the dye on one side of the boundary and reduce it on the other, each region acquiring the properties of the other. The process, if allowed to continue indefinitely will, of course, result in producing a uniform concentration of dye throughout both regions.

In a turbulent field, the masses involved in the interchange are called "eddies" and the process is known as eddy diffusion because of its similarity to molecular diffusion. The primary difference between the two processes lies in the analogy drawn between discrete particles, or molecules, moving in

Note: Discussion open until February 1, 1960. To extend the closing date one month, a written request must be filed with the Executive Secretary, ASCE. Paper 2150 is part of the copyrighted Journal of the Hydraulics Division, Proceedings of the American Society of Civil Engineers, Vol. 85, No. HY 9, September, 1959.

1. Asst. Prof. of Civ. Eng., Univ. of Calif., Berkeley, Calif.

free space, on the one hand, and the rather ill-defined lumps of fluid which are called eddies, on the other. Nevertheless, the final result, complete mixing of all fluid properties, is the same whether it occurs by molecular or eddy diffusion. In a turbulent regime, the effect of molecular diffusion is usually so small that it may be neglected.

The rate of change in concentration during eddy diffusion is determined fundamentally by two independent variables: the carrying capacity of the transverse flow and the extent of difference between the concentrations on either side of the arbitrary boundary. The latter variable can be expressed mathematically or evaluated experimentally as the lateral rate of change of concentration. The former is defined as the lateral coefficient of eddy diffusion, $D_z$, and is a characteristic of the turbulent field in which fluid dynamicists are particularly interested.

The coefficient of eddy diffusion has been defined in several ways. If eddies are treated as discrete entities which behave in a manner analogous to particles experiencing Brownian motion, the Einstein[1] equation is applicable,

$$D_z = \frac{1}{2} \frac{d(\sigma_z^2)}{dt} \tag{1}$$

where $D_z$ is the lateral coefficient of eddy diffusion, t is time the $\sigma_z$ is the standard deviation of the lateral displacement from the mean position of a statistically significant number of eddies. In a turbulent stream, eddy motions may be traced by introducing particles of a foreign substance which can be readily identified and the motions of which are equivalent to those of the water mass they displace.

Fick's laws of diffusion, which were derived from analogy with equations for heat conduction, have also been commonly applied to eddy diffusion. Fick's second law,

$$\frac{dc}{dt} = D_z \frac{d^2c}{dz^2} \tag{2}$$

where c is the concentration of diffusing substance, z is the lateral position, and t and $D_z$ are as previously defined, has been especially popular. It should be recognized, however, that when $D_z$ is not constant but is a function of t or z, solution of (2) is difficult and in many cases cannot be accomplished by formal procedures.

The mixing length concept of fluid mixing, usually credited to Prandtl, recognizes an analogy between fluid turbulence and the "mean free path" concept of gas dynamics. This results in a definition of eddy diffusion

$$D_z = \ell_z \sqrt{\overline{w'^2}} \tag{3}$$

where $\ell$ is the "mischungsweg" or mixing length $\sqrt{\overline{w'^2}}$ is the root mean square velocity fluctuation in the z-direction. This relation for $D_z$ possesses the advantage of incorporation of a property of the flow, the velocity fluctuation. However, the analogy to gaseous diffusion is rather loosely drawn with

the result that the mixing length idea has gradually given way to statistical descriptions of mixing phenomena.

The modern day statistical theories of turbulence stemmed largely from Taylor's theory of diffusion by continuous movements presented in 1921.(2) Taylor described the diffusion of discrete particles of fluid by means of the equation

$$D_z = \overline{w'^2} \int_0^t R_\xi \, d\xi \tag{4}$$

where $\overline{w'^2}$ is the mean square velocity fluctuation and $\xi$ is the time displacement between positions of the same fluid particle according to the Lagrangian scheme and $R_\xi$, the velocity fluctuation correlation coefficient is defined as

$$R_\xi = \frac{\overline{w'_{t_o} \; w'_{t_o + \xi}}}{\overline{w'^2_{t_o}}} \tag{5}$$

Shortly after Taylor's theory was presented, Richardson(3) noticed the failure of the Fickian laws of diffusion to account for the extremely wide range in values of the diffusion coefficient observed in atmospheric turbulence. He introduced the concept of "neighbor distribution" which for an average separation of particle pairs, L, results in the neighbor diffusion equation

$$\frac{\partial q}{\partial t} = \frac{\partial}{\partial L}\left[ F(L) \frac{\partial q}{\partial L} \right] \tag{6}$$

where q is the mean number of neighbors per unit length of L, the neighbor separation, and F(L) is a diffusion coefficient which relates to the scale of the diffusion phenomena. Based on some rather crude observations of atmospheric diffusion and the associated scales, Richardson suggested that

$$F(L) = e\, L^{4/3} \tag{7}$$

in which e was taken as a constant. This relation, although presented without basis in theory, has been designated as the "Four-Thirds Law." It has been applied to oceanographic diffusion by Richardson(4,5) and others(6) with varying degrees of success. The exponent four thirds was viewed by some investigators as a universal number despite the lack of satisfactory experimental support and the absence of a theoretical basis for this conclusion.

The four-thirds relationship remained without prospect of theoretical support until 1941 when Kolmogoroff(7,8) introduced a somewhat new theory of the spectrum of turbulence. Kolmogoroff's development is based on the fundamental concept that eddying motions are characterized by a wide range of length scales. Energy of eddy motion is then conceived to be passed down the spectrum through a succession of eddies of smaller size ultimately being dissipated by viscous action as heat. In this process, as the scale is reduced, the influence of the large eddies is felt less and less so that within the middle

range of the spectrum eddies are assumed to possess properties common to all types of turbulence. By definition, such eddies are isotropic.

Kolmogoroff's analysis is built on two hypotheses, both applicable to motions with large Reynolds numbers:

1) The small-scale components of the motion depend only on the viscosity, $\nu$, and the mean rate of dissipation of energy per unit mass of fluid, E.

2) There is a sub-range of small eddies in which mean properties depend only on the mean rate of dissipation of energy per unit mass of the fluid.

Batchelor[9,10] in reviewing Kolmogoroff's theory argued on dimensional grounds that the effect of variation in the parameters E and $\nu$ could only be to change the effective length and time scales of the motion, thus

$$L = f(E, \nu) \tag{8}$$

If the customary analogy between molecular and eddy diffusion is used, $\nu$ can be replaced with D. By dimensional analysis, there results

$$D = \text{Constant } E^{1/3} L^{4/3} \tag{9}$$

where L may be taken as the mean size of the eddies participating in the diffusion process. Turbulence theories proposed independently in 1945 by Onsager[11] and in 1948 by von Weizsäcker[12] lead to identical relationships.

It appears that the empirical proposal of Richardson was apparently a good one and in agreement with the Kolmogoroff similarity theory; however, the literature fails to reveal an experimental confirmation of the theory under carefully controlled conditions.

## Experimental Techniques

The essential requirements for experimental investigation of the Kolmogoroff principle are:

1) a test facility which will create a statistically homogeneous turbulent field in which the diffusion phenomenon can be studied, and

2) techniques for evaluation of the scale of turbulence, the rate of energy dissipation per unit mass of fluid, and the coefficient of eddy diffusion.

Statistically homogeneous turbulence in three dimensions is virtually impossible to produce in a laboratory. Conditions along the center line of a large conduit probably come closest to the ideal requirements, but boundary effects severely restrict the scales of turbulence which may be examined. Wind or water tunnel grids may be expected to produce homogeneity of turbulence in the field stream but only in planes parallel to the grids. Because the scale of turbulence diminishes with distance from the grid, this form of turbulence generator is not suited to a study which attempts to relate eddy scales and eddy diffusion at a constant rate of energy dissipation.

If the requirement of three dimensional homogeneity is relaxed and a two dimensional field is substituted, the experimental techniques are considerably simplified. A broad, shallow, open channel of sufficient length and bottom

roughness to minimize end effects meets the requirements of two-dimensional homogeneity very satisfactorily provided the diffusion phenomena is constrained to a single plane, i.e. the surface of the stream.

The experimental channel constructed for the studies was 4 feet wide, 8 inches deep and 38 feet in length (Figure 1) and was supported on leveling screws which permitted adjustment to uniform slopes ranging from 0 to 0.01. Two one-quarter horsepower propellor pumps were capable of delivering flows up to 1000 gpm to the stilling basin at the head of the flume. A by-pass valve between the stilling basin and the return flume facilitate discharge control.

Bottom roughness for the experimental channel consisted of expanded metal meshes as shown in Figure 2 which were stapled to the plywood bottom of the channel. Three mesh sizes designated by the nominal dimensions of the minor diagonal of the diamond pattern as 0.5, 1.0 and 1.5 inches, were employed in the investigation.

The requirement that the diffusion phenomenon be observed only in a plane where two-dimensional homogeneity could be achieved dictated the use of floating particles, the motions of which were influenced by turbulence near the stream surface. Use of discrete particle motions to statistically characterize the turbulent regime is in accord with the theories of Taylor(2) and Richardson.(3) Also, a simple direct method for statistical interpretation of particle motion in terms of eddy diffusion is available through Einstein's equation (Equation 1).

The particles employed in the studies were polyethylene discs approximately one-eighth of an inch in diameter and one-sixteenth of an inch thick. Polyethylene has a specific gravity of approximately 0.975 so that, when fully wet, discs of this material just barely float. The buoyancy and size of the discs used in these investigations were apparently satisfactory to prevent their being entrained in the flow and to insure that their motion was representative of the upper few millimeters of the flowing stream. Particles were released singly through a small glass funnel suspended about one-eighth of an inch over the water surface from a point gage assembly which could be moved on rails along the channel sides.

In accordance with diffusion theory, the position of each particle must be fixed at a certain time following the instant of release. Each point is then projected to a single axis. The distribution of particle positions along this axis can be defined then in terms of the standard deviation from the mean position. The procedure used in the investigations reported herein differed slightly in that particles were all intercepted from the flow at a fixed distance downstream from the point of release. However, since the theoretical pattern would be symmetrical about this arbitrarily selected axis, the total experiences, i.e., the total accumulated path length of all particles, would be identical by either technique. It is, therefore, reasonable to conclude that the standard deviation calculated from an array of particles along a fixed line of interception a distance, x, from the source is substantially equal to that of a pattern whose centroid is also x distant from the source.

Particles were collected from the surface of the experimental channel by inserting a scoop of ordinary galvanized window screen into the top one-quarter inch of the flow. In order to simplify the statistical analysis of the particle positions, the particle collector was compartmentalized with thin metal sheets spaced one centimeter apart across the full width of the channel.

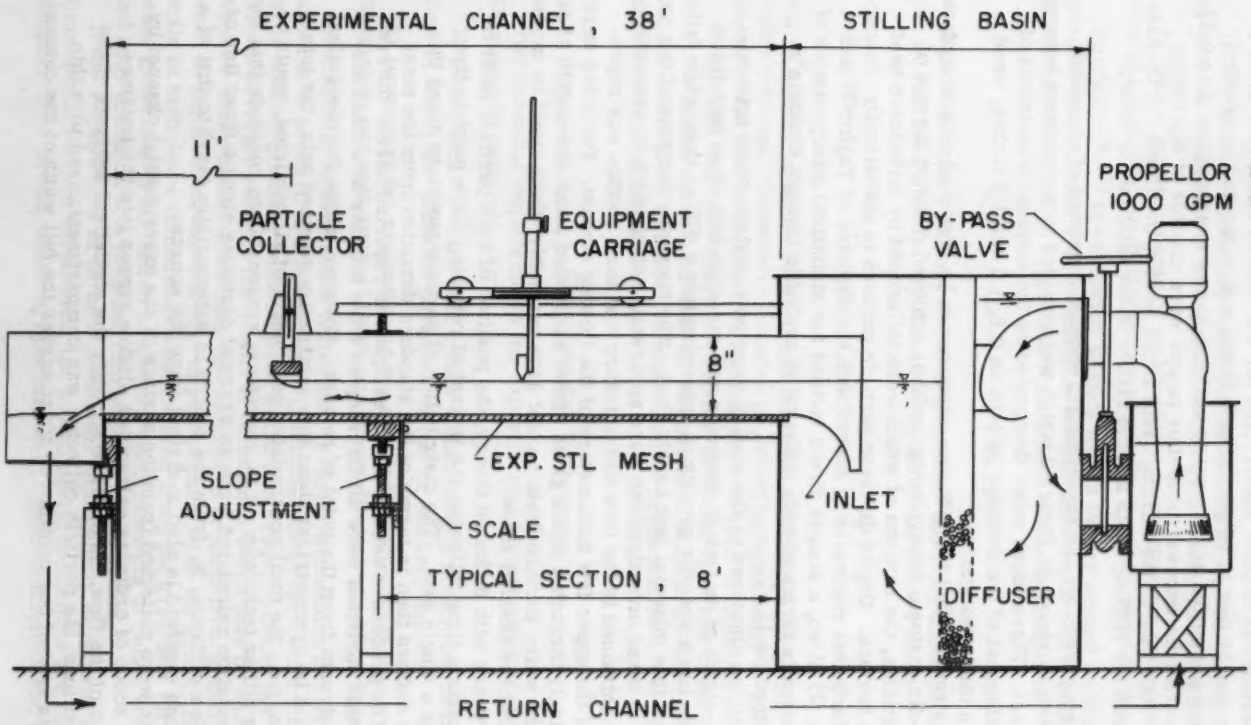


FIGURE 1 EXPERIMENTAL CHANNEL

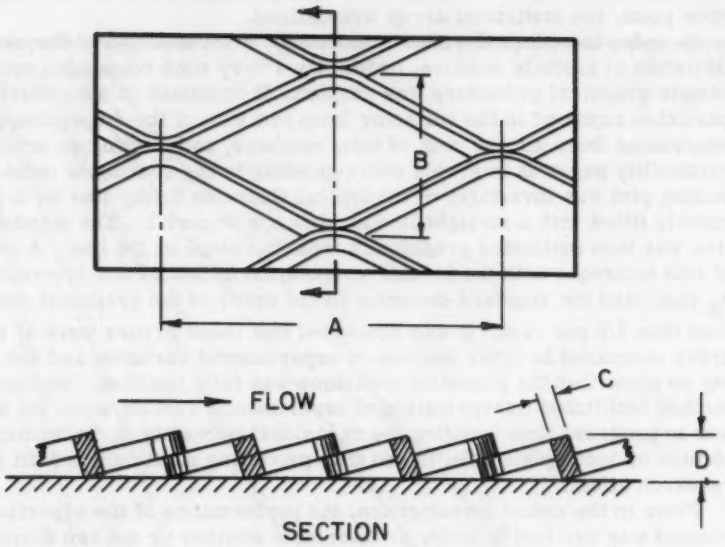


| NOMINAL WIDTH | LENGTH A | WIDTH B | THICKNESS C | DEPTH D |
|---|---|---|---|---|
| 0.5" | 1.22" | 0.48" | 0.063" | 0.193" |
| 1.0" | 2.01" | 0.96" | 0.106" | 0.236" |
| 1.5" | 3.03" | 1.39" | 0.154" | 0.327" |

FIGURE 2 CHARACTERISTICS OF ROUGHNESS MESHES

FIGURE 1 EXPERIMENTAL CHANNEL

By counting the number of particles in each compartment and recording these numbers with respect to the position of the compartment from a fixed reference point, the statistical array was defined.

In order to reduce the time required for determination of the standard deviation of particle position, ordinarily a very time consuming operation, a simple graphical procedure was adopted. It consisted of accumulating the particles captured in the collector from one side of the dispersion pattern, expressing them as per cent of total numbers, and plotting on arithmetic probability paper at intervals corresponding to the spacing of cells. The resulting plot was invariably of the typical Gaussian form; that is, it could be closely fitted with a straight line as shown in Figure 3. The standard deviation was then estimated graphically from the slope of the line. A comparison of this technique with the formal computation technique for determination of $\sigma_z$ indicated the standard deviation in the error of the graphical method was less than 1.0 per cent. It was concluded that these errors were of such small order compared to other sources of experimental variation and the time saving so great that the graphical technique was fully justified. Moreover, the method facilitated interpretation of experimental results while the experiment was in progress thus avoiding the occasional necessity of discarding inconclusive or incomplete results and thus producing maximum benefit from the research effort.

Prior to the actual investigation, the performance of the experimental channel was verified in order to determine whether or not two dimensional homogeneity was actually attained. Determinations of $\sigma_z$ at a fixed distance from the source over the width and along the length of the channel indicated that except for points very close to the channel walls, say less than 2 inches from the walls and within 5 or 6 feet of the entrance or exit channel, the turbulent structure was essentially homogeneous. During all subsequent tests, observations were confined to a smaller area about 2 feet wide and 15 feet long in the central portion of the channel.

## Results

Using the methods described above, it was possible to determine the standard deviation of the particle dispersion pattern at varying distances from the point of release thus defining, experimentally, the relationship between $\sigma_z$ and x. According to the basic Einstein diffusion equation (Equation 1), $\sigma_z$ is directly proportional to $x^{1/2}$ when the coefficient of diffusion and stream velocity are constant. Both the theoretical analyses offered by Taylor(2) and by Richardson(3) agree with this relation for large values of x but suggest that very close to the source, $\sigma_z$ is proportional to x. Thus, one would expect, if the theories are valid, to find that a dispersion pattern determined experimentally would be wedge-shaped near the source and would gradually approach a parabolic pattern as the distance from the source is increased (Figure 4). Also, the diffusion coefficient, which may be considered a function of x, would be expected to increase near the source in proportion to x, ultimately attaining a constant and maximum value distant from the source.

If the Einstein equation is modified by substitution of $dx/\bar{u}$ for dt, the diffusion coefficient becomes related to distance by

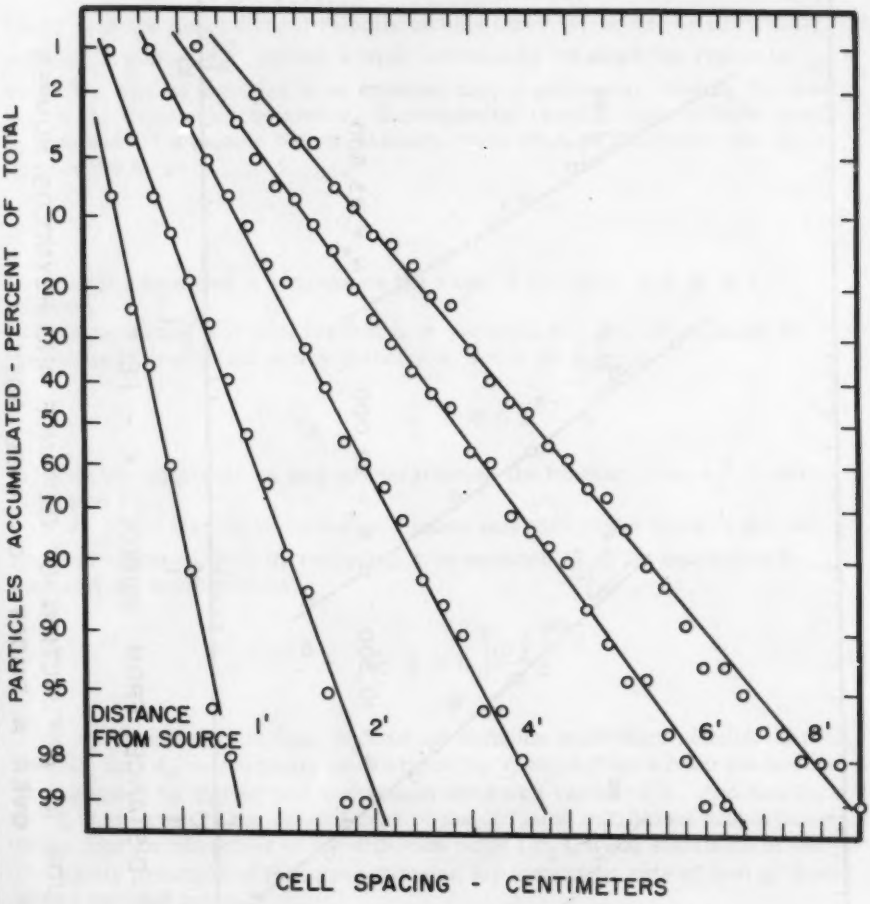


FIGURE 3 PARTICLE DISPERSION IN RELATION TO DISTANCE FROM SOURCE

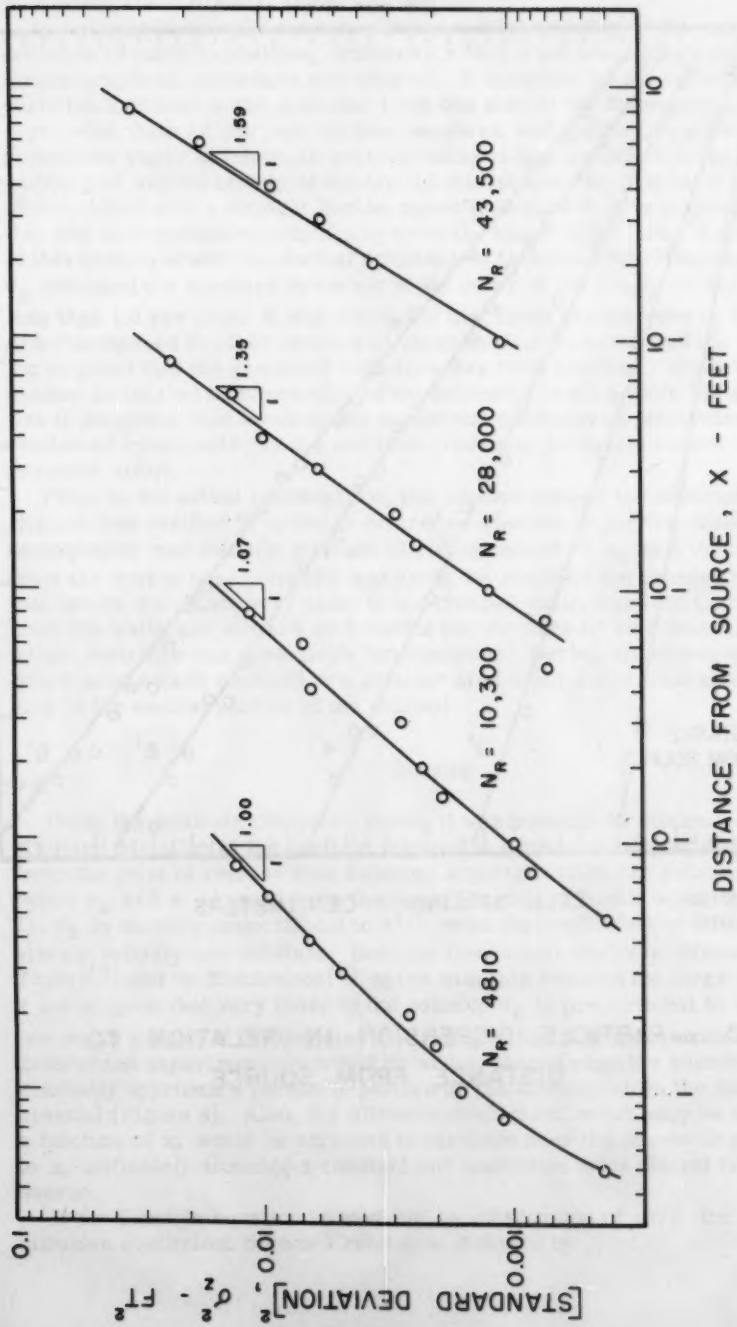


FIGURE 4 DISPERSION AS A FUNCTION OF DISTANCE AND REYNOLDS NUMBER OVER A SMOOTH CHANNEL BOTTOM

$$D_z = \frac{1}{2} \bar{u} \frac{d(\sigma_z^2)}{dx} \tag{10}$$

where $\bar{u}$ is the mean stream velocity and the other terms are as previously defined. A plot of $\sigma_z^2$ versus x thus indicates by its slope the region in which $D_z$ may be expected to be constant and, in particular, how $\sigma_z$ varies with x (or t) close to the source. Experimental results, such as those shown in Figure 4 for a smooth bottom channel, could often be fitted with straight lines of the form

$$\sigma_z^2 = m x^n \tag{11}$$

in which the exponent n represents the slope of the curve and m is a constant.

Differentiating (11) with respect to x produces the general equation for the diffusion coefficient at any distance x, from the source

$$D_z = \frac{1}{2} \bar{u} m n x^{n-1} \tag{12}$$

in which the constants m and n characterize the tangent to the $\sigma_z^2$-x curve (Equation 11).

If $\sigma_z$ itself may be regarded as a crude measure of the scale of the diffusion phenomena, then by replacing x in equation 12 by its equivalent in terms of $\sigma_z$ there results

$$D_z = \frac{1}{2} \bar{u} m n \left[\frac{\sigma_z^2}{m}\right]^{\frac{n-1}{n}} \tag{13}$$

If $n = 1$, the special case of constant diffusion coefficient results. If $n = 2$, both $D_z$ and $\sigma_z$ are directly proportional to x, the distance from the source, as suggested by Taylor and Richardson for small values of x. And finally, if $n = 3$, there results the special case of the diffusion coefficient proportional to the four-thirds power of the diffusion scale ($\sigma_z$), i.e. a statement of the similarity principle of turbulent diffusion for a constant rate of energy dissipation per unit mass.

In Figure 4 the value of n is seen to range from 1.0 to 1.59 depending both on x and on the Reynolds number, $\bar{u}y/\nu$. There were indications in these and all similar series that at sufficiently large values of x the value of n reached 1.0 and that n tended to increase as the source was approached. The maximum values of n observed for the polyethylene particle experiments seldom exceeded 2.0. The increase in n with Reynolds number suggests that the scale and intensity of turbulence also increased so that the region of constant $D_z$ was virtually pushed out of the experimental region and could not be directly observed.

It was apparent from preliminary results with floating particles that verification of a "four-thirds" law or the similarity principle would not be possible by direct observation of the dispersion pattern in laboratory scale channels. The sub-range of eddy sizes to which the similarity concept would apply

FIGURE 4 DISPERSION AS A FUNCTION OF DISTANCE AND REYNOLDS NUMBER OVER A SMOOTH CHANNEL BOTTOM

must have been much smaller even than the size of particles employed. To further support this conclusion, a limited number of studies with fluorescien dye streams were conducted. By injecting the dye at the surface of the stream through a fine glass capillary the shape of dispersion pattern much closer to the source could be examined. Such dye streams were photographed with time exposures on high speed film under ultra violet light.

Assuming that the dispersion pattern produced on the photographs defined limits of $\pm 2\sigma_z$ $_z$, it was noted, as shown in Figure 5, that the value of n frequently exceeded 2.0 and occasionally approximated the value of 3.0 theoretically required for conclusive verification of Kolmogoroff's relation. It is clear that direct corroboration in the laboratory of the applicability of equation 9 by inspection of individual dispersion patterns will require much finer measurements than were possible in these studies.

However, the relationship between $D_z$, the eddy diffusion coefficient, and $L_a$, the mean eddy size, can be determined through a comparison of the properties of several different turbulence fields. In order to accomplish this comparison it was necessary to relate characteristics of the dispersion pattern, viz $\sigma_z$, to the size of eddies which brought about dispersion. By equating the basic definitions of eddy diffusion by the Einstein and Taylor equations, one obtains

$$\frac{1}{2}\frac{d(\sigma_z^2)}{dt} = \overline{w'^2}\int_0^t R_\xi \, d\xi \qquad (14)$$

In order to integrate the right hand side of (14) it is essential to know the form of $R_\xi$. Many experimental observations, particularly those of Dryden,[13] Laufer,[14] Favre, Gaviglo, and Dumas[15,16] and Ippen and Raichlen[17] show that the $R_\xi - \xi$ curve may be closely approximated by an equation of the form

$$R_\xi = e^{-k\xi} \qquad (15)$$

Substituting into (14), integrating, and replacing t with $x/\bar{u}$, produces the general equation

$$\sigma_z^2 = \frac{2\overline{w'^2}}{k}\left[\frac{k}{\bar{u}}x - \left(1 - e^{-\frac{k}{\bar{u}}x}\right)\right] \qquad (16)$$

With the aid of equation (16) and an experimental knowledge of $\sigma_z$, x, and $\bar{u}$, it is possible to determine both k and $\overline{w'^2}$ as well as those other quantities derivable from the basic equation. It will be noted that the shape of the $\sigma_z^2$-x curve is determined only by the eddy scale reciprocal, $k/\bar{u}$, the velocity fluctuation being only a translational term which positions the curve along the vertical axis. Thus, $k/\bar{u}$ can be determined without knowing $\overline{w'^2}$ by simply fitting a curve of relative $\sigma_z^2$ versus x to experimental data over a suitable range of x. In fact, one need only know two pairs of values of $\sigma_x^2$ and x to obtain an estimate of eddy scale. Once $k/\bar{u}$ has been established, $w'^2$ can be calculated from Equation 16. Since the velocity is ordinarily known, k can be determined thus permitting calculation of the Lagrangian eddy size

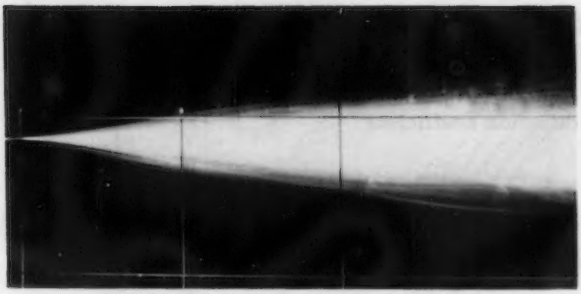

FLUORESCEIN DYE STREAM
UNDER ULTRA-VIOLET LIGHT

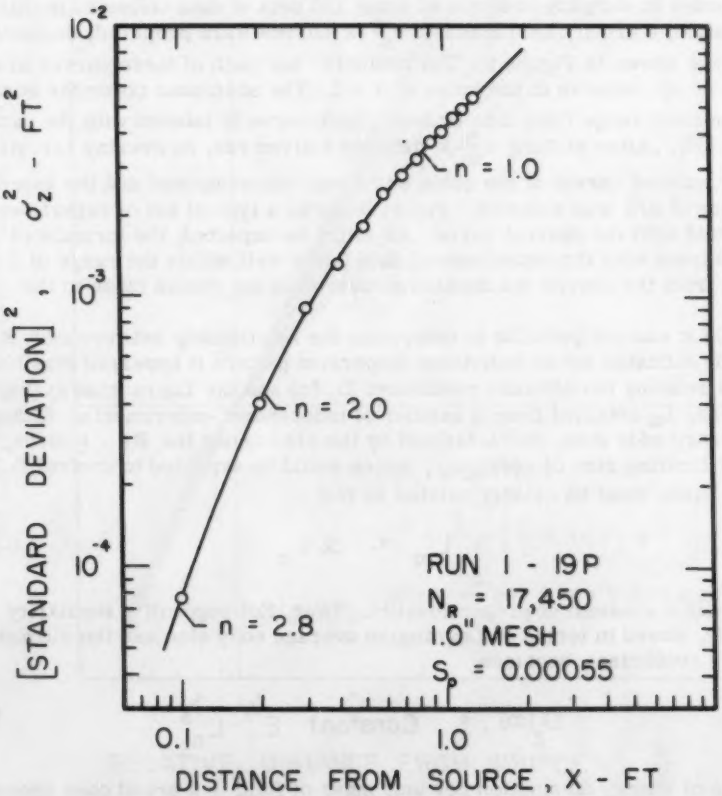


FIGURE 5 DISPERSION NEAR A DYE SOURCE

$$L_a = \bar{u} \int_0^t e^{-kt}\, dt = \frac{\bar{u}}{k} \tag{17}$$

the eddy diffusion coefficient

$$D_z(\infty) = \frac{\overline{w'^2}}{k} \tag{18}$$

and the mixing length

$$\ell_z = \frac{\sqrt{\overline{w'^2}}}{k} \tag{19}$$

In order to simplify analysis of some 150 sets of data collected in this investigation, a group of normalized $\sigma_z^2$-x curves were prepared, samples of which are shown in Figure 6. The ordinates for each of these curves are the values of $\sigma_z^2$ relative to the value at x = 1. The abscissas cover the normal experimental range from 1 to 20 feet. Each curve is labeled with the parameter $k/\bar{u}$. After plotting $\sigma_z^2$-$\dot{x}$ data for a given run, an overlay carrying the normalized curves at the same scale was superimposed and the appropriate value of $k/\bar{u}$ was selected. Figure 7 shows a typical set of experimental data fitted with the general curve. As might be expected, the formulated curve agrees with the experimental data fairly well within the range of 1 to 10 feet from the source but departs somewhat in the region close to the source.

While it was not possible to determine the relationship between eddy size and eddy diffusion for an individual dispersion pattern it appeared feasible to attempt relating the ultimate coefficient $D_z(\infty)$ and the Lagrangian average eddy size, $L_a$ obtained from a number of independent experiments. Although the average eddy size, characterized by the area under the $R\xi$ - $\xi$ curve, is not that limiting size of eddy, $L_\infty$, which would be expected to control $D_z(\infty)$ the two sizes must be closely related so that

$$L_\infty = \alpha L_a \tag{20}$$

where $\alpha$ is a constant of proportionality. Thus, Kolmogoroff's similarity principle, stated in terms of Lagrangian average eddy size and the ultimate diffusion coefficient, becomes

$$D_z(\infty) = \text{Constant}\ E^{1/3} L_a^{4/3} \tag{21}$$

The rate of energy dissipation per unit mass of fluid in a broad open channel is defined as

$$E = U g S_e \tag{22}$$

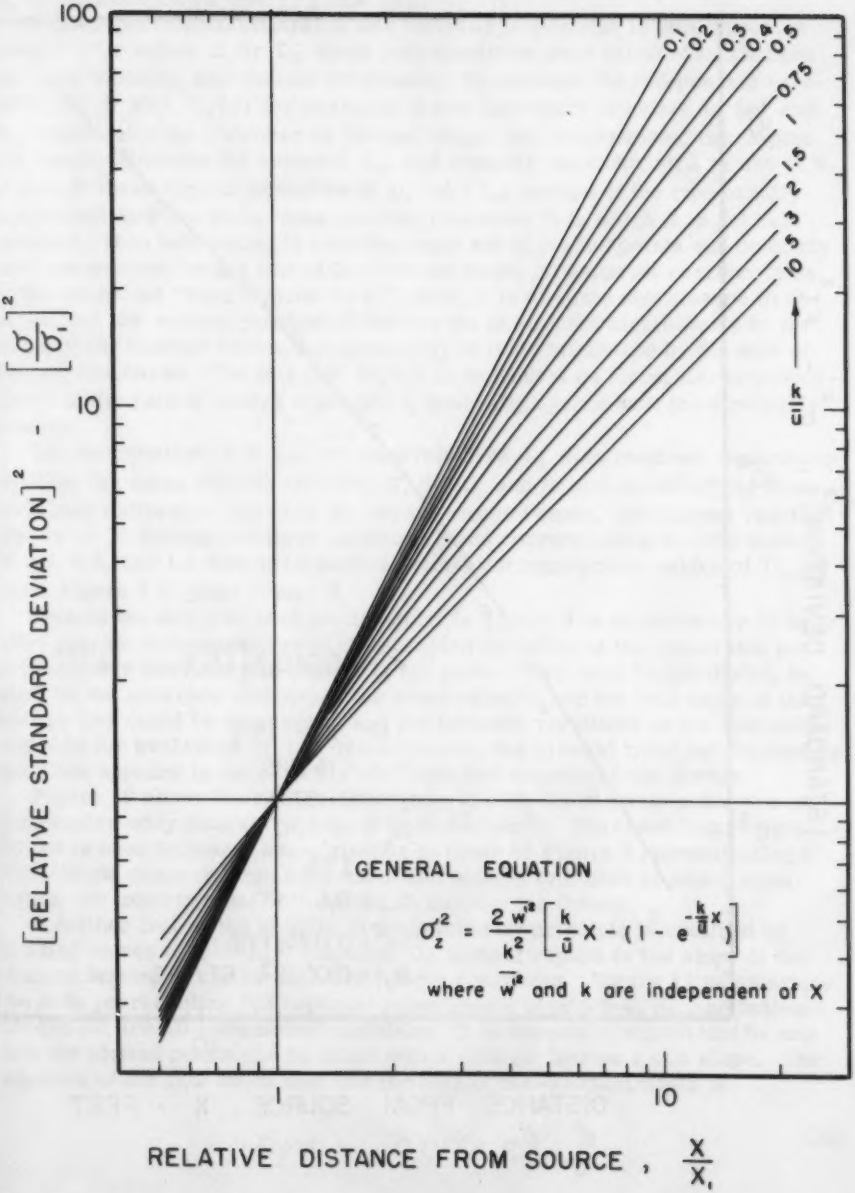


FIGURE 6 NORMALIZED DISPERSION-DISTANCE CURVES

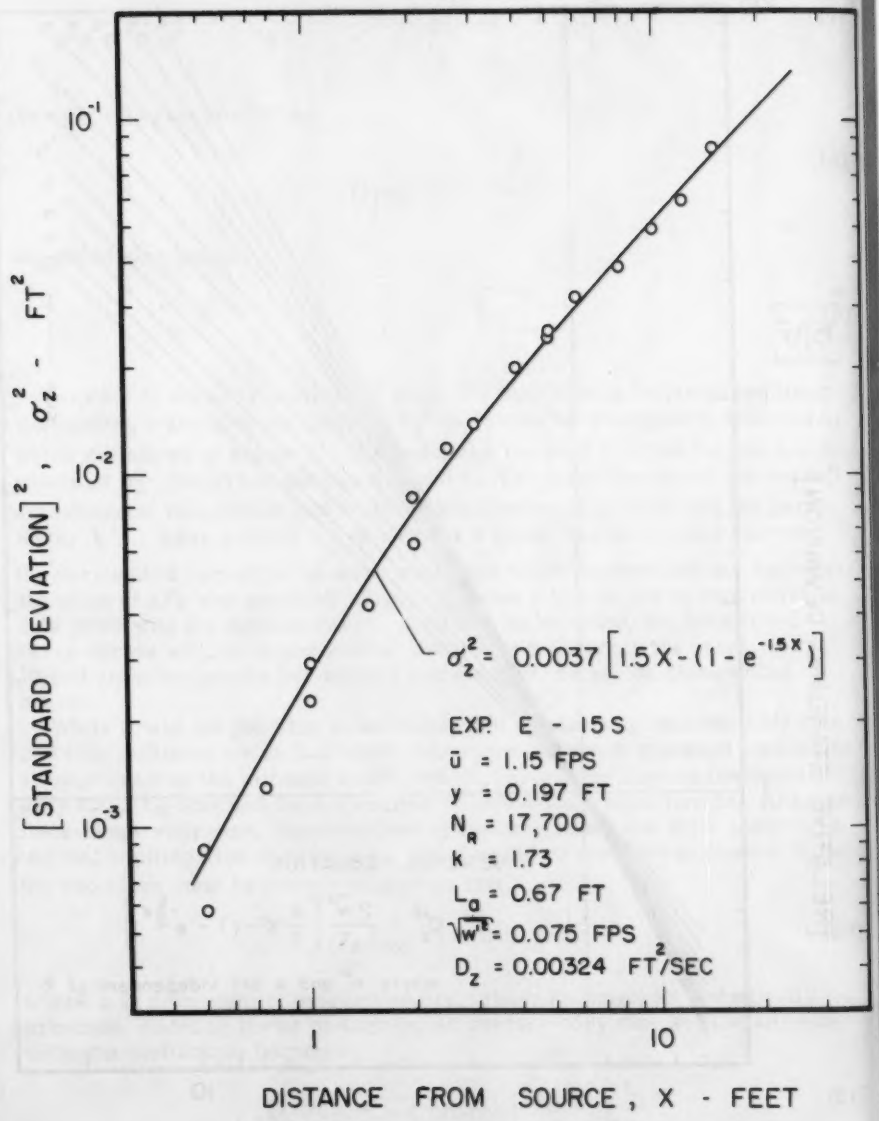


FIGURE 7 GENERAL POINT SOURCE SOLUTION FITTED TO EXPERIMENTAL DATA

where U is the mean stream velocity, g is the acceleration of gravity, and $S_e$ is the slope of the energy grade line.

In the experimental channel it was virtually impossible to attain precise control over either E or $L_a$ since both quantities were affected by changes in slope, velocity, and channel roughness. To examine the independent variability of E with $D_z(\infty)$ for example, it was necessary to relate $D_z(\infty)$ and $L_a$ empirically for a number of channel slopes and roughnesses, cross-plot the resulting curves for constant $L_a$, and compute the associated values of E. Figure 8 shows typical examples of $D_z(\infty)$ - $L_a$ curves of the type usually associated with the Richardson relation (Equation 7) in which E is not held constant. It is interesting to note that each set of plotted points can be fairly well represented with a line of four-thirds slope, an apparent corroboration of the so-called "Four-Thirds Law." Also, it is of some significance to observe that the vertical position of the curves is affected significantly by the slope of the channel bottom but apparently is little influenced by the size of bottom roughness. The fact that $D_z(\infty)$ is dependent on slope, i.e. is proportional to the rate of energy dissipation, generally agrees with the similarity concept.

The computation of E for constant values of $L_a$ also required empirically relating the mean channel velocity, U, to $L_a$ and in turn selecting $S_e$ from a channel calibration curve of $S_e$ versus channel slope, and channel velocity. Values of E determined from equation 22 and corresponding to eddy scales of 0.2, 0.5, and 1.0 feet were plotted against the appropriate values of $D_z(\infty)$ from Figure 8 to yield Figure 9.

Despite the fact that each plotted point in Figure 9 is supported by 50 to 100 separate determinations of the standard deviation in the dispersion pattern there is considerable scatter in the plots. This must be attributed, in part, to the accuracy with which the mean velocity and the true slope of the energy line could be determined and the inherent variations in the statistical methods for evaluation of $L_a$. Nevertheless, the general trend established by the plots appears to agree fairly well with that expected from theory.

Figure 10 shows the coefficient of lateral eddy diffusion as a function of Lagrangian eddy size at constant E (0.05 $ft^2/sec^3$). The trend line in the figure is seen to have a shape similar to those of Figure 8 approximating a four-thirds slope at large eddy sizes and tending to flatten at small sizes. Again, the experimental data appear to support the theory.

A further test of the validity of the similarity principle is obtained by plotting values of $E^{1/3}L_a^{4/3}$ against $D_z$ without regard to the slope of the channel bottom or the condition of bottom roughness. Figure 11 summarizes the data representing 105 separate experiments in which U, $S_e$, and bottom roughness are all independent variables. It is especially significant to note that the plotted points can be fitted with a straight line on a unit slope. The equation of the line which best fits the data of these experiments is

$$D_z(\infty) = 0.0136\, E^{1/3} L_a^{4/3} \qquad (23)$$

where $D_z$ is the coefficient of the lateral eddy diffusion, E is the rate of energy dissipation per unit mass, and $L_a$ is the Lagrangian eddy size. The constant is taken as representative of all degrees of bottom roughness produced by the three roughness meshes employed in the experiments.

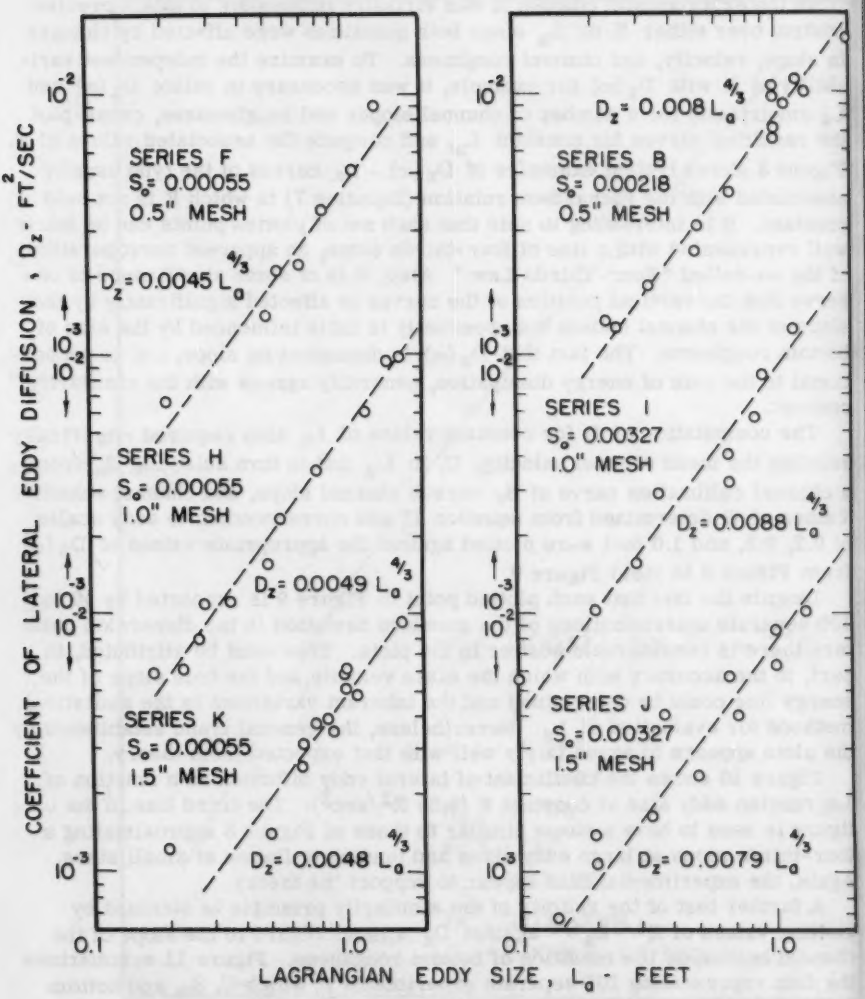


FIGURE 8 EFFECT OF EDDY SIZE ON EDDY DIFFUSION

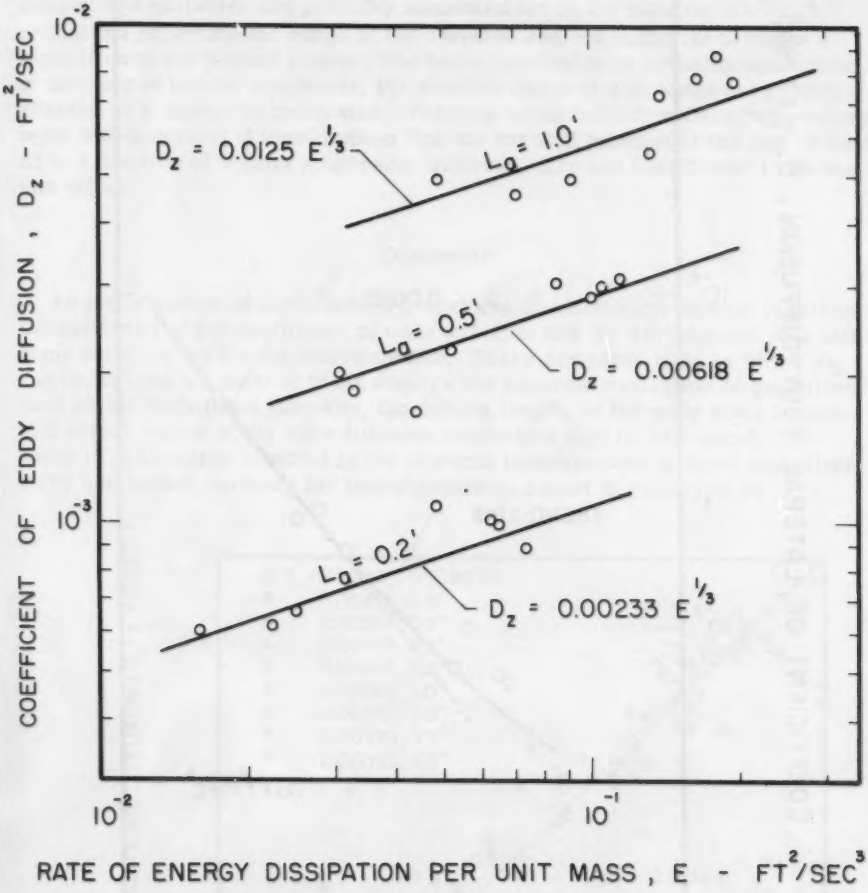


FIGURE 9 COEFFICIENT OF EDDY DIFFUSION AS A FUNCTION OF RATE OF ENERGY DISSIPATION PER UNIT MASS FOR CONSTANT EDDY SIZE

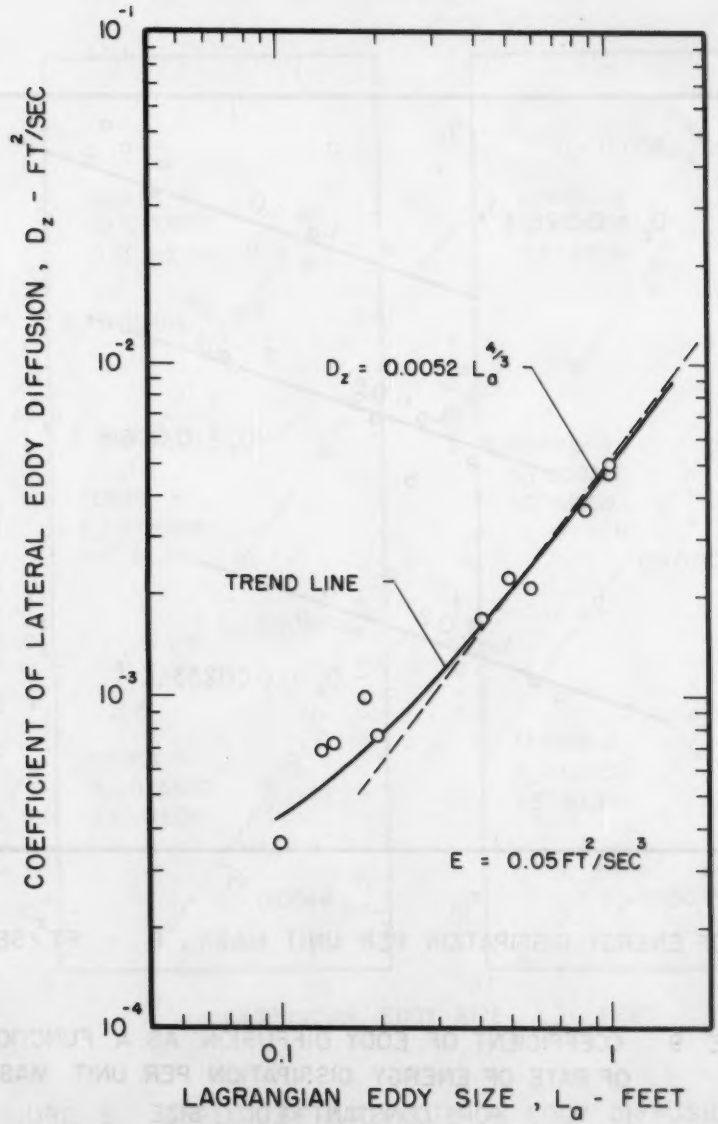


FIGURE 10 COEFFICIENT OF EDDY DIFFUSION AS A FUNCTION OF EDDY SIZE FOR CONSTANT RATE OF ENERGY DISSIPATION PER UNIT MASS

The fact that all the data from the series used to prepare Figure 11 are rather equally distributed about the best fit line indicates that the scatter is probably due to experimental errors alone. It may also be concluded that the independent variables are probably accounted for in the quantity $E^{1/3}L_a^{4/3}$ or that the experimental range of the variable was not sufficient to cause a separation in the plotted points. The latter conclusion is probably applicable in the case of bottom roughness, the absolute value of which was not greatly affected by a change in mesh size. There is some indication from exploratory tests with a smooth channel bottom that the vertical position of the line of best fit is a function of bottom roughness; however, data are insufficient to define this effect.

## Discussion

An investigation of the diffusion properties of a turbulent stream requires the definition of the coefficient of eddy diffusion and the development of a technique satisfactory for its determination. There are many ways in which $D_z$ can be defined but most of these require the separate evaluation of quantities such as the turbulence intensity, the mixing length, or the eddy scale in order that actual values of the eddy diffusion coefficient may be calculated. Because of difficulties involved in the physical measurement of these quantities there has been a tendency for investigators to resort to empirical or

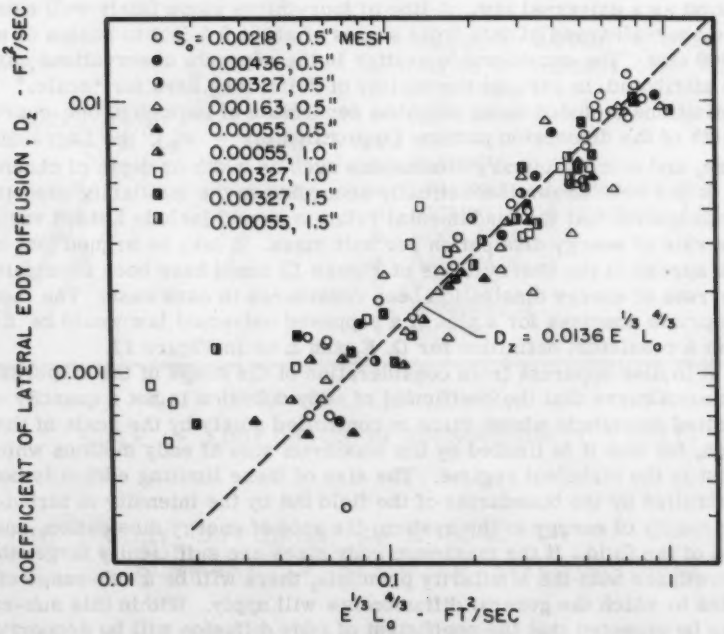


FIGURE 11 EDDY DIFFUSION AS A FUNCTION OF SCALE AND RATE OF ENERGY DISSIPATION

semi-empirical "laws" which relate two properties of the flow, usually $D_z$ and one other characteristic, through constants of proportionality and appropriate exponents. Often the empirical equation is only a convenient device useful for rough estimation but bearing no resemblance in form or content to the true theoretical relationship. Occasionally the researcher who has proceeded with only a partially developed theory can, with the aid of considerable intuition and astute observation, hit upon a relationship which comes close to the truth but which is not quite complete. This appears to have been the case with the semi-empirical relationship first proposed by Richardson and which has been referred to as the "Four-Thirds Law."

Richardson observed that the coefficient of eddy diffusion was nearly proportional to the four-thirds power of some measure of the scale of the phenomenon causing diffusion. He proposed a theory of "neighbor diffusion" which involved the statistical averaging of "neighbor separations" of adjacent particles. The mean neighbor separation he took to be a measure of "scale." Unfortunately, Richardson's neighbor diffusion theory is difficult to apply, and except for a few studies on ocean surfaces, it has been little used.

Pearson[6,18] has summarized the relationship between the coefficient of eddy diffusion and the scale of the diffusion phenomenon by reporting the observations of many independent investigators, including himself, for a wide variety of scales. Figure 12 is a typical plot of the type Pearson prepared, including all of the data reported by him together with some observations collected during the investigations which are reported herein. It is possible to see from the figure why one might be inclined to regard Richardson's relation as a universal law. A line of four-thirds slope fairly well establishes the over-all trend of data from scales of about 0.1 foot to scales of more than 1000 feet. The considerable scatter in the separate observations can probably be attributed, in part, to the variety of definitions used for "scale." These definitions included mean neighbor separation of particles, one-quarter of the width of the dispersion pattern (approximately = $\sigma_z$), the Lagrangian eddy size, and some arbitrary dimensions such as width or depth of channel.

It has been shown theoretically according to the similarity concept of Kolmogoroff that the fundamental relation should include a third variable, the rate of energy dissipation per unit mass. It may be argued that much of the spread in the observations of Figure 12 could have been eliminated had the rate of energy dissipation been considered in each case. The most appropriate abscissa for a plot of a supposed universal law would be $E^{1/3}L^{4/3}$ with a consistent definition for D, E, and L as in Figure 11.

It is also apparent from consideration of the shape of the dispersion-distance curve that the coefficient of eddy diffusion is not a quantity of unlimited magnitude whose value is controlled solely by the scale of the phenomenon, but that it is limited by the maximum size of eddy motions which may exist in the turbulent regime. The size of these limiting eddies is not only controlled by the boundaries of the field but by the intensity of turbulence, the supply of energy to the system, the rate of energy dissipation, and properties of the fluid. If the maximum eddy sizes are sufficiently large, then, in accordance with the similarity principle, there will be a sub-range of eddy sizes to which the general diffusion law will apply. Within this sub-range it may be expected that the coefficient of eddy diffusion will be proportional to the four-thirds power of the eddy size, but on the upper side of this range diffusion will become decreasingly dependent on scale until it ultimately reaches its maximum constant value.

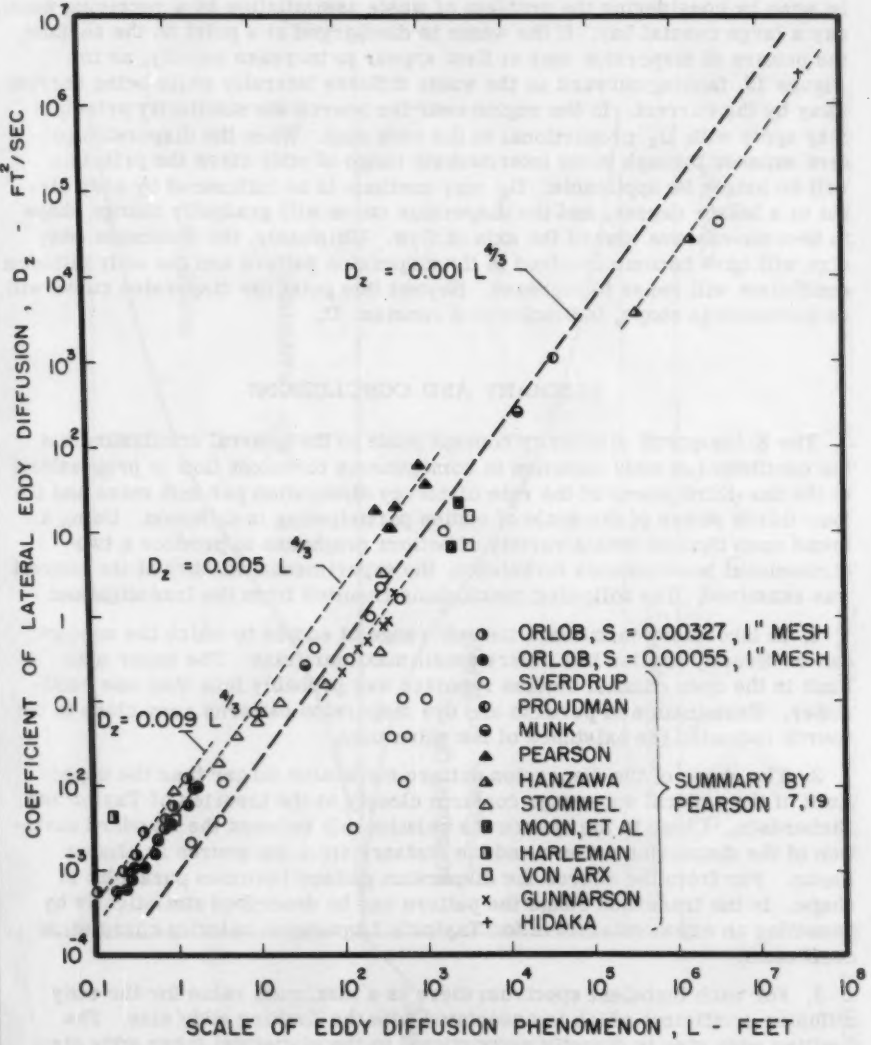


FIGURE 12 EDDY DIFFUSION AS A FUNCTION OF SCALE - SUMMARY OF REPORTED INVESTIGATIONS

The significance of the concept of a limiting diffusion coefficient can best be seen by considering the problem of waste assimilation by a receiving water, say a large coastal bay. If the waste is discharged at a point on the surface, the pattern of dispersion may at first appear to increase rapidly, as in Figure 13, fanning outward as the waste diffuses laterally while being carried away by the current. In the region near the source the similarity principle may apply with $D_z$ proportional to the eddy size. When the dispersion pattern expands through some intermediate range of eddy sizes the principle will no longer be applicable. $D_z$ may continue to be influenced by eddy size but to a lesser degree, and the dispersion curve will gradually change shape to become concave toward the axis of flow. Ultimately, the maximum eddy size will have become involved in the dispersion pattern and the eddy diffusion coefficient will cease to increase. Beyond this point the dispersion curve will be parabolic in shape, indicative of a constant D.

## SUMMARY AND CONCLUSIONS

The Kolmogoroff similarity concept leads to the general conclusion that the coefficient of eddy diffusion in homogeneous turbulent flow is proportional to the one-third power of the rate of energy dissipation per unit mass and the four-thirds power of the scale of eddies participating in diffusion. Using a broad open channel with a variety of bottom roughness to produce a two-dimensional homogeneous turbulence, the experimental validity of the concept was examined. The following conclusions resulted from the investigation:

1. In laboratory turbulence the sub-range of eddies to which the concept can be directly applied has a very small maximum size. The upper size limit in the open channel studies reported was probably less than one centimeter. Examination of particle and dye dispersion patterns very close to the source indicated the existance of the sub-range.

2. The shape of the dispersion pattern for scales larger than the upper limit of the critical sub-range conform closely to the theories of Taylor and Richardson. Close to the source the relationship between the standard deviation of the dispersion pattern and the distance from the source is almost linear. Far from the source the dispersion pattern becomes parabolic in shape. In the transition range the pattern can be described statistically by assuming an exponential form for Taylor's Lagrangian velocity correlation coefficient.

3. For each turbulent spectrum there is a maximum value for the eddy diffusion coefficient which is associated with the limiting eddy size. The limiting eddy size is directly proportional to the statistical mean eddy size.

4. The Kolmogoroff similarity principle adequately describes the relationship between the ultimate lateral eddy diffusion coefficient $D_z(\infty)$, the Lagrangian mean eddy size $L_a$, and the rate of energy dissipation per unit mass E, in statistically homogeneous flow in broad open channels. The equation

$$D_z(\infty) = 0.0136\, E^{1/3} L_a^{4/3}$$

characterizes 105 turbulence conditions investigated.

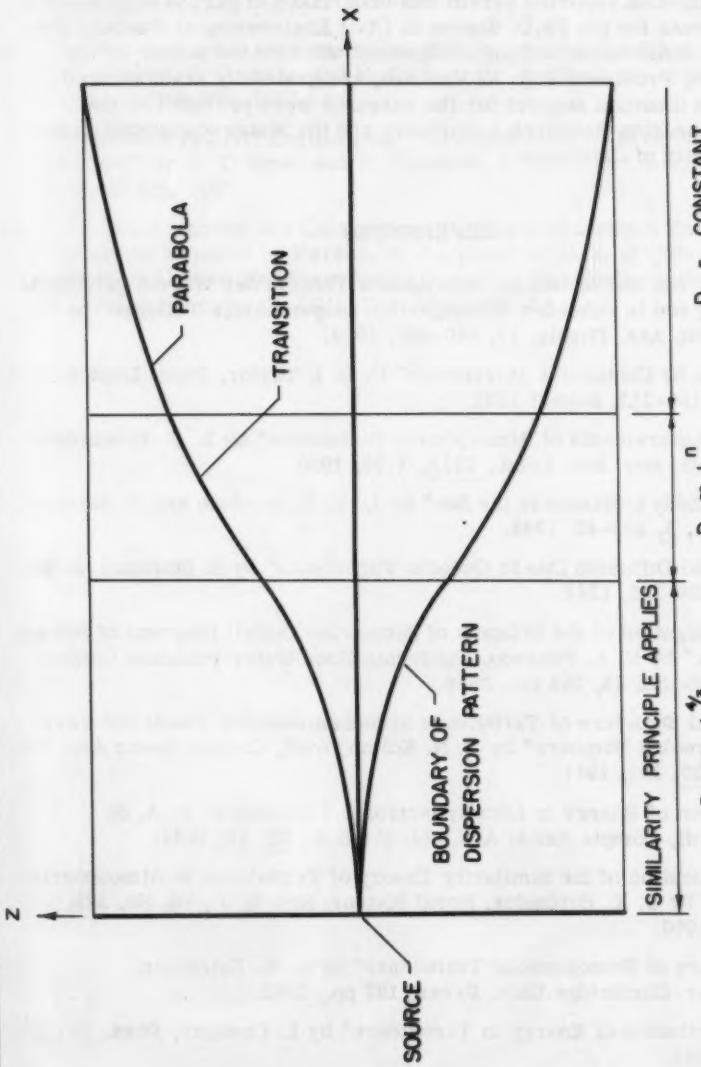


FIGURE 13 GENERAL DISPERSION PATTERN FROM A POINT SOURCE

## ACKNOWLEDGMENTS

The investigation reported herein was undertaken in partial fulfillment of the requirements for the Ph.D. degree in Civil Engineering at Stanford University. The consultation and encouragement afforded the author by his thesis advisor, Professor John K. Vennard, are gratefully acknowledged. Facilities and financial support for the research were provided by the Sanitary Engineering Research Laboratory and the Water Resources Center of the University of California.

## REFERENCES

1. "Über die von der molekular-kinetischen Theorie der Wärme geforderte Bewegung von in ruhenden Flüssigkeiten suspendierten Teilchen" by A. Einstein, Ann. Physik, 17, 549-560, 1905.
2. "Diffusion by Continuous Movements" by G. I. Taylor, Proc. London Math. Soc., 20, 196-211, August 1921.
3. "Some Measurements of Atmospheric Turbulence" by L. F. Richardson Phil. Trans. Roy. Soc. Lond., 221A, 1-28, 1920.
4. "Note on Eddy Diffusion in the Sea" by L. F. Richardson and H. Stommel, J. Meteor., 5, 238-40, 1948.
5. "Horizontal Diffusion Due to Oceanic Turbulence" by H. Stommel, J. Mar. Res., 8, 199-225, 1949.
6. "An Investigation of the Efficacy of Submarine Outfall Disposal of Sewage and Sludge" by E. A. Pearson, California State Water Pollution Control Board, Pub. No. 14, 154 pp., 1956.
7. "The Local Structure of Turbulence in Incompressible Fluids for Very Large Reynolds Numbers" by A. N. Kolmogoroff, Compte Rendu Aca. Sci. U.S.S.R., 30, 301, 1941.
8. "Dissipation of Energy in Locally Isotropic Turbulence" by A. N. Kolmogoroff, Compte Rendu Aca. Sci. U.S.S.R., 32, 16, 1941.
9. "The Application of the Similarity Theory of Turbulence to Atmospheric Diffusion" by G. K. Batchelor, Royal Meteor. Soc. Q. J., 76, No. 328, 133-146, 1950.
10. "The Theory of Homogeneous Turbulence" by G. K. Batchelor, Cambridge: Cambridge Univ. Press, 197 pp., 1953.
11. "The Distribution of Energy in Turbulence" by L. Onsager, Phys. Rev., 68, 286, 1945.
12. "Das Spektrum der Turbulenz bei grossen Reynoldsschen Zahlen," by von Weizsäcker, Z. Phys., 124, 614-627, 1948.
13. "A Review of the Statistical Theory of Turbulence" by H. L. Dryden, Proc. Roy. Soc. London, 156A, 1935.
14. "Investigation of Turbulent Flow in a Two Dimensional Channel" by J. Laufer, NACA Rep. 1053, 1951.

15. "Appariel de measures de la correlation dans le temps et l'espace" by A. Favre, J. Gaviglo, and R. Dumas, Proc. 8th Congr. Appl. Mech., Istanbul, 307-314, 1952.

16. "Quelque measures de correlation dans le temps et l'espace en soufflerie" by A. Favre, J. Gaviglo, and R. Dumas, Proc. 8th Congr. Appl. Mech., Istanbul, 314-324, 1952.

17. "Turbulence in Civil Engineering: Measurements in Free Surface Streams" by A. T. Ippen and F. Raichlen, J. Hydr. Div. ASCE, Paper 1392, 27 pp., 1957.

18. "The Measurement and Calculation of Stream Reaeration Ratio" discussion of paper by Person, E. A., paper by D. J. O'Connor, Seminar, Dissolved Oxygen Relationships in Streams, Taft Sanitary Engrg. Center, U.S.P.H.S., Cincinnati, Ohio, Oct. 30-31, 1957.

Journal of the

HYDRAULICS DIVISION

Proceedings of the American Society of Civil Engineers

CONTENTS

DISCUSSION

Page

Some Experiments With Emergency Siphon Spillways, by Warren B. McBirney. (Proc. Paper 1807, October, 1958. Prior Discussion: 2012. Discussion closed.)
by Warren B. McBirney (closure) . . . . . 105

Evaporation of Lake Ontario, by Ira A. Hunt, Jr. (Proc. Paper 1934, February, 1959. Prior Discussion: none. Discussion closed.)
by Max A. Kohler . . . . . 109

Problems Concerning Use of Low Head Radial Gates, by Thomas J. Rhone. (Proc. Paper 1935, February, 1959. Prior Discussion: 2097. Discussion closed.)
by J. R. Bowman . . . . . 113

Calibration of a Submerged Broad-Crested Weir, by Richard A. Smith. (Proc. Paper 1960, March, 1959. Prior Discussion: none. Discussion closed.)
by P. K. Kandaswamy and N. Rajaratnam . . . . . 119
by T. R. Anand . . . . . 124

Tabular Solution of Open Channel Flow Equations, by H. A. Babcock. (Proc. Paper 1961, March, 1959. Prior Discussion: none. Discussion closed.)
by R. Silvester . . . . . 125
by Ivan M. Nelidov . . . . . 127
by Walter J. Tudor . . . . . 131
by Warren W. DeLapp . . . . . 133

(Over)

Note: Paper 2182 is part of the copyrighted Journal of the Hydraulics Division, Proceedings of the American Society of Civil Engineers, Vol. 85, HY 9, September, 1959.

Page

Relationships Between Pipe Resistance Formulas, by W. L. Moore. (Proc. Paper 1962, March, 1959. Prior Discussion: 2097. Discussion open.)
by K. Szesztay . . . . . 137
by Henry J. Miles . . . . . 141
by M. B. McPherson . . . . . 143
by Nicholas Bilonok . . . . . 155
by J. V. Dawsey . . . . . 157

Hydraulic Analysis of Surge Tanks by Digital Computer, by Mr. Nicholas Barbarossa. (Proc. Paper 1996, April, 1959. Prior Discussion: none. Discussion closed.)
by Charles Jaeger . . . . . 159

Two Methods to Compute Water Surface Profiles, by J. M. Lara and K. B. Schroeder. (Proc. Paper 1997, April, 1959. Prior Discussion: 2076, 2138. Discussion closed.)
by R. Silvester . . . . . 163

# SOME EXPERIMENTS WITH EMERGENCY SIPHON SPILLWAYS[a]

## Closure by Warren B. McBirney

WARREN B. McBIRNEY,[1] M. ASCE.—The writer is indebted to Messrs. Fred W. Blaisdell and Harold W. Humphreys for their interest in preparing a discussion and in offering for consideration the drop inlet type of structure.

Since much of the discussion centers around the definition of a siphon, it might be well to analyze the two definitions given. The first, to which the writer subscribes, defines a siphon "as a spillway which requires that the liquid be lifted above the headpool level." This definition is supported by Russell,(1) Addison,(2) and Rouse.(3) The Bureau of Reclamation so classifies such a structure, though this position admittedly is based on applied considerations and not theoretical ones.

The second definition, which the authors suggest as being appropriate, is "a closed conduit, a portion of which lies above the hydraulic grade line." Three Bureau structures are named as qualifying as siphons, the Heart Butte and Shadehill morning-glory spillways in the Dakotas, and the Hungry Horse morning-glory in Montana. The writer believes none of these operate as siphons, even by the authors' definition. All three spillways were studied extensively by model experiments. In general it can be said that certain portions of the profiles showed negative pressures for the unsubmerged flow conditions, but those pressures prevailed in areas below the crest sections which received radial or near-radial flow, and not between certain elevations for the full circumference. Thus, the low pressures were similar to those on an ogee shape, and were related to tendencies for flow separation from the boundaries because of imperfect profiles. Since the upper nappe surfaces were essentially at atmospheric pressure no siphon head could exist because the flow was of the open channel type.

The possibilities of extremely low pressures occurring with submerged flow conditions were indeed recognized. At Heart Butte a combination of nine air inlets and deflectors was installed 11.5 feet below the crest and an aerated flow deflector placed on the crown side of the shaft 31.5 feet below the crest. Further, the tunnel diameter diverged from 11 to 14 feet in diameter around the bend. Pressure tests at submerged flow showed negative pressures no greater than about -5 feet of water in certain areas, with no indication that low pressures existed around the entire circumference, as would have been the case if a closed conduit siphon head had been acting.

There was less opportunity for low pressures in the Shadehill spillway because of the large spillway and tunnel diameters and the short drop of 33 feet

a. Proc. Paper 1807, October, 1958, by Warren B. McBirney.

1. Hydr. Research Engr., Div. of Eng. Laboratories, Bureau of Reclamation, Denver, Colo.

to the invert of the bend. Negative pressures not exceeding -3 feet of water occurred for weir-flow discharges less than 60 percent of design capacity, and all measured pressures were well above atmospheric at capacity flow. Even so, a flow deflector was installed on the crown side of the shaft 14 feet below the crest to insure open channel flow from the deflector downstream to the tunnel outlet.

The Hungry Horse morning-glory was studied in one of the most thorough investigations ever conducted by the Bureau. The negative pressures on the profile were deliberately created to increase the discharge coefficient and were restricted to areas below portions of the crest receiving radial or near-radial flow. Other negative pressures were relieved by an air vent. An air intake structure of 36 square feet cross-section was installed on the crown side of the shaft 31 feet below the crest. This conduit had sufficient air capacity to prevent the shaft and tunnel from flowing full for any flow or crest head thought possible at the site. The writer as well as the research engineers responsible for these tests believe there is no possibility of the Hungry Horse spillway and tunnel ever flowing full.

None of these structures in model or prototype has shown any evidence of siphonic action in the sense that a full conduit was acting to influence the rate of flow at higher elevations in the shaft or tunnel. No priming or depriming aids were built since the structures were not envisioned as siphons and every effort to prevent siphon action was made. The air demand of each structure was more than satisfied with oversized conduits to prevent unsteady rates of intake. This is not the type of partialization desired by the writer.

With the above description of the operation of these spillways completed, the writer is now prepared to admit that a morning-glory or drop inlet spillway flowing submerged with an unaerated shaft of sufficient drop in elevation will exhibit flow characteristics akin to those in the downstream leg of a saddle or volute siphon. It is doubtful, however, whether the engineer who produces such a cavitation structure would derive much credit for his design.

The head-discharge curve in Figure A of the discussion, for the drop inlet closed conduit spillway, is very similar to a typical morning-glory head-discharge curve. Placing an antivortex flat plate over an inlet 3 inches in diameter may appear to offer control of the vortex and a uniform proportioning of air and water. Trial of a similar scheme in a model of the Trinity Dam morning-glory, northern California, model size 24 inches in diameter at the crest, brought near-disastrous results to the clear plastic of the shaft. Air was sucked under the plate intermittently instead of steadily, pressures in the shaft varied rapidly between -10 and -30 feet of water (prototype), the forebay supplying the structure was soon set in rhythmic motion, and the model vibrated violently. Such action in the prototype would cause serious damage in a short time.

The writer suggests that the authors employ a high frequency response pressure cell and oscillograph to a piezometer centered in an antivortex plate over a drop inlet spillway. Lack of visible fluctuations in the head pool for a 3-inch-diameter inlet may not be adequate proof of stability in the setup.

Near the end of their discussion the authors applied a linear multiplication factor to compare operation of the Bureau saddle siphons with the drop inlet spillways. Such a comparison by this means is not believed to be valid for the following reasons:

1. Even assuming both types of structures to be siphons, scale relationships for siphons are still very much in doubt and are probably not linear.

2. The authors compare by the multiplication factor a head on the drop inlet which "caused the Illinois spillway to prime" to the heads for maximum capacity flows in the standard and proposed designs. The latter heads were reached long after both siphons began priming. Actually, the standard siphon started to prime with about 0.13 foot of head and the proposed siphon required about 0.015 foot of head. Both heads are less than the 0.17 foot shown by the authors for the Illinois spillway.

Neither the authors in their discussion nor the writer in his paper offered any information on the effects of changing the rates of rise in the forebays of respective spillways. The Bureau test setup was not flexible enough to vary the rate of rise for any discharge, but other experimenters in the world have been able to do so. Findings are that the lower the rate of rise for a given discharge the lower will be the head required to cause the siphon to prime. Thus, it is quite probable that the authors' and writer's spillways will prime at lower heads for lower rates of rise.

The authors state that extending skirts from the antivortex plate downward below the weir crest modifies the structure to the form of a vortex siphon spillway and that the head-discharge curve then obtained is similar to those shown for the standard and proposed siphons. This would seem to be excellent evidence that there are fundamental differences in the two types of structures and that only one of them should be classified as a siphon.

The writer does not doubt that the drop inlet closed conduit spillway has many uses, but in its current form it does not appear to fit requirements of the Bureau of Reclamation for an emergency spillway.

## REFERENCES

1. "Hydraulics," George E. Russell, p 213, Henry Holt and Company, 1942.

2. "A Treatise on Applied Hydraulics," Herbert Addison, pp 200-202, John Wiley and Sons, Inc., 1945.

3. "Elementary Mechanics of Fluids," Hunter Rouse, p 121, John Wiley and Sons, Inc., 1946.

# EVAPORATION OF LAKE ONTARIO[a]

Discussion by M. A. Kohler

MAX A. KOHLER,[1] F. ASCE.—Major Hunt states that there are several methods of computing evaporation—mass transfer, water budget and energy budget—only the first two of which he has applied to Lake Ontario. In addition to the methods cited by the author, there is the evaporation-pan approach as well as several others which constitute combinations of the four. It should also be emphasized that there exists a multitude of mass-transfer evaporation equations which have been derived by numerous investigators.

Considering, first, the mass-transfer approach, it will be noted that the author's equation (Eq. 7) relates evaporation to the vertical gradient of horizontal wind speed over the lake and that the empirical constant was derived from data collected at Lake Hefner, Okla.(1) Although one might expect to obtain satisfactory estimates of normal monthly wind speed over the water from shore anemometers, corresponding estimates of the vertical gradients are likely to be appreciably in error. In the Weather Bureau's analysis of the Lake Hefner data,(2) several mass-transfer equations were derived empirically which require wind movement instead of wind gradient. One of the equations is

$$E = 0.00304\ U_4\ (e_0 - e_2) \qquad (A)$$

where $E$ is the lake evaporation in inches per day, $U_4$ is the 4-meter wind movement in miles per day, $e_0$ is the saturation vapor pressure at the temperature of the water surface (inches of mercury), and $e_2$ is the 2-meter vapor pressure over the water, also inches of mercury. The constant of this equation is based on records for 115 days when the water-budget data were judged to be accurate within 5 percent. The correlation coefficient is 0.956—much higher than the author cites for his equation.

Equation (A) has been applied to Lake Ontario using the author's data (Table 7) with the results shown in Table A. It will be noted that Eq. (A) provides a better fit with the water budget than does the author's Eq. (7), on a monthly basis as well as for the year as a whole.

The Weather Bureau(3) has recently completed a series of United States maps showing:

1. Mean annual free-water evaporation
2. Mean annual class A pan evaporation
3. Annual class A pan coefficient (ratio of free-water to pan evaporation).
4. Percent of annual class A pan evaporation occuring during the summer (May-Oct).

a. Proc. Paper 1934, February, 1959, by Ira A. Hunt, Jr.

1. Chf. Research Hydrologist, U. S. Weather Bureau, Washington, D. C.

Table A. LAKE ONTARIO EVAPORATION

| Month | Wind ($U_4$)[a] mi/day | Vapor pressure[b] difference ($e_0 - e_2$) inches of Hg | Evaporation in feet Eq.(A) | Eq.(7) | Water budget |
|---|---|---|---|---|---|
| Jan | 402 | .081 | .26 | .23 | .19 |
| Feb | 389 | .077 | .21 | .19 | .10 |
| Mar | 307 | .073 | .18 | .16 | .06 |
| Apr | 284 | .039 | .08 | .09 | .04 |
| May | 192 | .001 | .00 | .00 | .04 |
| Jun | 163 | .013 | .02 | .02 | .00 |
| Jul | 181 | .132 | .19 | .18 | .11 |
| Aug | 190 | .157 | .23 | .22 | .28 |
| Sep | 220 | .191 | .32 | .27 | .32 |
| Oct | 231 | .150 | .27 | .23 | .38 |
| Nov | 292 | .100 | .22 | .20 | .35 |
| Dec | 395 | .076 | .24 | .21 | .34 |
| Annual | | | 2.22 | 2.00 | 2.21 |

a. At Lake Hefner, 4-meter wind averaged 0.90 that at 8-meters. This factor was applied to the data in the author's Table 7 and converted to miles per day.

b. The author's vapor-pressure difference values are incorrectly labeled as "millibars". Strictly speaking, Eq. (A) requires the 2-meter vapor pressure over the water rather than the average for several stations around the lake.

5. Standard deviation of annual class A pan evaporation.

The computations(4) were based on records for the period 1946-55. In the course of deriving the free-water map, evaporation was computed from solar radiation (or percent sunshine), dewpoint, air temperature and wind for six meteorological stations adjacent to Lake Ontario. The computed values (ft/yr) are as follows:

| | | | |
|---|---|---|---|
| Toronto | 2.27 | Oswego | 2.36 |
| Buffalo | 2.37 | Syracuse | 2.50 |
| Rochester | 2.56 | Canton | 2.19 |

It would appear from these results that the 10-year mean evaporation from the lake is near two and one-quarter feet—a value in close agreement with our mass-transfer and the author's water-budget results.

Having essentially substantiated the author's water-budget value (2.21 ft/yr) by two independent approaches, it is indeed unfortunate that a question must be raised concerning the value used for lake precipitation. Early results from the island network on Lake Michigan have led the author to conclude that annual precipitation over Lake Ontario is only 2.30 ft. as compared to 2.92 ft. on the tributary drainage. The observational program is still in progress on Lake Michigan and final conclusions must await further analysis. Nevertheless, present indications are not entirely in accord with the author's interpretation.

Table B shows record-mean summer, winter and annual precipitation for the island stations and comparative data for a group of lake-shore stations. There can be little doubt that the islands (and the lake) receive less summer

precipitation that would be indicated by an average of the shore stations. But is this deficiency compensated by an excess during the winter months? The records from South Manitou (and possibly Beaver Light Station) indicate this is the case.

The author concludes that at least part of the differences among the island data result from the fact that the larger islands produce an increase of precipitation. It would seem that any heating effect should be greatest at the downwind side of a small island (and likely even beyond) whereas St. James and the Light Station are on the northern and southern portions of Beaver Island, respectively. Some of those concerned with the project have felt for some time that virtually all the differences could be explained by relative windiness at the gage sites.

In July 1958, anemometers were installed at four of the island stations (gage-orifice height) which were read in the latter part of the following October. Mean wind speeds (mph) for the period were as follows:

| | |
|---|---|
| St. James, Beaver Island | 4.04 |
| Beaver Island Light Station | 2.05 |
| Ile Aux Galets | 7.02 |
| Shoe Island | 7.61 |

Without going into details in this discussion, examination of the wind data and photographs of the gage exposures show conclusively that the relative catch of the island gages is highly correlated with windiness.

Table B. LAKE MICHIGAN PRECIPITATION, (SIX-YEAR MEANS, 1952-1958), IN INCHES

| STATION | Summer | Winter | Annual |
|---|---|---|---|
| St. James, Beaver Island | 13.19 | 12.87 | 26.06 |
| Beaver Island Light Station | 13.34 | 14.91 | 28.25 |
| South Manitou Island | 13.68 | 15.04 | 28.72 |
| North Manitou Island | 12.46 | 14.56 | 27.02 |
| South Fox Island | 13.39 | 12.21 | 25.60 |
| Gull Island | 13.02 | 13.29 | 26.31 |
| Ile Aux Galets | 10.79 | 9.04 | 19.83 |
| Shoe Island* | 11.80 | 8.14 | 19.94 |
| Shore stations (weighted)+ | 14.87 | 13.86 | 28.73 |

* Two years (1956-58) for which the shore-station precipitation averaged 14.96, 13.22 and 28.18 for the summer, winter and annual periods, respectively.

\+ All gages in the group are shielded. Unshielded gages at the same sites receive a few percent less precipitation, on the average.

In the light of Wilson's[5] studies of wind vs. gage catch, it would now appear that annual precipitation over Lake Michigan may not be significantly less than that observed at a network of shore stations.

Assuming that the average annual precipitation observed at a network of eight stations along the shores of Lake Ontario is equivalent to that over the lake, the value in Column 6 of the author's Table 1 becomes 2.76 ft. The water-budget evaporation then becomes 2.67 ft. instead of 2.21 ft. Since this revised value is appreciably higher than that derived by any of the other methods, the writer has attempted to check the results for a different period of record (1946-55) as follows:

| | |
|---|---|
| Precipitation (average of 8 shore stations) | 2.84 feet |
| Runoff (104% of 1934-53 as indicated by average of 4 tributary basins) | 5.04 |
| Inflow (Niagara River at Buffalo, N. Y., plus Welland Canal) | 32.69 |
| Outflow (St. Lawrence River at Ogdensburg, N. Y.) | 38.63 |
| Change in stage (dropped 1.05 ft. in 10 years) | 0.11 |
| Computed evaporation (1946-55) | 2.05 |

It is entirely possible that the evaporation was less in 1946-55 than for the longer period 1934-53, but much of the difference (2.05 and 2.67 ft.) is believed to be erroneous. Without belaboring possible sources of errors in water-budget computations, it should be pointed out that bank-storage effects would be of proper sign with respect to the two periods—the lake level dropped 0.11 ft. per year during the period 1946-55 and rose 0.11 ft. per year during 1934-53. Even so, any realistic assessment of the reliability of the water-budget for this particular lake will show that an error of one-half foot in the annual evaporation is not unlikely. A bias of only one percent in the inflow and outflow items amounts to about 0.7 ft. over the lake.

## REFERENCES

1. Water-loss Investigations: Lake Hefner Studies, Base Data Report, U. S. Geol. Survey Prof. Paper 270, 1954.
2. Kohler, M. A., Lake and Pan Evaporation, Water-loss Investigations: Lake Hefner Studies, Technical Report, U. S. Geol. Survey Prof. Paper 269, p. 137, 1954.
3. Evaporation Maps of the United States, U. S. Weather Bureau Tech. Paper (in process).
4. Kohler, M. A., T. J. Nordenson, and W. E. Fox, Evaporation from Pans Lakes, U. S. Weather Bureau Research Paper 38, May 1955.
5. Wilson, W. T., Discussion of paper, Precipitation at Barrow, Alaska, Greater than Recorded, Trans. Am. Geophys. Union, Vol. 35, pp. 206-207, Apr. 1954.

# PROBLEMS CONCERNING USE OF LOW HEAD RADIAL GATES[a]

## Discussion by J. R. Bowman

J. R. BOWMAN,[1] M. ASCE.—Mr. Rhone's paper constitutes a significant contribution toward a better understanding of the hydraulic characteristics of tainter (radial) gates. The author and the USBR should be congratulated for sharing with the profession the knowledge gained through research supported by public funds; in many instances, the results of basic research carried out by public agencies has been imprudently labeled "Restricted" or "Not for General Distribution."

### Discharge Characteristics

Quite often it is desirable to derive accurate rating curves for discharge under a tainter gate, without recourse to a model test program specifically organized for this purpose. This is often the case for smaller regulating works whose total costs do not warrant expenditures for model tests. In a few instances, it has been possible to check or modify analytical predictions by means of field measurements; more often than not, however, comprehensive field tests will not be feasible, with the result that the responsibility for accurate discharge predictions will rest solely with the designer.

The problem of how best to determine part gate discharge probably has been encountered as long as tainter gates have been in use. Where the gate sill is located at the weir crest, the rating curves for the gate will be similar to those of a vertical-lift gate, provided that the centerline of trunnions is not appreciably higher than the centerline of the gate. Where the trunnions are located at the elevation of headwater, or higher, the approach angle $\theta$ exerts considerable influence on the value of the discharge coefficient, as shown in Figure 3. In cases in which the gate sill is located downstream from the weir crest, a shifting control is encountered; The control point moves gradually from the gate sill, at small openings, to the weir crest as full gate opening is approached. Cases in which the gate sill is located upstream from the crest are not often encountered, inasmuch as such a gate setting usually results in increased costs of associated structures which may more than offset any saving in gate costs.

In the development of rating curves for a tainter gate whose sill is located at the weir crest, the writer, as well as many of his predecessors, has utilized a method whose validity is largely confirmed by the data presented in Figure 4. When the approach angle $\theta$ lies generally between 75 and 105 degrees, the free discharge coefficient can be applied to all gate openings,

a. Proc. Paper 1935, February, 1959, by Thomas J. Rhone.
1. Civ. Engr., Erik Floor and Assocs., Inc., Chicago, Ill.

with an average error of less than 5 percent. The writer is acquainted with a few such cases in which field measurements and predicted values differed by not over 5 percent.

Although no simple and accurate method has yet been devised for computing the discharge under a tainter gate whose sill is located downstream from the weir crest, Mr. Rhone has presented information which may well serve as the basis for the effective utilization of a combination of methods.

On the basis of analyses of a number of rating curves based on model studies, the writer can make the following generalizations:

1) For gate openings ranging from near zero (gate closed) up to 15 or 20 percent of full gate, with discharge coefficients related to the head on the weir crest, the application of the modified weir formula (first equation) results in discharge coefficients that vary from unrealistically high values at near zero opening to values nearly equal to the free discharge coefficient at somewhat larger openings. ("Full gate" is defined herein as the gate opening at which the upper nappe breaks clear of the bottom edge of the gate.)

2) For the same range in gate openings, but with discharge related to the head on the gate sill, application of the orifice formula results in a nearly constant range in discharge coefficients. This observation is substantiated by the curves of Figure 6.

3) For larger gate openings, the discharge coefficient, expressed in terms of the head on the weir crest, is nearly constant and can be closely related to the free discharge coefficient.

In cases in which extreme accuracy has not been required, the writer has made use of an approximation which combines both analytical and graphical methods, and which expresses discharge as a function of gate opening; the procedure, for a given headwater condition, is as follows:

1) Determine the depth of water on the gate sill at free discharge, considering this depth as "full gate." For the majority of downstream settings on ogee crests, it can be assumed that critical depth will occur in the immediate vicinity of the gate sill. Any corrections in depth or discharge, due to end contraction, velocity of approach, etc., should be made at this time.

2) Compute and plot discharge versus gate opening from zero opening to approximately 25 percent of "full gate" by means of the orifice equation and the discharge coefficients of Figure 6.

3) Draw a straight line, passing through the full gate point of step (1) and tangent to the curve of step (2). This completes the rating curve for a given headwater condition.

In conjunction with step (2) above, it should be stated that, although the definition of gate opening shown in Figure 6 represents good academic practice, a good deal of manipulation is required for the precise determination of any gate opening. It is suggested that computations could be simplified by expressing gate opening as a vertical distance above the gate sill, and by adjusting discharge coefficients accordingly; any differences in gate settings and/or crest shape then would be accounted for by the approach angle $\theta$, which could be determined graphically with sufficient accuracy for any purpose.

In reference to the author's apparent bewilderment concerning the results shown in Figure 7, it should be apparent that, for gate sills located downstream from the crest, the approach angle and, consequently, the coefficient of discharge should be less than for a weir crest setting. This trend is amply illustrated by the author's Figure 6.

The author's dream of large models set up for the sole purpose of research in the field of gate discharge relationships is heartily shared by the writer, whose interests in such matters, unfortunately, are not supported by the means for carrying out such a program. It should be of interest to learn whether the Bureau contemplates such a comprehensive program in basic research.

## Pressure Characteristics

The results of the pressure profile studies are very well explained by the author; as such, they incite very little comment on the part of the writer. He would like to be informed as to the basis for derivation of the profile used as a datum in the series of tests. In passing, it is of interest to note that the spillway at American Falls, which was designed a good many years ago and without the benefits of present-day knowledge, is in no imminent danger of failure due to negative pressures on the ogee.

## Gate Seals

It is obvious that this portion of the paper deals primarily with seals that are currently being developed or applied by the Bureau of Reclamation. It is not improbable that there are as many different preferred combinations of seal types and methods of application as there are gate designers. However, merely describing several popular combinations would likely exceed the limitations placed on the length of a paper.

Although it is universally conceded that low head tainter gates should be equipped with side seals, it does not necessarily hold that they must also be provided with bottom seals attached to the gates themselves. In a good many early installations, the bottom edge of the skin plate was arranged to bear on a creosoted timber, which was bolted into the supporting structure so that its top face was flush with the canal floor or weir crest. At Dix Dam in Kentucky, vertical-lift spillway gates sealing against timber sills were installed in the early 1930's; the original timbers continue to provide practically a drop-tight seal after more than 25 years of service. In a number of fairly recent installations, the skin plate rests on a soft metal, such as babbitt or lead, which has been melted and poured into a structural channel, or other suitable member, embedded in the floor or weir surface. Such installations have not always met with the anticipated degree of success; their shortcomings generally stem from one of two sources:

1) In cases concerning small gates, the weight of the gate does not provide adequate indentation of the soft metal, with the result that a uniform degree of contact is not achieved.

2) In the case of a rather deep gate, the hydrostatic pressure at the sill of a closed gate induces a wire-drawing action; this results in pinhole or sheet jets under the skin plate.

Where rubber bottom seals are necessary, the writer ordinarily does not subscribe to the practice of placing the seal on the downstream face of the skin plate; he prefers to place the seal on the upstream face, so that hydrostatic pressure can assist in effecting final closure. In his opinion, the only practical difficulty that might arise from the latter practice is that an upstream seal presents a local obstacle to streamline flow and to direct mathematical treatment.

In the application of side seals, the writer is strongly in agreement with the author in that a nominal amount of seal preset is necessary to assure positive contact between the seal and the embedded seal plate. If no preset were provided, a number of factors could reduce (and have been known to reduce) the effectiveness of the seal:

1) Inaccuracies in field alignment of seal plates and/or seals can result in excessive out-of-true humps and sags.

2) A certain amount of lateral play accompanies the vertical movement of tainter gates; it may be limited to a fixed amount by rollers or skids, or to a variable amount by limiting forces developed within the seals themselves.

3) Field observations indicate that the contact face of a seal acquires some permanent set, resulting from age and usage; the softer the contact face or the more flexible the seal bulb (as for "J-seals"), the greater the amount of permanent set.

Seal preset does, of course, introduce frictional forces in addition to the amount attributable to hydrostatic pressure alone. This has led many to consider the possible application of retractible side seals, wherein all frictional forces would be absent while the gate is being raised or lowered; full hydrostatic pressure would be utilized to force the seals into contact with the seal plates only after the gate has reached its closed position. Prominent among those individuals was the late L. F. Harza; several years ago, he conducted a series of model studies devoted to exploring the possible application of retractible seals to tainter crest gates. A significant observation derived from his studies is the fact that the retractible body of the seal must have considerable inherent stiffness, so that the activating water pressure at lower levels can effect complete closure at headwater level, where hydrostatic pressure equals zero. Moreover, the required stiffness would tend to reduce the flexibility along the contact face to an extent that could require extensive modification in order to regain a portion of the contact flexibility originally lost.

The Bureau's angle seal (or "L-seal") appears to represent a compromise between the two most popular types of "J-seal" mountings. The L-seal incorporates the simple "compression" mounting of the J-seal, in which the seal leaf is directly attached to the skin plate; it also takes advantage of the greater leaf flexibility of the J-seal's "deflection" mounting, while circumventing the "outboard" mounting requirements of the latter. Perhaps the most outstanding advantages of the J-seal are its versatility and low cost; several manufacturers of industrial rubber products offer a wide standard range in J-seal sizes and molded corners. The writer would be very much interested in learning how the L-seal negotiates the bottom corners of a radial gate.

His small contribution to an engineering handbook[9] has made the writer aware that a comprehensive coverage of the problems besetting the designer

of tainter gates would be a voluminous undertaking. He also wonders whether the limited audience would even pay the printer's costs.

The writer gratefully acknowledges the cooperation of Mr. Richard D. Harza, A.M. ASCE, of the Harza Engineering Company, Chicago, Ill., in his consent to make public certain observations derived from the unpublished works of the late Leroy F. Harza.

## BIBLIOGRAPHY

9. Bowman, J. S., and Bowman, J. R., "Spillway Crest Gates" section of Handbook of Applied Hydraulics (C. V. Davis, editor-in-chief), Second Edition; McGraw-Hill, New York, 1952.

# CALIBRATION OF A SUBMERGED BROAD-CRESTED WEIR[a]

## Discussions by P. K. Kandaswamy, N. Rajaratnam, and T. R. Anand

P. K. KANDASWAMY,[1] M. ASCE and N. RAJARATNAM[2].—The author has presented a very interesting paper on broad-crested weirs with upstream and downstream slopes. The new method of approach presented therein to find out the modularity limit based on the Froude Number at the center of the weir crest is commendable.

The flow over a weir of any shape can be classified as modular or non-modular as explained below. When the discharge over the weir depends only on the upstream head and is independent of the tail-water head, its performance is said to be modular. When with an increase in tail water depth, this independence ceases and the discharge depends upon both the upstream and downstream head, its performance is said to be non-modular. The limit between these two ranges is called the "modular limit" or "modularity limit."

In the modular range, the discharge over a broad-crested weir with vertical upstream and downstream faces is given by the general equation.

$$Q = C\ B\ H^{3/2} \qquad (1)$$

where

Q is the discharge in cusecs,
C is the coefficient of discharge,
B is the length of the weir in feet normal to the direction of flow and
H is the head in feet over the crest of the weir.

Investigations(1,2,3,4) by various research workers have shown that the coefficient C varies mainly with H/L where L is the width of the crest in the direction of flow and is independent of the velocity of approach represented by the term $\frac{H}{P}$ where P is the height of the weir crest above the approach channel floor. The curve given in Figure 1 shows the variation of C with H/L for a broad crested weir with vertical upstream and downstream faces.

When the broad crested weir is provided with upstream and downstream slopes, the flow pattern and hence the discharge characteristics are likely to be different. Considering the downstream slope first, it is known that when water flows over a broad crested weir, the critical depth occurs over the crest. The exact location of the critical depth section is difficult to define as can be seen from Figure 2. To be sure, the stage of the flow changes from

a. Proc. Paper 1960, March, 1959, by Richard A. Smith.
1. Executive Engr., (Research), Irrig. Research Station, Poondi, India.
2. Junior Engr., (Research), Irrig. Research Station, Poondi, India.

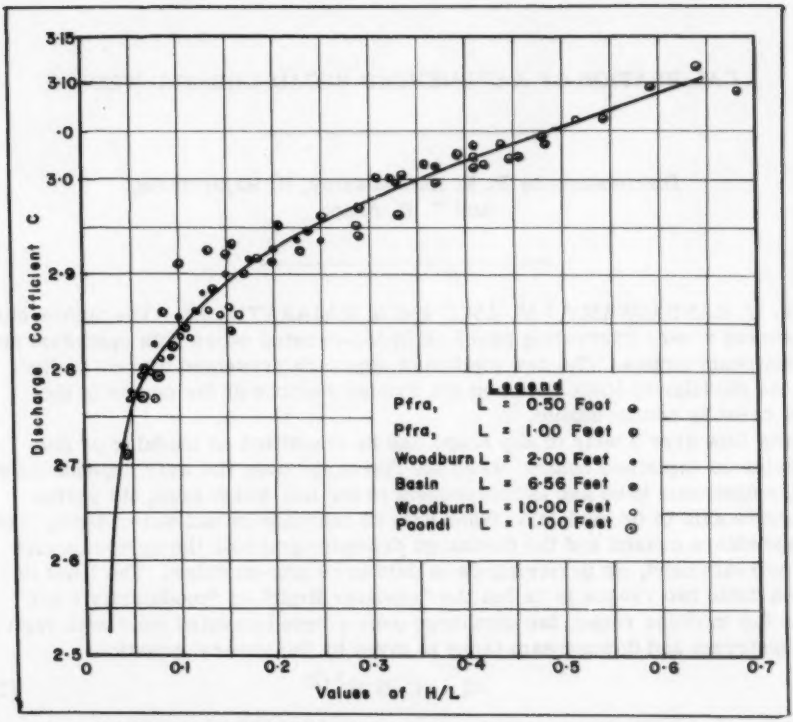


Fig-1 STANDARD COEFFICIENT CURVE FOR BROAD CRESTED WEIRS.

(From Ref-4)

the sub-critical to the supercritical condition over the crest. Hence, so long as the downstream slope provided is steeper than the critical slope for the range of discharges involved, as it happens to be in the case considered by the author, any change in the super-critical downstream slope is not likely to affect the flow pattern over the crest. Consequently, the discharge coefficient C in the equation $Q = C B H^{3/2}$ will be independent of the downstream slope. If in any case, the downstream slope is milder than critical slope for the discharges involved, the tail-water may back up and the modularity limit may occur at some particular slope which may be termed as the "modularity slope."

It has been observed in a general way, that the discharge coefficient for a broad-crested weir increases as the steepness of the upstream slope decreases. To incorporate the effect of upstream slope in the general formula, equation (1) is modified as

$$Q = C \gamma B H^{3/2} \qquad (2)$$

where $\gamma$ is known as the "slope factor." The variation of $\gamma$ with H/L is shown plotted in Figure 3 for values of upstream slope varying from 1/100

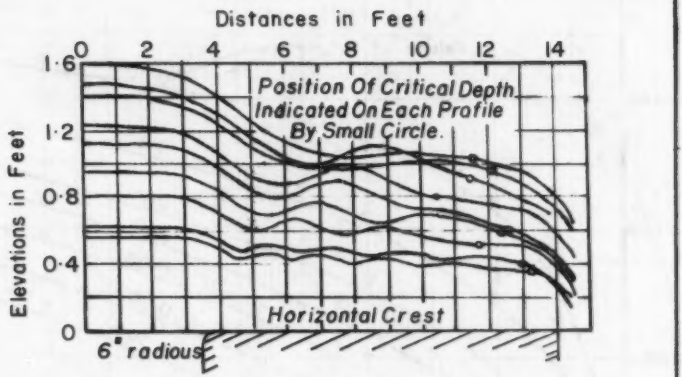


Fig·2· WATER-SURFACE PROFILES AND POSITIONS OF CRITICAL DEPTH ON WEIR WITH HORIZONTAL CREST (From Ref· 3)

to 1/1000. The results are taken from a series of experiments conducted in the Irrigation Research Station, Poondi on bye-washes which are flush escapes for floods provided in small tanks in the State of Madras. Further experiments have to be conducted to collect more information for steeper slopes up to 1/100.

The author has measured the depth of flow at a point located slightly downstream from the center of the weir crest and has calculated the corresponding Froude number. This has been used for defining the modularity limit, that is the stage at which flow changes from modular to non-modular range. When conducting similar experiments at this Research Station, the writers have observed that the water surface over the crest is undulating and that sometimes the same depth occurs at more than two sections. Hence, the writers feel that it may not be very reliable to base any solid conclusion on the depth measured at the section mentioned previously.

Considering the functioning of a broad crested weir in the modular range, any increase above the crest up to the modularity limit does not affect the upstream level. This apparent anamoly has been explained by the writers[5] with the conception of the critical depth section occurring as a control section over the crest and of the celerity of the breaking surge. In the paper referred above, it has been concluded that until the modularity limit is attained, the critical depth occurs somewhere on the crest. In fact, it can be seen that with a steady increase in the tailwater level, the critical depth keeps on moving downstream over the crest up to the modularity limit when it falls into the relatively deeper downstream portion. This conclusion agrees indirectly in a qualitative manner with that of the author that the change in control occurs when the Froude number is approximately 0.78 at the section chosen.

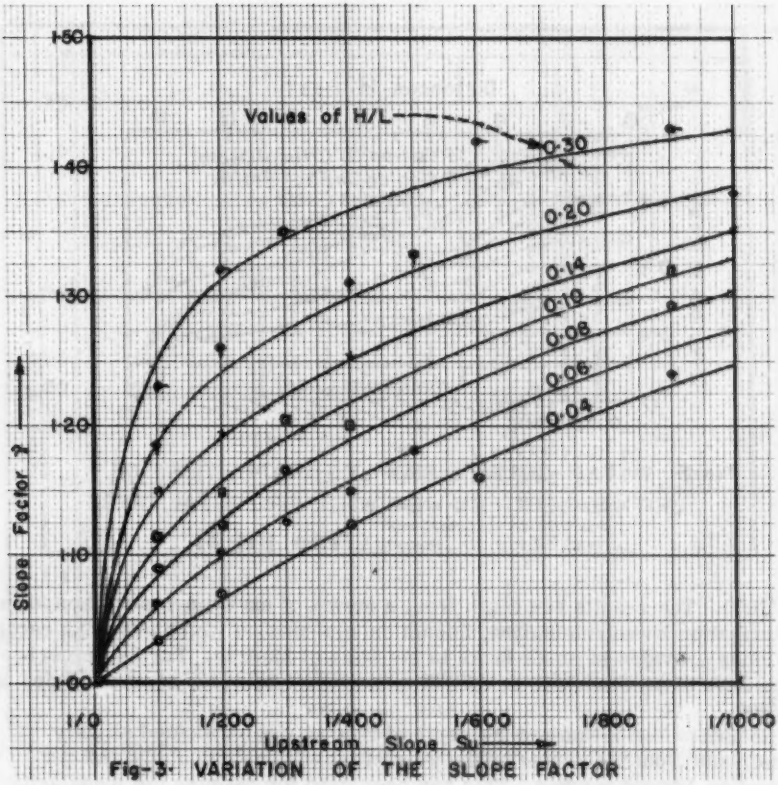


Fig-3· VARIATION OF THE SLOPE FACTOR

Further, the discharge for a broad crested weir in the non-modular range is given by the relation(2)

$$Q = Q_m f \qquad (3)$$

where Q is the actual non-modular discharge,

Qm is the modular discharge for the given upstream head and f is a reduction factor which is a function of the submergence ratio $\frac{Z}{H}$ and $\frac{H}{L}$, Z being the height of the tail water above the crest.

The variation of the reduction factor f with the submergence ratio $\frac{Z}{H}$ for a weir called Kodiveri Anicut(5) is given in Figure 4. Studies on Dowlaishwaram Anicut(6) indicate the variation of f with H/L. For a broad crested weir with upstream and downstream slopes, it is likely that

$$f = \phi\left\{\frac{Z}{H}, \frac{H}{L}, S_u, S_d\right\} \qquad (4)$$

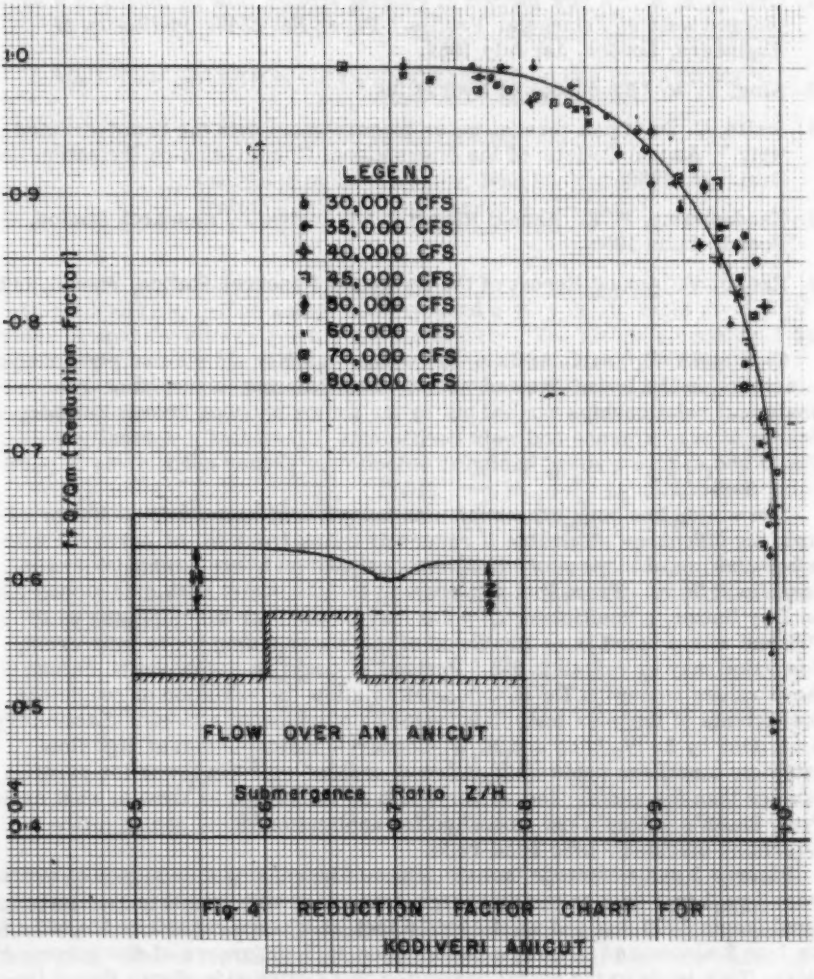


Fig 4 REDUCTION FACTOR CHART FOR KODIVERI ANICUT

where Su is the upstream slope and $S_d$ is the downstream slope of the weir. The nature of the function can be studied by detailed experimentation.

## REFERENCES

1. Woodburn J. G. "Tests of Broad-crested weirs" Transactions of the American Society of Civil Engineers, Vol. 96, 1932.

2. Crump, E. S. "A new method of gauging stream flow by means of a submerged weir of Triangular Profile." Paper No. 2848. Institution of Engineers, London, 1st July 1952.

3. King, H. W. "Hand-book of Hydraulics."

4. Smith, C. D. "Open channel water measurement with the broad-crested weir." Annual Bulletin of the International Commission on Irrigation and Drainage, 1958.

5. Kandaswamy, P. K. Annual Report of the Irrigation Research Station, Poondi, India 1958.

6. Rao, J. V. Annual Report of the Irrigation Research Station, Poondi, India. 1951.

T. R. ANAND,[1] A.M. ASCE.—The writer heartily agrees that previous literature on the broad-crested weir coefficients was incomplete. The analytical relationships worked out by the author between Froude number, degree of submergence and weir coefficients (illustrated graphically in Fig. 3 and 4) give a sound basis for selection of proper coefficients in particular cases.

The writer has been concerned with selection of weir coefficients for estimating discharge obtainable if reservoir dykes (rock fill or earth fill with adequate top and slope protection) are designed as broad-crested weirs to pass flood flows. From Fig. 4 it appears that for weirs with side slopes 1 on 1 or flatter, a coefficient 'C' = 3.0 may be used for submergence up to 70% and where there is no likelihood of tail water rising above weir crest, this value may be raised to 3.2. Perhaps it would be necessary to reduce these values somewhat for design work to allow for variation of roughness coefficients of the weir materials, velocity of approach etc. etc. Laboratory work done by L. W. Long and N. W. Conner(1) indicates that at high flow rates the discharge coefficient of broad-crested weirs is lower for paraffin surface than for glass. The writer would be interested to know to what extent Prof. Smith's values were modified for application in the design office to determine discharge over road-beds.

Figures 2 and 4 indicate that the effect of increasing side slopes of weirs from 1 on 1 to 1 on 2 on the discharge capacity is very small (e.g. if weir crest length 1000 feet and total head 10 feet, discharge capacity = 134,500 c.f.s. for 1 on 2 slopes and 127,000 c.f.s. for 1 on 1; % difference of discharge = 5% only). This leads to the useful derivation that flatter side slopes do not increase discharge rating significantly and considerable savings may be made by building weirs to say 1-1/2 on 1 slope instead of 1 on 2, or flatter, provided other conditions such as structural stability, hydraulic gradient, etc. etc. are satisfied.

## REFERENCE

1. "Tests on Broad-Created Weirs with two different surface adhesion Conditions"; L. W. Long, N. W. Conner. North Carolina State College Engg. Research School - Bulletin No. 61, March 1956, 26 p.

1. Engr., The Shawinigan Eng. Co. Ltd., Montreal, Canada.

# TABULAR SOLUTION OF OPEN CHANNEL FLOW EQUATIONS[a]

Discussions by R. Silvester, Ivan M. Nelidov, Walter J. Tudor, and Warren W. DeLapp

R. SILVESTER[1].—The author has provided a very useful table giving values of specific energy readily and accurately. The author's equation 3 has appeared previously.(1) The analysis of the dimensionless form has been restricted to the rectangular channel. It can be modified to include other shapes as follows:

$$\frac{E_s}{d_c} = \frac{d}{d_c} + \frac{Q^2}{2ga^2 d_c} \quad \text{now} \quad \frac{Q^2}{g} = \frac{a_c^3}{(b_\omega)_c} = \frac{d_c^3 (b'_\omega)_c^3}{(b_\omega)_c}$$

where $b_w$ is the water surface width and $b'_w$ is the width of a rectangular channel equivalent in area to the original channel; the suffix c denotes values at the critical depth.

$$\text{thus} \quad \frac{E_s}{d_c} = \frac{d}{d_c} + \frac{1}{2}\left[\frac{d_c^3 (b'_\omega)_c^3}{a^2 d_c (b_\omega)_c}\right]$$

$$\text{or} \quad \frac{E_s}{d_c} = \frac{d}{d_c} + \frac{1}{2}\left(\frac{d_c}{d}\right)^2 \left[\frac{(b'_\omega)_c^3}{b'^2_\omega (b_\omega)_c}\right]$$

As seen in the accompanying sketch values of $b_w$ and $b'_w$ can easily be determined for trapezoidal channels for any stage operating. For other shapes a scale drawing could provide values close enough for most practical problems. Where depths are being determined an initial estimate based on the original equation could be the basis of a correction applied for the shape factor.

This procedure may appear a little arduous in order to obtain one or two specific values as illustrated in the problems cited. But the table could be used in the step method solution of backwater profiles. It can be shown that

$$dx = \frac{E_2 - E_1}{S_o - S_f} \quad \text{or} \quad \frac{dx}{d_c} = \frac{E_2/d_c - E_1/d_c}{S_o - S_f}$$

a. Proc. Paper 1961, March, 1959, by H. A. Babcock.

1. Senior Lecturer in Civ. Eng. (Hydraulics), University of Western Australia, Nedlands, Australia.

where dx is the length of channel over which $S_f$ is the friction gradient and $E_1$ and $E_2$ are the specific energies at the upstream and downstream ends respectively; $S_o$ is the bed slope.

By knowing the stage at each end of a section of channel, length dx, the specific energy can be determined from the table supplied by the author. For a rectangular channel this is done directly. For other shapes the correction outlined above can be used.

The correction in fact is only applied to the velocity head term and, as can be seen in the author's Figure 1, this is small for mild slopes once $d/d_c > 1.5$. Below this value down through the critical depth and for steep slopes the correction assumes importance. The velocity head is found by subtracting $d/d_c$ from the value of $E_s/d_c$ as read in the table. An example should assist to illustrate the points raised.

Example

A channel of bottom width 25 ft, side slopes 1 on 1-1/2 and bed slope 0.00079 delivers 900 cusecs into a reservoir whose depth at the junction is 10 ft. It is required to find the distance upstream at which the depth is within 2 percent of normal; Manning's n = 0.025.

Note: Graphs and a nomograph for ease in determining normal and critical depths and other terms in the calculation of $S_f$ are contained in articles by the writer[2,3] to which the reader could refer for checking the computations.

$$Q = \frac{K}{n}\sqrt{S_o}$$

$$900 = \frac{K}{0.025}\sqrt{0.00079}$$

ie. $K = 800$

-thus the normal depth

$$d_o = 6.0 \text{ ft.}$$

$$M_c = \frac{Q}{\sqrt{g}} = \frac{900}{\sqrt{32.2}}$$

$$= 159$$

$$d_c = 3.28 \text{ ft.}$$

- since $d_o > d_c$ and $d > d_o$

curve is M1 (3)(4).

Thus the total length of the backwater profile is $3445 \times 3.28 = 11{,}330$ ft. It may be remarked here that the same problem was solved by the conventional step method in reference 3 where the answer given was 14,360 ft; but if it were reworked using the average values of friction and kinetic energy terms for each channel section, as above, the answer would become 11,300 ft: Actually using the table without the shape factor correction results in a length of 11,100 ft.

## REFERENCES

1. J. R. D. Francis. Fluid Mechanics for Eng. Students. Edward Arnold Ltd., London 1958.

2. R. Silvester. "Flow in Open Channels" J. Inst. Engrs. Aust. Vol. 25, 1953, P. 155.

3. R. Silvester. "New Graphs Aid Open Channel Calculations" Water Power, 1954, P. 339.

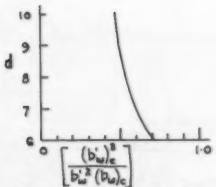


| d | $d/d_c$ | $E_s/d_c^{(a)}$ | $\frac{1}{2}(d_c/d)^2$ | [ ] | correction | $E_s/d_c^{(b)}$ | $(E_s-E_1)/d_c$ | K | $S_f \times 10^3$ | $(S_o-S_f)\times 10^3$ | $dx/d_c$ |
|---|---|---|---|---|---|---|---|---|---|---|---|
| 6.1 | 1.86 | 2.004 | 0.144 | 0·70 | 0.100 | 1 960 | | 820 | 0.75 | 0.04 | |
| | | | | | | | 0.040 | | | | 800[c] |
| 6.25 | 1.91 | 2.038 | 0.128 | 0.69 | 0.090 | 2.000 | | 860 | 0.73 | 0.06 | |
| | | | | | | | 0.065 | | | | 520 |
| 6.5 | 1.98 | 2.108 | 0.128 | 0.66 | 0.085 | 2.065 | | 925 | 0.60 | 0.19 | |
| | | | | | | | 0.072 | | | | 300 |
| 6.75 | 2.06 | 2.178 | 0.118 | 0.65 | 0.077 | 2.137 | | 1000 | 0.50 | 0.29 | |
| | | | | | | | 0.066 | | | | 203 |
| 7.0 | 2.135 | 2.245 | 0.110 | 0.62 | 0.068 | 2.203 | | 1080 | 0.43 | 0.36 | |
| | | | | | | | 0.138 | | | | 345 |
| 7.5 | 2.285 | 2.380 | 0.095 | 0.59 | 0.056 | 2.341 | | 1200 | 0.36 | 0.43 | |
| | | | | | | | 0.146 | | | | 304 |
| 8.0 | 2.44 | 2.524 | 0.084 | 0.56 | 0.047 | 2.487 | | 1360 | 0.26 | 0.53 | |
| | | | | | | | 0.142 | | | | 206 |
| 8.5 | 2.59 | 2.665 | 0.075 | 0.52 | 0.039 | 2.629 | | 1510 | 0.23 | 0.56 | |
| | | | | | | | 0.144 | | | | 244 |
| 9.0 | 2.74 | 2.807 | 0.067 | 0.50 | 0.033 | 2.773 | | 1700 | 0.17 | 0.62 | |
| | | | | | | | 0.156 | | | | 246 |
| 9·5 | 2.90 | 2.960 | 0.060 | 0.49 | 0.029 | 2.929 | | 1860 | 0.14 | 0.65 | |
| | | | | | | | 0.147 | | | | 223 |
| 10.0 | 3.05 | 3.104 | 0.054 | 0.48 | 0.026 | 3.076 | | 2050 | 0.12 | 0.67 | |
| | | | | | | | | | | Total : | 3445 |

(a) value as taken from table.

(b) value corrected for shape factor.

(c) equal to $0.040/0.05 \times 10^{-3}$.

IVAN M. NELIDOV,[1] F. ASCE.—The writer was attracted by the method presented by the author for facilitating solution of open channel problems.

In accordance with the preference of the writer for graphical solution of hydraulic problems he wishes to present a graphical interpretation of this problem for trapezoidal channels.

Since for critical flow the velocity head is $h_{vc} = \frac{A_c}{2T_c} = \frac{V^2}{2g}$ and $V_c = \sqrt{\frac{A_c}{T_c}}\, g$, then $Q_c = A_c V_c = \frac{A_c^{3/2}}{T_c^{1/2}} g^{1/2}$ and $Q_c/g^{1/2} = \frac{A_c^{3/2}}{T_c^{1/2}} = F_1$.

For trapezoidal channel:

$$F_1 = \frac{(B + md_c)^{3/2}}{(B + 2md_c)^{1/2}} d_c^{3/2} = m \frac{(B/m + d_c)^{3/2}}{(B/m + 2d_c)^{1/2}} d_c^{3/2}$$

The curves representing $F_1$ in terms of $d_c$ and $B/m$ are plotted on Fig. 2.

For the specific energy related to critical depth the following expression can be obtained:

$$\frac{E_s}{d_c} = \frac{d}{d_c} + \frac{V^2}{2gd_c} = \frac{d}{d_c} + \frac{1}{2gd_c} \frac{Q_c^2}{A^2} = \frac{d}{d_c} + 1/2\left(\frac{d_c}{d}\right)^2 \left(\frac{A_c}{d_c}\right)^3 \left(\frac{d}{A}\right)^2 \frac{}{T_c}$$

1. Civ. & Structural Engr.

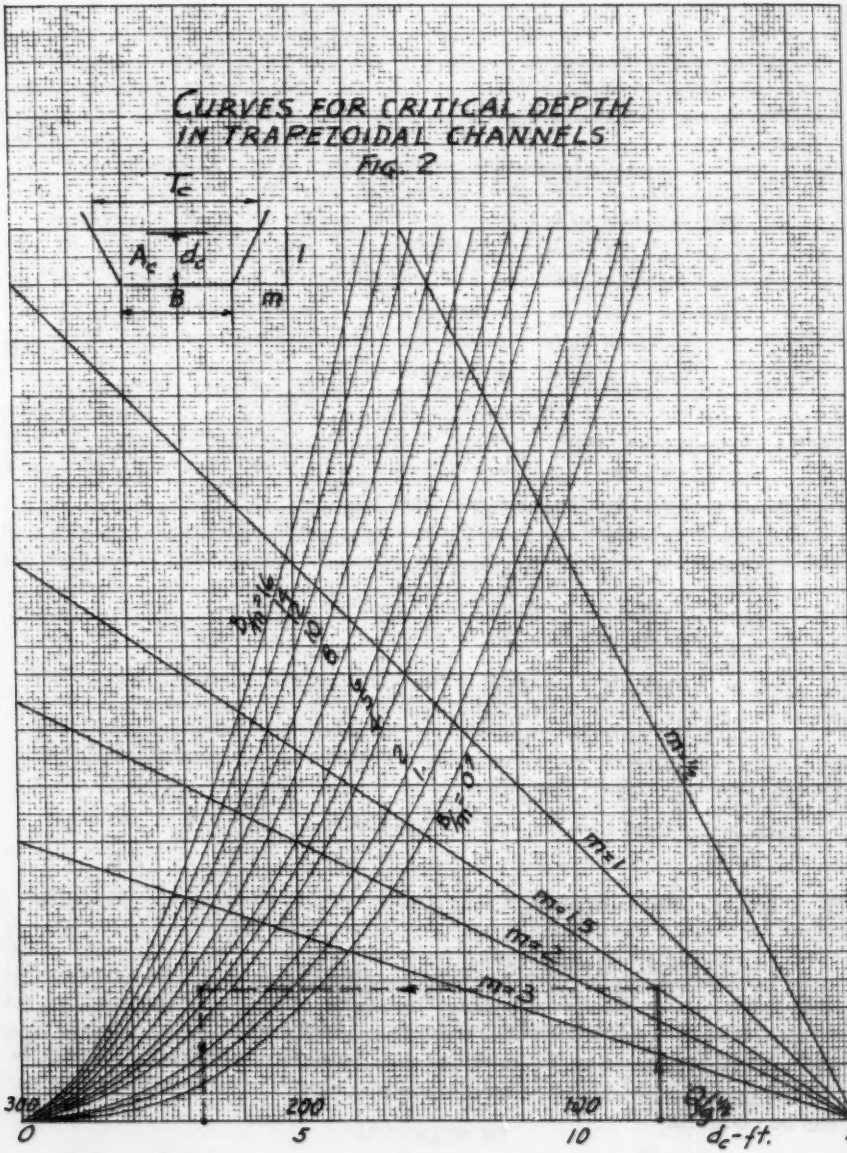
CURVES FOR CRITICAL DEPTH
IN TRAPEZOIDAL CHANNELS
FIG. 2
$T_c$
$A_c$
$d_c$
B
1
m
m=0
m=.5
m=1
m=1.5
m=2
m=3
300
200
100
0
0
5
10
15
$d_c$-ft.

$$= \frac{d}{d_c} \div 1/2 \left(\frac{d_c}{d}\right)^2 \frac{(B \div md_c)^3}{(B \div 2md_c)(B \div md)^2} = F_2, \text{ where:}$$

$$F_2 = \frac{d}{d_c} \div 1/2 \left(\frac{d_c}{d}\right)^2 \frac{(B/md_c \div 1)^3}{(B/md_c \div 2)} \quad \overline{(B/md_c \div d/d_c)^2}$$

The curves representing $F_2 = E_s/d_c$ are plotted on Fig. 3 in terms of $d/d_c$ and $B/md$. The application of these curves will be illustrated on the examples of the author.

Example 1. Data as per author, except that the side slopes are 1.5 to 1, or $m = 1.5$. Then, $Q_c/g^{1/2} = 400./5.67 = 70.7$ and $B/m = 9./1.5 = 6$. From curves on Fig. 2 we obtain $d_c = 3.25$ ft. and $E_s/d_c = 7./3.25 = 2.15$. With this value, we obtain $d_r/d_c = .57$ and $d_t/d_c = 2.11$ from curves on Fig. 3. This gives us $d_r = .57 \times 3.25 = 1.85$ ft. and $d_t = 2.11 \times 3.25 = 6.85$ ft.

Example 2. Data as per author, except side slope factor $m = 2$. Then $Q/g^{1/2} = 300./5.67 = 53.$ and $B/m = 10./2 = 5$. From curves on Fig. 2 we obtain $d_{c1} = 2.50$ ft. and $d_1/d_{c1} = 6./2.5 = 2.4$. With $B/md_{c1} = 10./2 \times 2.5 = 2.$ we obtain from curves on Fig. 3 $E_{s1}/d_{c1} = 2.43$ and $E_{s1} = 2.43 \times 2.5 = 6.07$ ft.

For the narrow section, with the same side slopes, we obtain: with $Q/g^{1/2} = 53.$ from Fig. 2 and $B/m = 9/2 = 4.5$, $d_{c2} = 2.65$ ft.; neglecting losses, $E_{s2}/d_{c2} = 6.07/2.65 = 2.29$. Then, from Fig. 3 and with $B/md_{c2} = 9./2 \times 2.65 = 1.7$, we obtain $d_2/d_{c2} = 2.32$ and $d_2 = 2.32 \times 2.65 = 6.15$ ft.

Example 3. With data by the author and side slope factor $m = .5$, also with $Q_c/g^{1/2} = 250./5.67 = 44.1$ and $B/m = 8./.5 = 16$, we obtain $d_c = 2.95$ ft. Then $d_1/d_c = 5./2.95 = 1.7$. From Fig. 3 with $B/md_c = 8./5 \times 2.95 = 5.43$ we find $E_1/d_c = 1.83$. $E_{s2}/d_c = 1.83 - .5/2.95 = 1.83 - .17 = 1.66$; with this we obtain $d_2/d_c = 1.48$ and $d_2 = 1.48 \times 2.95 = 4.39$ ft.

For circular conduits if we consider the central angle $\alpha$ subtending the water width T, the same will have an expression $T = D\text{Sin}\, 1/2\,\alpha$, where D is the diameter of the conduit; the depth of water will be $d = D/2(1\text{-Cos}\, 1/2\,\alpha)$ and the area of cross section $A = D^2/8\,(\alpha - \text{Sin}\,\alpha)$. The U. S. Bureau of Reclamation tables contain coefficients necessary for plotting curves similar to those for trapezoidal channels. (Table 12a, p. 48a, Ed. 1923). The relationship between the critical depth ratio to diameter $d_c/D$ is given by coefficients $Q_c/D^5/2$, which we will call $f_1(d_c/D)$, so that $Q_c = f_1(d_c/D)D^5/2$; the relationship between $d/D$ and the area is given by the coefficients $A/D^2$ (p. 48), which we will call $f_2(d/D)$, so that $A = f_2(d/D)D^2$. Then $F_2 = E_s/d_c$ $= d/d_c \div 1/2 \dfrac{Q^2c}{gd_c\ A^2} = \dfrac{d/D}{d_c/D} \div 1/2 \dfrac{f_1{}^2(d_c/D)}{f_2{}^2(d/D)}$, which can be plotted for various ratios of $d/D$ and $d_c/D$.

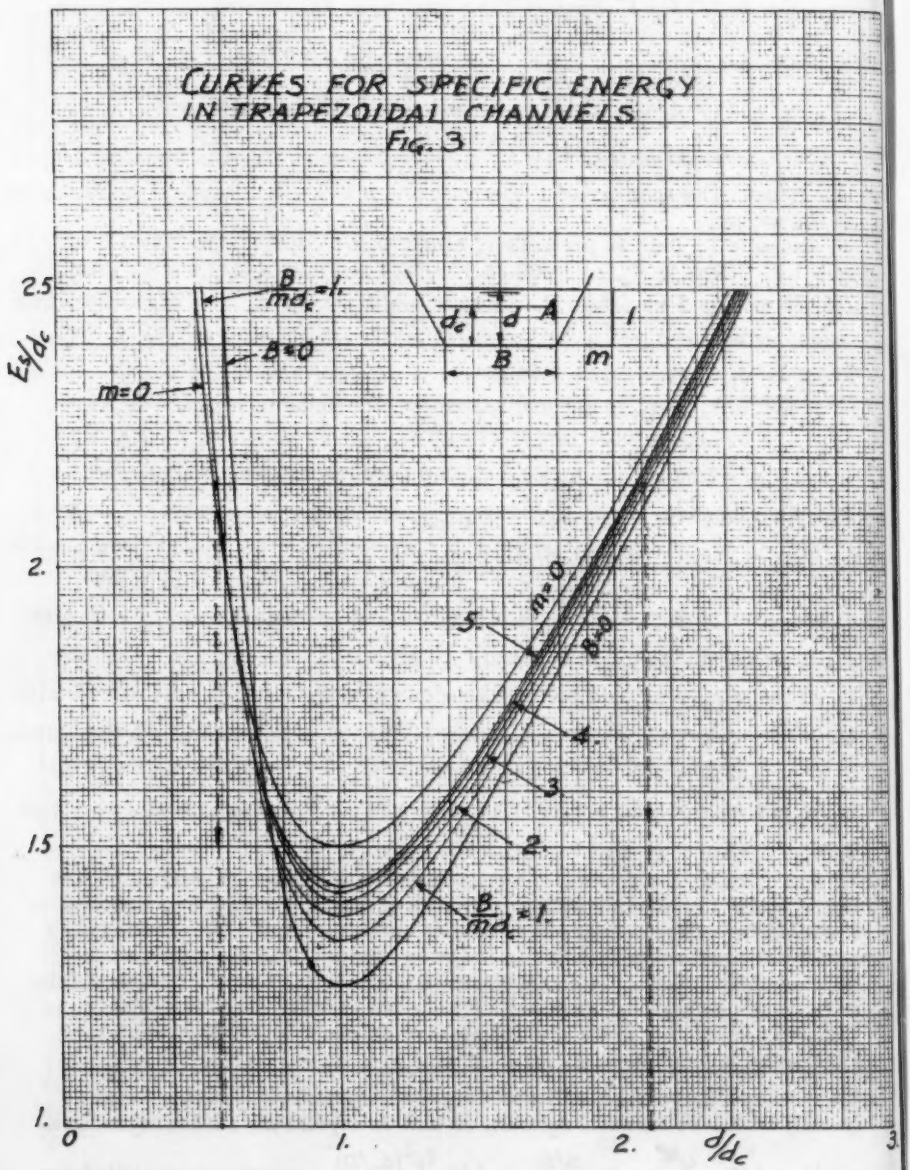
CURVES FOR SPECIFIC ENERGY
IN TRAPEZOIDAL CHANNELS
FIG. 3
E/dc
d/dc
B/mdc=1.
B=0
m=0
dc
d
A
B
m
1
2.5
2.
1.5
1.
0
1.
2.
3
5.
4.
3.
2.

WALTER J. TUDOR,[1] A.M. ASCE.—The cubic equation which arises in hydraulic problems can be obtained from the author's equation (3)

$$\frac{E_s}{d_c} = \frac{d}{d_c} + \frac{1}{2}\left(\left(\frac{d_c}{d}\right)\right)^2$$

by multiplying by $d_c d^2$ and substituting

$$\frac{d_c^3}{2} = \frac{q^2}{2g},$$

to yield $$d^3 - E_s d^2 + \frac{q^2}{2g} = 0.$$

This cubic always has two positive roots or depths (that is, tranquil and shooting) when $E_s$ and the constant term are positive. A nomographic solution for the extraction of these two positive roots is shown on Figure 4.

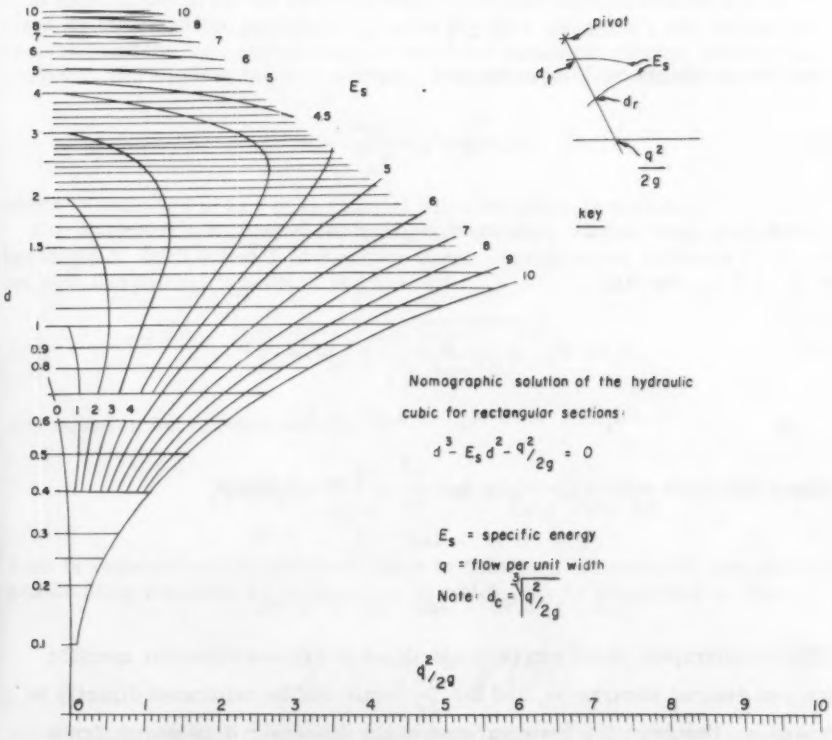


Fig. 4

1. Engr. Civ. Dept., Harza Eng. Co., Chicago, Ill.

As an example illustration of the diagram consider the author's first example. The cubic equation to be solved is

$$d^3 - 7d^2 + 30.6 = 0.$$

Since the scale of $\frac{q^2}{2g}$ extends only to 10, set $d = 2d_1$ to obtain

$$8 d_1^3 - 28 d_1^2 + 30.6 = 0$$

or

$$d_1^3 - 3.5 d_1^2 + 3.83 = 0$$

A straight edge through $\frac{q^2}{2g} = 3.83$ and the pivot point intersects the curves $E_s = 3.5$ at $d_1 = 1.33$ and $d_1 = 3.1$.

$$\therefore d_r = 2.66 \text{ and } d_t = 6.2.$$

The author's second example is solved as follows:

$$E_s = 6 + \left(\frac{30}{6}\right)^2 / 2g = 6.388,$$

so that the pertinent cubic equation is

$$d^3 - 6.388 d^2 + \frac{30^2}{2g} = 0$$

or

$$d^3 - 6.39 d^2 + 17.2 = 0.$$

Let $d = 1.5 d_1$, so that

$$3.38 d_1^3 - 14.3 d_1^2 + 17.2 = 0$$

or

$$d_1^3 - 4.23 d_1^2 + 5.09 = 0.$$

Enter the chart with $E_s = -4.23$ and $\frac{q^2}{2g} = 5.09$ to obtain

$$d_1 = 1.30 \quad \text{and} \quad d_2 = 3.92.$$

$$\therefore d_r = 1.95 \quad \text{and} \quad d_t = 5.88.$$

This nomographic chart can be constructed to various sizes for specific cases and desired accuracies, and the $\frac{q^2}{2g}$ scale can be calibrated directly in terms of q. However, the main purpose of the discusser is to demonstrate the nomographic solution of the hydraulic cubic.

WARREN W. DeLAPP,[1] F. ASCE.—The author has demonstrated that the dimensionless specific-energy function, in either graphical or tabular form, can be a useful tool in the solution of certain open channel flow problems. The fact that the method presented permits the inclusion of energy losses, either as a numerical value or in terms of the velocity head, gives it a distinct advantage over previously published procedures. This was pointed out to the writer by the author some time ago when the latter was a graduate student in a course in open channel flow given by the writer, and since that time the method has been included in the course material.

The use of the diagram and table of the paper are restricted to the rectangular cross section, and the method cannot be used for the trapezoidal section because the ratios involved change with the geometry of the channel. There are, however, two other shapes, less commonly used, for which a similar procedure may be used. These are the triangular and parabolic channel cross sections. Since the determination of the depth for a given energy for these sections is even more difficult than for the rectangular channel, considerable work can be saved through the use of the author's methods if either of these shapes are being used.

A general criterion for critical flow is found in most textbooks and is derived by the substitution of Q/A=V in the author's Equation 1 and setting the derivative of the expression equal to zero for minimum energy. Noting that dA/dd=T, the width at the free surface, results in the expression

$$\frac{Q^2}{g} = \frac{A^3}{T} \tag{9}$$

which is satisfied in any open channel when the depth is critical.

Consider now a symmetrical triangular channel, vertex down, with a vertex angle $\beta$. Both A and T in Equation 9 may be expressed in terms of d and $\tan \beta/2$ and the critical depth is given by

$$d_c = \sqrt[5]{\frac{2Q^2}{g \tan^2 \beta/2}} \tag{10}$$

The equation for specific-energy is

$$E_s = d + \frac{Q^2}{2gA^2} = d + \frac{Q^2}{2g d^4 \tan^2 \beta/2} \tag{11}$$

This is reduced to dimensionless form by following the author's procedure and dividing Equation 11 by Equation 10 which may be simplified to yield

$$\frac{E_s}{d_c} = \frac{d}{d_c} + \frac{1}{4}\left(\frac{d_c}{d}\right)^4 \tag{12}$$

which can be shown by the same procedure to be valid for an unsymmetrical triangular section as well.

The parabolic channel may be defined by the equation $T=kd^{1/2}$ and

1. Prof. of Civ. Eng., Univ. of Colo., Boulder, Colo.

proceeding as above from Equation 9 the critical depth is

$$d_c = \sqrt[4]{\frac{27\,Q^2}{8gk^2}} \tag{13}$$

and the dimensionless specific-energy equation

$$\frac{E_s}{d_c} = \frac{d}{d_c} + \frac{1}{3}\left(\frac{d_c}{d}\right)^3 \tag{14}$$

It is evident that, as for the rectangular section, either Equation 12 or Equation 14 may be used in graphical or tabular form for the solution of problems involving their respective shapes and that the curves which they represent are independent of the values of $\beta$ and k.

It may be of interest to note that the pressure-momentum function, frequently used in connection with the hydraulic jump, may also be expressed in dimensionless form for each of the above channel shapes. For the rectangular channel of width b the pressure-momentum is given by

$$P + M = \frac{\gamma b d^2}{2} + \frac{\gamma Q^2}{gbd} \tag{15}$$

in which $\gamma$ is the specific weight of the fluid. The critical depth is

$$d_c = \sqrt[3]{\frac{Q^2}{b^2 g}} \tag{16}$$

and making the substitution $Q^2 = d_c^3\, b^2\, g$ and dividing by $d_c$ gives the dimensionless form of the equation

$$\frac{P+M}{\gamma b d_c^2} = \frac{1}{2}\left(\frac{d}{d_c}\right)^2 + \frac{d_c}{d} \tag{17}$$

In the same way the expression for the triangular channel is

$$\frac{P+M}{\gamma \tan\beta/2\; d_c^3} = \frac{1}{3}\left(\frac{d}{d_c}\right)^3 + \frac{1}{2}\left(\frac{d_c}{d}\right)^2 \tag{18}$$

and for the parabolic section

$$\frac{P+M}{\gamma k\, d_c^{5/2}} = \frac{4}{15}\left(\frac{d}{d_c}\right)^{5/2} + \frac{4}{9}\left(\frac{d_c}{d}\right)^{3/2} \tag{19}$$

Equation 17 for the rectangular channel is shown graphically in Figure A, curves for the other channel being similar in form. The use of the curve is, of course, quite simple. Knowing either of the depths, say $d_2$, for a hydraulic jump, the ratio $d_2/d_c$ is calculated. The ratio $d_1/d_c$ is then selected from the point on the curve having the same abscissa value as $d_2/d_c$ and the value of $d_1$ then calculated. Although the conjugate depths for a rectangular

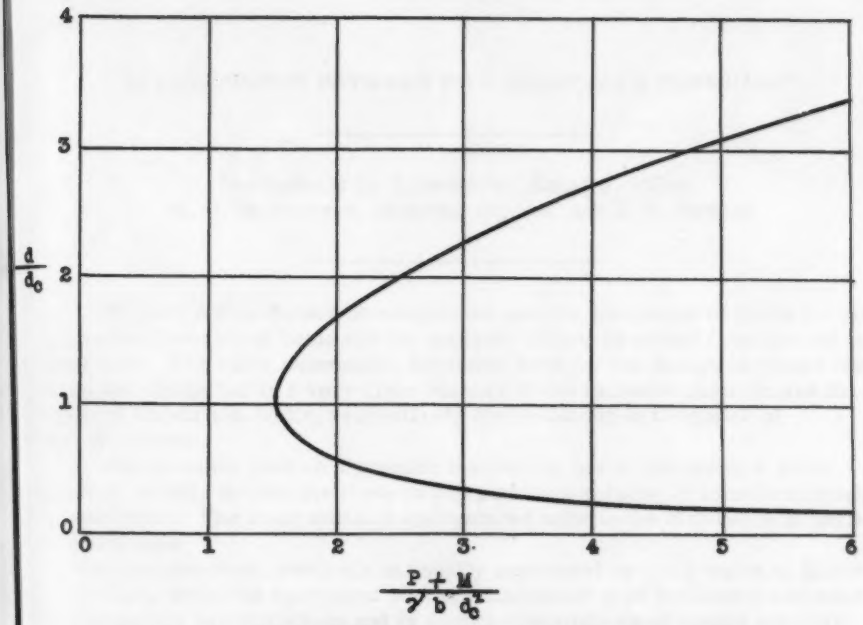


**Figure A. Dimensionless pressure-momentum diagram.**

channel may be found readily by other means, this is not true for the other shapes. The conjugate depths for the latter can, however, be easily determined from a graph such as Figure A drawn to an appropriate scale, or from a table similar to the author's for a higher degree of accuracy.

# RELATIONSHIPS BETWEEN PIPE RESISTANCE FORMULAS[a]

Discussions by K. Szesztay, Henry J. Miles,
M. B. McPherson, Nicholas Bilonok, and J. V. Dawsey

K. SZESZTAY[1].—Recent investigations into the movement of fluids provide a common theoretical basis for the analysis of flow in closed conduits and in open beds. The older exponential formulae used for the design of closed conduits are compared in a very clear manner to the inclusive formula and diagram of Colebrook-White, respectively Rouse-Moody in the paper of Mr. W. Moore.

These formulae rest on a sounder theoretical basis and are of a more general validity so that their use in computations relating to open beds would be desirable. The main obstacle encountered here is the difference in units of roughness.

The roughness of open beds is usually expressed by the $n$ value of Kutter-Ganguillet, while the equivalent particle diameters $k$ of Nikuradse are used in theoretical investigations and in design computations of closed conduits.

Combining the Kármán-Prandtl formula for rough pipes and the Manning formula H. Rouse developed for the relationship between the two roughness parameters the formula:(1)

$$0{,}093\ \frac{R^{1/6}}{n} = 2 \log \frac{R}{k} + 2{,}35 \quad [\text{ft}] \tag{1}$$

In order to study the effects of factors which cannot be taken into account analytically (kinematic viscosity $\nu$ and the gradient $S$) and errors in observation, a statistical investigation has been carried out recently. The evaluation of the 116 data obtained experimentally, respectively by measurement, and extending over the entire turbulent range in both open beds and closed conduits, yielded the following direct relationship of two variables (Fig. 1):(3)

$$\frac{1}{n} = 19{,}8 \log \frac{915}{k} \quad [\text{cm}] \ , \tag{2-a}$$

respectively

$$\frac{1}{n} = 19{,}8 \log \frac{30}{k} \quad [\text{ft}] \ , \tag{2-b}$$

Owing to the scatter due to the simplifying assumptions and uncertainties mentioned above, the statistical investigation failed to reveal the effective of values of $R$.

In his paper Mr. W. Moore points to a very important prerequisite for the more widespread application of the lately developed formulae, which although

a. Proc. Paper 1962, March, 1959, by W. L. Moore.

1. Cand. of Eng. Sc. Researche Institute for Water Resources, Budapest, Hungary.

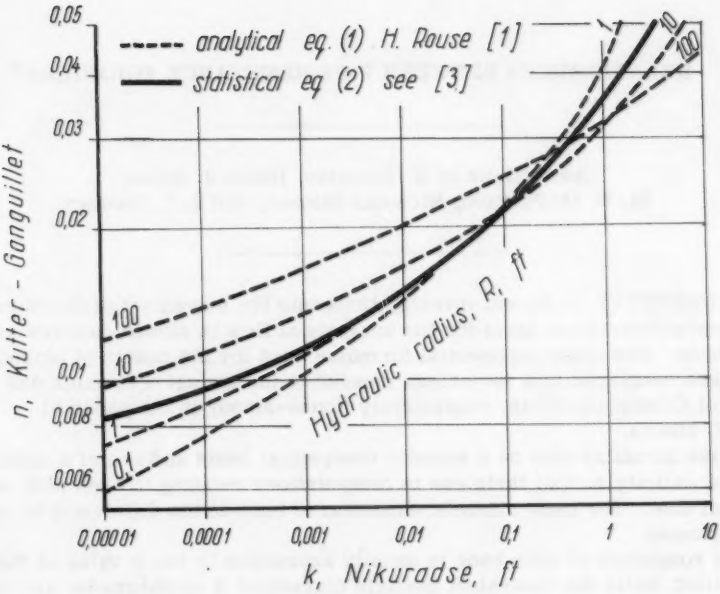


Fig. 1

of a more general validity, are of a more complicated form. This is the problem of readily usable graphs, whereby the need of successive approximations can be eliminated. An easy solution can generally be found to this problem in case of conduits having a circular cross section, all characteristics thereof being the function of a single parameter, the diameter. In the case of the most common type of open canals, the trapezoidal cross section, the situation is considerably more involved.

Graphs were recently issued by the Research Institute for the hydraulic design of canals and pipelines.(4) Attempts have been made therein to give a direct solution for the dimensioning of the optimum trapezoidal canal cross section for any given Q discharge, S terrain slope and n, respectively k, roughness conditions.

The problem will not be unambigous, unless certain shape characteristics of the trapezoidal cross section are either assumed as constant, or considered as a direct function of the water depth (or any other dimension). Similar basic assumptions for the construction are shown in Fig. 2.

Variations in the shape characteristic $\beta = \underline{a/h}$ with the waterdepth h, have been adopted after studies on stable beds (Lacey, Lindley, Girskan and others) and on basis of empirical data. The relationship between the bank slope $\varrho$ and the waterdepth h represents a statistical summary of solutions commonly used for unlined beds. It should be noted, that the method to be presented below can be extended by the construction of an adequate number of graphs to constant, respectively to any arbitrary, $\beta$ and $\varrho$ values.

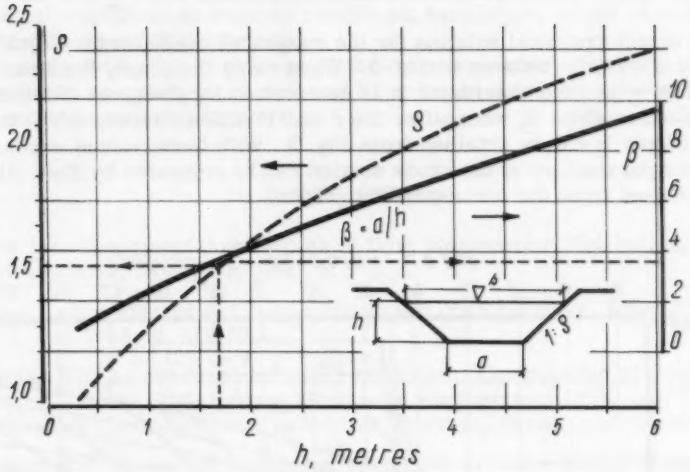


Fig. 2

Having selected the values of $\underline{\beta}$ and $\underline{\varphi}$, respectively the corresponding condition equations, the construction of the graphs constitutes a unambigous hydraulic problem. The first step is to establish the relationships

$$a = \beta h \qquad (3\text{-}a)$$

$$b = \beta h + 2g h \qquad (3\text{-}b)$$

$$P = \beta h + 2h\sqrt{1+g^2} \qquad (3\text{-}c)$$

$$A = h^2(\beta + g) \qquad (3\text{-}d)$$

$$R = \frac{h^2(\beta+g)}{\beta h + 2h\sqrt{1+g^2}} \qquad (3\text{-}e)$$

($\underline{P}$ is the wetted perimeter, $\underline{A}$ the cross sectional area), expressing the variation of the hydraulic parameters of the cross section with waterdepth.

In the relationship expressing the conveying capacity of the beds

$$Q = A\,v = A\,c\,\sqrt{R\,S} \qquad (4)$$

the velocity factor $\underline{c}$ is computed from the expression

$$c = -\sqrt{32\,g}\,\log\left(0{,}0676\,\frac{k}{R} + \frac{0{,}222\,\nu}{R\sqrt{g\,S\,R}}\right) \qquad (5)$$

($g$ = 981 cm/sec$^2$, the constant of gravity) developed as a transformation of the Colebrook-White formula by E. S. Crump.(2)

The inclusion of the second term in Eq. (5), expressing the effect of viscosity and slope, is not necessary in case of conduits and canals carrying water unless $k < 1$ cm, respectively $n < 0{,}017$.(3)

Consequently, with the substitutions according to Eqs. (3-d), (3-e) and (5) the discharge expressed by Eq. (4) is - for any given roughness coefficient

k - actually a unambiguous function of the surface slope S and the waterdepth h.

A direct graphical solution for the roughness coefficient n = 0,025 (respectively k = 7 cm) is shown in Fig. 3. When using the graph, the mean flow velocity v and the waterdepth h is determined for the given discharge Q and surface slope S, whereafter the $\beta$ and $\varphi$ values corresponding to the waterdepth h can be obtained from Fig. 2. With these values available, all further parameters of the cross section can be computed by Eqs. (3), or can be obtained from the corresponding graphs.

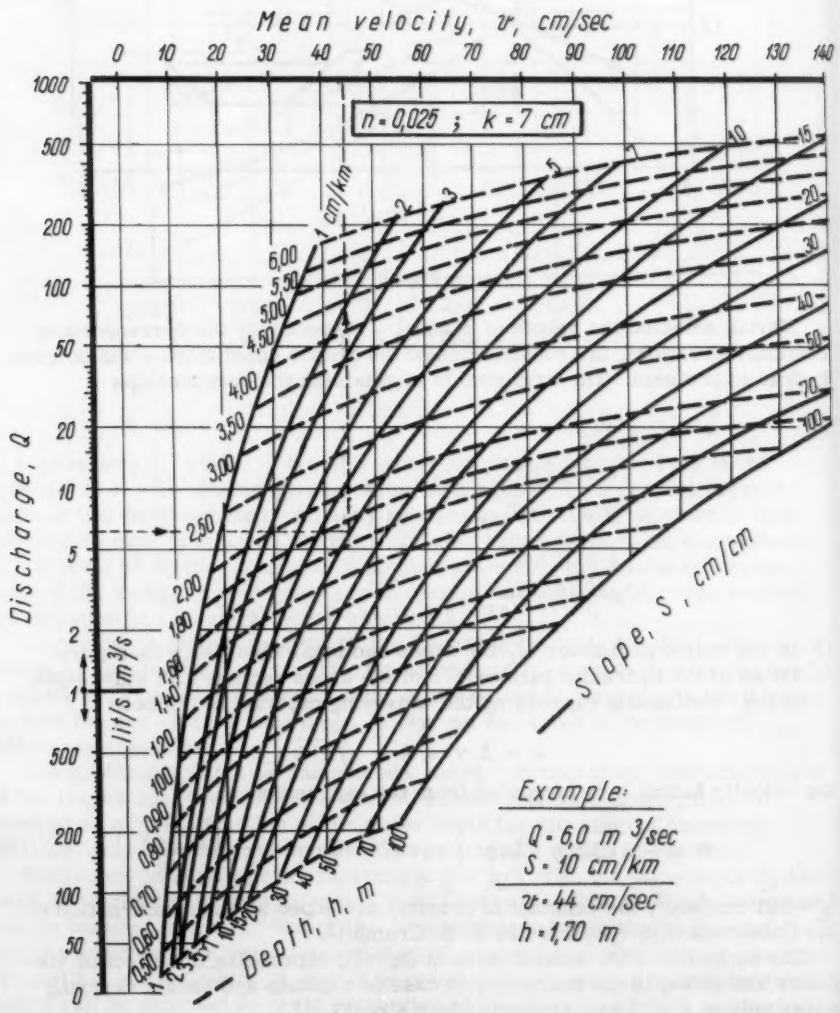


Fig. 3

The values obtained from the graphs may be used as a first approximation even if local conditions as regards roughness, bank slope, or the ratio a/h differ from those adopted originally.

By compiling a series consisting of an adequate number of sheets, the direct solution according to Figs. 2 and 3 can be extended for any combination of n, $\varrho$ and a/h occurring in practice.

## REFERENCES

1. Rouse H.: Fundamental principles of flow, Engineering Hydraulics, John Wiley and Sons, New York, 1950, p. 115.

2. Crump E. S.: Flow of fluids in conduits and open channels, Proc. ICE, part 3, Aut 1956 pp. 522-526.

3. Szesztay K.: Az áramlási sebesség számítása (Computation of flow velocity) Vizügyi Közlemények (Hydraulic Engineering) 1957. No. 1-2. (In Hungarian with summary in English, German, French and Russian).

4. Szesztay K.: Tervezési segédletek csatornák és csővezetékek hidraulikai méretézéséhez (Graphical aids for computation of flow in open channels and conduits) Vizgazdálkodási Tudományos Kutató Intézet, Tanulmányok és Kutátasi Eredmények (Proc. of the Research Institute for Water Resources) Budapest, 1957. No. 2.

HENRY J. MILES,[1] M. ASCE.—Professor Moore's paper is a valuable contribution to a better understanding of the subject of pipe friction. The writer is particularly interested in this paper as he had independently derived a similar relationship between exponential formulas and the general resistance diagram, and for many years in his classes in hydraulics has been using this idea for introducing the overall concept of fluid friction. As the author points out, the large number of exponential formulas is not only confusing to the beginner but also gives the wrong impression of the interrelationship of $h_f$, D, Q, and V unless it is realized that each formula applies only to a limited range of Reynolds number.

The writer has used a slight modification of the author's formula (6), namely

$$h_f = \frac{C_o \nu^{2-m} L V^m}{2g D^{3-m}} \qquad (1)$$

In the range of laminar flow the plot of f vs. $N_R$ is a straight line on the general resistance diagram with a negative slope of 1. Therefore, m = 1 and the formula becomes

$$h_f = \frac{C_o \nu L V}{2g D^2} \qquad (2)$$

For high Reynolds numbers the slopes of the lines approach 0, m approaches 2, and the formula becomes

1. Prof. of Civ. Eng., The University of Arizona, Tucson, Ariz.

$$h_f = \frac{C_o L V^2}{2g D} \qquad (3)$$

the viscosity term having disappeared completely. For intermediate Reynolds numbers, as the author points out, the value of m varies from about 1.7 to 2.

Thus it is possible to visualize the general picture of friction loss as Reynolds number increases: $h_f$ varying initially as V and inversely as $D^2$, and gradually changing to the relationship of varying directly as $V^2$ and inversely as D; viscosity initially playing an important role but gradually decreasing in importance until it finally disappears from the equation. It is also apparent from observing the slopes of the lines on the general resistance diagram that the rougher pipes approach complete turbulence at much lower Reynolds numbers than the smoother ones.

It will be noted in the writer's formula (1) that the sum of the exponents of D and V always totals 3. This tendency can be observed in the various exponential formulas proposed in the past by Hazen-Williams, Scobey, Barnes, Lea, and others. Since the sum of the exponents of D and V in these exponential formulas does not always total exactly 3, the question arises as to whether the discrepancy is caused by slight errors in the empirical formulas, or whether the idea of representing corresponding values of f and $N_R$ on the general resistance diagram by smooth curves is only approximate and introduces small errors.

In conclusion, it is interesting to use the methods proposed by the author to compute the approximate numerical relationship between the e/D ratios of Nikuradse and Hazen-Williams C. The latter formula can be written in the form

$$h_f = \frac{3.02 L V^{1.85}}{C_1^{1.85} D^{1.17}} \qquad (4)$$

If the exponents of V and D are adjusted slightly so that they total 3, the formula can be equated to the writer's formula (1)

$$h_f = \frac{3.02 L V^{1.84}}{C_1^{1.85} D^{1.16}} = \frac{C_o f^{2-m} L V^m}{2g D^{3-m}} \qquad (5)$$

from which it is obvious that m must equal 1.84. If this value of m and the kinetic viscosity of water at 60° F. are inserted in this equation it reduces to

$$C_o = \frac{1267}{C_1^{1.85}} \qquad (6)$$

which, if substituted in the author's formula (5)

$$f = \frac{C_o}{N_R^{2-m}}$$

reduces to

$$C_1^{1.85} = \frac{1267}{f N_R^{0.16}} \qquad (7)$$

If corresponding values of f and $N_R$ are read from the general resistance diagram for each e/D line at the point where its negative slope is 2-m or 0.16, and substituted in this last equation, Table IV is obtained. If these values are plotted on semi-logarithmic coordinates, the resulting curve approaches asymptotically $C_1 = 160$.

Corresponding Values of Nikuradse's e/D and Hazen-Williams' $C_1$ for Water at 60°F.

| e/D | $C_1$ |
|---|---|
| .05 | 93 |
| .04 | 97 |
| .03 | 102 |
| .02 | 108 |
| .015 | 113 |
| .01 | 118 |
| .008 | 121 |
| .006 | 124 |
| .004 | 128 |
| .002 | 135 |
| .001 | 140 |
| .0008 | 142 |
| .0006 | 144 |
| .0004 | 146 |
| .0002 | 150 |
| .0001 | 153 |
| .00005 | 155 |
| .00001 | 158 |
| .000001 | 159 |

M. B. McPHERSON,[1] M. ASCE.—Since the emphasis in the author's presentation is directed towards a precise interpolation of the 'general resistance diagram,' it is necessary to review limitations and assumptions which must be considered in using the diagram.

## General Resistance Diagram

Colebrook,(5) noting that the general trend for new commercial pipe data was a continuous transition between the characteristics of hydraulically

1. Research Engineer, Philadelphia Water Dept., Philadelphia, Pa.

"smooth" and artificially "rough" pipes, arrived at an asymptotic "transition law" of good approximation based upon integration limits for these extremes given by Nikuradse. The Colebrook "transition law" is graphed in Fig. D-1, a photo-copy of Fig. 1, p. 136 of reference (5).

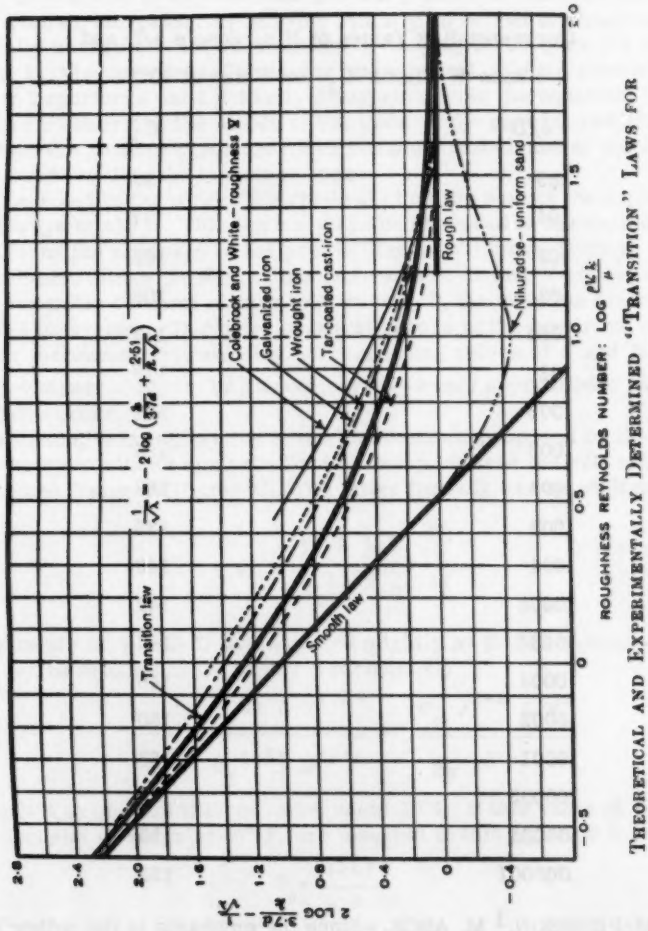


THEORETICAL AND EXPERIMENTALLY DETERMINED "TRANSITION" LAWS FOR VARIOUS ROUGH SURFACES.

Figure D-1

Reproduction of Figure 1, p. 136, Reference (5).
(Note that $\lambda = f$, $k = e$, $d = D$, $V_* = V\sqrt{f/8}$ and $R = N_R$).
(The expression for the "transition law" is equivalent to Equation 167 by Rouse(3)).

"Roughness V" represents a non-uniform artificial sand grain roughness in which 5% (much larger size than the remainder) was cemented in a diamond pattern in a test pipe by Colebrook. The original raw data for the three classes of new commercial pipe were selected from a variety of published American and private British references. Colebrook determined the equivalent sand grain roughness, e, for each individual commercial test pipe directly and indirectly by means of the Karman-Prandtl "smooth" and "rough" pipe relations. From these calculations for each pipe, he then determined the "mean" e for each class. The extremes and mean for each class are summarized in Table D-1. Using the calculated mean e for each class together with the raw test flow data, Colebrook then determined empirically the "mean transition curves" of Fig. D-1 for each of the three classes of commercial roughness. Rouse[3] has compared a variety of test data (mostly small diameters) with the Colebrook "transition law" in his Fig. 110. It is to be noted that Colebrook interpreted his results in terms of a system of transition curves, whereas only his semi-empirical "transition law" has been incorporated in the general resistance diagrams presented by Rouse[6] and Moody[7] as being "a close approximation to the actual resistance law."[6] Inasmuch as the majority of the tests supporting the validity of the transition region curves of the general resistance diagram were for new pipes of small diameter, there remains some question as to the probable accuracy in the use of this diagram for large pipes.

(Disc. 1962)

TABLE D-1

Review of Colebrook Summaries -- Ref. (5), pp. 152-153

New Pipe--Flow of Water

"Asphalted (tar coated) Cast Iron Pipes"

| Diameter, inches | Approximate e, inches |
|---|---|
| 4 | .0090 |
| 6 | .0042 |
| 8 (3 tests) | .0024, .0060, .0067 |
| 12 (3 tests) | .0027, .0030, .010 |
| 16 (2 tests) | .0025, .0084 |
| 24 | .0055 |
| 40 | .0074 |
| 44 | .0062 |
| 48 | .0047 |
| 61 | .0016 |

For the Three Types Considered by Colebrook:

| Type | "Mean" e | Approx. Max. e | Approx. Min. e |
|---|---|---|---|
| Galv. Iron* | 0.006-in.(.0005-ft.) | 0.011-in. | 0.001-in. |
| Asph. C. I. | 0.005-in.(.0004-ft.) | 0.010-in. | 0.0016-in. |
| Wrought Iron | 0.0017-in.(.00014-ft.) | 0.0038-in. | 0.0004-in.** |

(* 0.35 to 4-in. pipes; ** asphalted)

Note: "Approximate" means that the figures cited were read by the writer from a graph of plotted points.

The mean G. I. transition curve of Fig. D-1 would lead to values of f up to 5% higher than the "transition law." If the range of calculated e values for G. I. pipe given by Colebrook (Table D-1) are applied to the general resistance diagram, Figure 1, the variation in f about that for the mean e is of the order of plus and minus 15% for a 4-inch pipe at a Reynolds number of $10^5$. This is a reminder that the first four equivalent uniform sand grain roughnesses for new commercial pipe tabulated in Fig. 1 are mean values. (Ranges of values, such as those given by Streeter,[18] would seem to be less misleading). Most references suggest that the accuracy of estimating f in the "rough" region (for which there is a paucity of supporting data) is probably within about plus or minus 10%: for "smooth" pipes the probable variation is about plus or minus 5%. Recall also that the supporting data for the transition region analysis was selected from laboratory and field data considered representative of new, clean straight pipe without fittings (Colebrook made arbitrary head loss deductions for bends and fittings from some of the field measurements).

The universality of the "smooth" pipe characteristic for steady near-incompressible conditions has been demonstrated using oil, air and water (reference (3), p. 203). Nikuradse's experiments as well as all the commercial pipe tests used by Colebrook and subsequent adaptations were confined to water flow. The trends of the functions for new commercial pipe with a random or 'statistical' type of roughness are indeed remarkably similar. However, the preciseness of the general resistance diagram implied by the "exponential equations" of the author does not appear to be justified. The author leaves the impression that the characteristics of new commercial pipe are fully established and completely understood. The extensive studies of artificial random sand grain roughness by Colebrook and White[28] and square-groove machined-roughness patterns by Streeter[19] indicate that much more remains to be evaluated. Rouse[20] warned some time ago against leaning too heavily upon a single linear dimension e, in attempting to describe any roughness other than uniform. In reference (6) Rouse recommended the Colebrook relation "as a close approximation to the actual resistance law." From the standpoint of velocity distribution, Robertson[21] states that the effect of commercial pipe roughness "has not yet been explained in terms of our knowledge of the action of artificial roughness." The line of demarcation for m = 2 is arbitrary and by no means exact. These remarks are not intended to disparage the vast and invaluable knowledge acquired to date, but to warn against the false sense of exactness implied by a too-literal interpretation of the trend-curves as in the author's "exponential equations."

## Empiricism in Design Practice

The writer assumes that the instruction in fluid mechanics tendered American undergraduate civil engineers for more than a decade has left at least a residual impression, and is confident that contemporary designers (mostly young men) are conversant with sound mechanics principles and the limitations inherent in commonly used empirical relations. He assumes also that a comparison between the Hazen-Williams formula and the general resistance diagram, similar to the presentation by Vennard,[22] is offered to the majority of civil engineering students. The timely, comprehensive paper

by Hinds[12] in 1946 coincided with the advent of widespread intensive fluid mechanics instruction in this country. There has certainly been a visible upgrading in American design practice since that time and it is hoped that the author's pessimism does not truly reflect prevailing conditions except in the extreme. The relatively contemporaneous heated discussions on formulae to which the author alludes[10,14] are specific to British practice; some of the formulae in these references are peculiar to British usage.

## New Express or Feeder Mains

Responsible designers usually appraise the expected initial, or "new," capacity of this type of main by means of the general resistance diagram. Since designs are normally based upon 'future' requirements, an estimate of both new and aged roughnesses is necessary. Recourse is made to well-documented and carefully selected data such as presented by the U.S.B.R.[23] and/or to local records in estimating pertinent or critical (design-wise) values of e.

The author has made some valuable and timely comments under the heading "Equivalent Pipe Concept." However, the numerical values of Table II, used to support some of his arguments, pass beyond the realm of design practicality. In water works design, an overall arterial, feeder, or express main head loss exceeding about twenty feet per mile (equivalent to nearly one pound per city block) at peak flow can seldom be tolerated. This criteria is equivalent to a flow of less than 3 cfs in the 12-inch pipe and less than 0.5 cfs in the 6-inch pipe of Table II. Even ignoring the unrealistically excessive losses cited, it is implied that the field data from which the pipes would be 'calibrated' would be sufficiently precise to assign three significant figure coefficients and exponents to the "exponential equation." Such precision is rarely attained and should not be expected for typical distribution system field conditions.

Equation (20) represents nothing more than a restatement of the equivalent pipe concept and has been used for a variety of purposes in this or similar form for several decades. The equivalent pipe procedure is occasionally employed in modern network analyses as a computation aid (for instance, to reduce two pipes in one street to a single resistance for simplification, if justified). Subsequently it will be shown that the procedures proposed under the heading "Exponential Equations and Complex Pipe Systems" have little place in the analysis of distribution networks. Further, the writer submits that when a distribution problem is as simple as the "complex" cases vaguely mentioned by the author, there is no logical excuse for using an empirical fit to the general resistance diagram except possibly for a first trial; to be consistent, the diagram itself should be used in determining the final answer. The author states that with a twenty-fold variation in Q (quite hypothetical) the exponential equation will agree with the diagram within 5%. For his first example in the Appendix, this statement might appear to be correct: the head loss for the 0.544 coefficient given would be about 0-2% below that for the diagram. However, there is an arithmetical error in the example and the head loss should be 4.88-feet and the coefficient should be 0.454. A twenty-fold increase in Q for the corrected equation will yield a head loss about 17% below that for the diagram. The C for the corrected example is 145, which is not likely to be associated with a small, 12-inch main.

Regardless, a more pertinent comparison would be for a doubled flow for which the corrected equation would lead to a loss about 2% below that for the diagram while a C of 145 in the Hazen-Williams formula indicates a loss about 4% below the diagram. (Since field test data is often acquired during periods of near-average demand and since peak hour flows in large arterial systems are typically two to three times the annual average, a rate approximately double the test rate should represent a reasonable estimate of the probable maximum).

## Distribution Network Design

Network analyses commonly comprise over 90% of waterworks distribution design problems. At the present time there are two rather widely used mechanical means for the detailed calculation of head losses in complex gas and water distribution networks: by direct analogy using the McIlroy Network Analyzer,[24] and by iteration via the Hardy Cross relaxation procedure using a digital computer.[25]

Calculations on a digital computer are restricted to a constant m-value (1.85 normally used for water service), since a large number of exponential equations are being solved simultaneously. Introduction of a varied relaxation factor (differing values of m) would hopelessly prolong the iteration process. With the McIlroy Analyzer, the m for individual pipes can be arranged to fall anywhere between 1.85 and 2. Thus, in an analogue calculation, it would not be impossible to assign different values of m to individual pipes.

However, the purpose of these calculations is normally for the design of facilities to meet peak demands under future conditions (head losses for peak demands under existing conditions can be estimated more easily and more expeditiously by means of extrapolation of direct field tests). In this connection it would perhaps prove fruitful if some of the principal assumptions normally implicit in network analyses were reviewed:

a. Neither all the arterial pipes in a system nor all segments of the pipes 'calibrated' are accessable for field head loss measurements. Field head loss measurements can seldom be made over a sufficient range of flow, even if induced, to cover peak demands. (Design of large arterial networks is generally governed by peak-hour conditions). Field head loss measurements over a range of significantly different rates of flow are very expensive; measured values normally would have to be extrapolated to greater rates for future peak conditions.

b. After 'skeletonizing' the system to an arterial network, loads (or 'draw-offs') must be somewhat arbitrarily consolidated and arranged as to their location. The proportion of the total demand assigned each load is based upon annual averages. (The most reliable information, meter readings and leak-and-waste-survey data, is usually in terms of an average demand rate).

c. Due to the normal absence of adequate information, it is commonly assumed that each local load fluctuation has been and will be proportional to the total system demand.

d. Future total system demands, future friction coefficients and the relocation, proportion and variations of loads for the future are all necessarily judgment projections.

These and additional but less important approximations would thoroughly discourage a designer were it not that 'control' analyses of existing networks performed under these assumptions usually check out remarkably well with field system-head-loss measurements. One aspect of this fortunate coincidence has been at least partially explained by McIlroy.(26) He made a study of the effect of random errors in assumptions of values of C or f for the individual pipelines in networks and found a "pronounced tendency for rather severe, randomly distributed, individual errors to cancel themselves in the determination of total head losses." He concluded from his study that "there appears to be no strong reason to insist on the use of rigorous expressions in a solution which is not based on precise data." And further, "For network-analysis work, the widely used Hazen-Williams formula is entirely adequate, if the same degree of judgment is applied to the results as is necessary in the use of — (other) —methods."(27)

For the several reasons outlined in the preceding paragraphs of this section, the writer is forced to reject as obviously unrealistic (and clearly not proven) the statement by the author: "Although the methods for analysis of networks will not be considered here, it is pertinent to note that exponential resistance relations will be most convenient for use in this type of analysis."

## The Hazen-Williams Formula

Although the Hazen-Williams formula does not deserve very serious consideration in the design of express or feeder mains, some relation with a constant m-value is not only convenient but practically necessary for network analysis. This equation can be compared to any point on the general resistance diagram in the turbulent flow region. The statement "Thus the Hazen-Williams formula with its exponent of 1.85 corresponds to a combination of relative roughness and Reynolds number lying along the line m = 1.85 on the Moody diagram" is completely incorrect. Fig. D-2, a photo-copy of Fig. 5, p. 258 of the author's reference (14) clearly shows the comparative relation between C and f. The equivalent friction coefficient for the Hazen-Williams formula can be expressed as

$$f_{H.W.} = \frac{1060}{C_{H.W.} N_R^{0.15} D^{0.015}}$$

for water at 60° F. Comparing Fig. 1 and Fig. D-2, it can be seen that the "m = 1.85" curve in Fig. 1 is for a variable C, ranging between about C = 140 and C = 150, since the points of intersection of the "m = 1.85" line in Fig. 1 do not collectively describe a single-valued exponent. Obviously, neither can the Hazen-Williams formula be described by a single line on the diagram.

## Lamont's and Other Data

The author's Fig. 2 is a redraft of Lamont's Fig. 3. The table which should have accompanied the author's Fig. 2 is given here as Table D-2. Lamont did not give the original data. All but twenty of the experiments cited have been used previously in the works of Colebrook or others. The five highest curves in Fig. 2 happen to be for new G. I. pipes with a diameter ranging between

*Fig. 5*

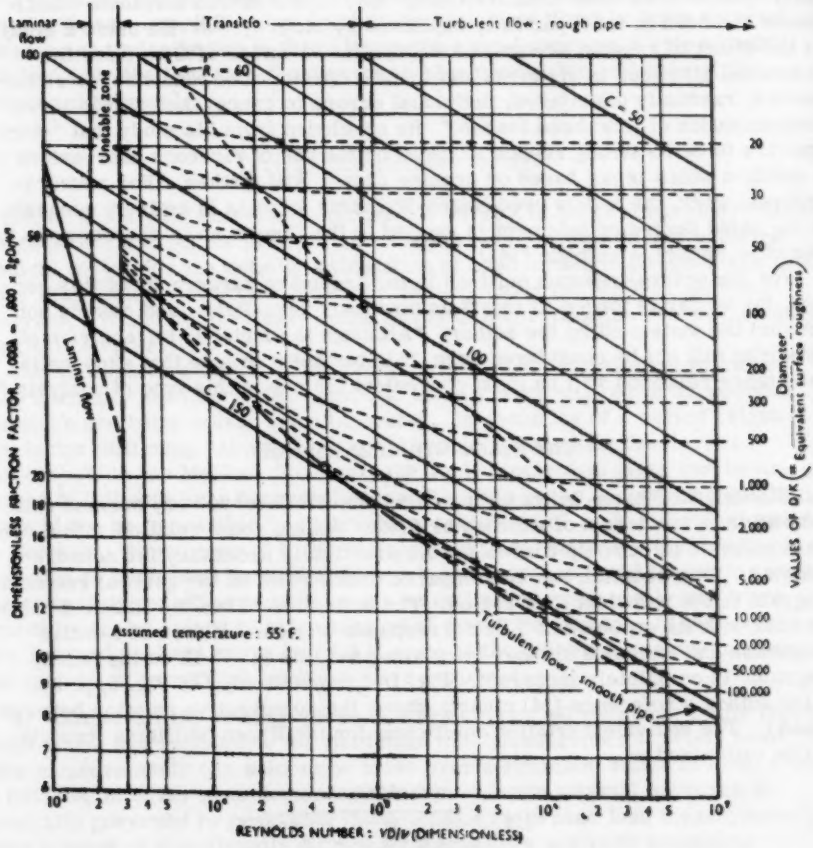


HAZEN-WILLIAMS FORMULA

(The formula has been plotted at $V = 4$ feet per second. There is little difference in the positions of the lines at other velocities.)

Figure D-2

Reproduction of Figure 5, p. 258, Reference (14).

(Note that $\lambda = f$, and $k = e$)

TABLE D-2

Reproduction of "Table 1- Summary of Experimental Records for New Pipes", p. 253 Reference (14) by Lamont (Describes pipes of Lamont's Fig. 3, redrawn by the author a his "Fig. 2- Resistance Records on New Pipes").

| Type of pipe | No. of expts. | Range of experiments | | | Equivalent surface roughness k: inch | | |
|---|---|---|---|---|---|---|---|
| | | Diam: inches | Velocity: ft/sec. | Reynolds Number | Range | Mean | Recommended design value |
| Uncoated cast iron | 3 | 3.24 to 19.68 | 1.175 to 16.168 | $2.43\times10^4$ to $7.06\times10^5$ | 0.0060 to 0.0130 | 0.0089 | 0.010 |
| Coated cast iron | 14 | 3.83 to 61.0 | 0.3947 to 33.80 | $2.88\times10^4$ to $6.48\times10^6$ | 0.0007 to 0.0085 | 0.0040 | 0.005 |
| Galvanized iron | 9 | 0.350 to 4.110 | 0.556 to 20.50 | $3.40\times10^2$ to $5.15\times10^5$ | 0.0016 to 0.0110 | 0.0040 | 0.005 |
| Wrought iron | 18 | 0.3604 to 8.0481 | 0.1844 to 22.50 | $8.02\times10^2$ to $9.11\times10^5$ | 0.0003 to 0.0040 | 0.0020 | 0.002 |
| Coated steel | 4 | 0.47 to 10.12 | 0.249 to 11.05 | $7.57\times10^2$ to $4.09\times10^5$ | 0.0006 to 0.0050 | 0.0018 | 0.002 |
| Uncoated steel | 10 | 0.62 to 12.09 | 0.75 to 46.00 | $3.75\times10^3$ to $1.28\times10^6$ | 0.0003 to 0.0032 | 0.0011 | 0.0015 |
| Asbestos cement | 3 | 2.97 to 5.77 | 0.72 to 5.68 | $1.90\times10^4$ to $1.80\times10^5$ | Smooth pipe | Smooth pipe | Smooth |
| Spun concrete lined | 6 | 3.61 to 60.0 | 0.53 to 15.65 | $2.67\times10^4$ to $1.18\times10^6$ | Smooth to 0.0011 | Smooth pipe | Smooth |
| Spun bitumen lined | 7 | 10.000 to 46.25 | 0.648 to 9.42 | $1.41\times10^5$ to $1.24\times10^6$ | Smooth pipe | Smooth pipe | Smooth |
| Smooth pipe* | 16 | 0.24204 to 3.9995 | 0.145 to 32.30 | $6.30\times10^2$ to $8.74\times10^5$ | Smooth to indefinite | Smooth pipe | Smooth |
| Concrete | 7 | 13.10 to 21.6 | 2.08 to 20.0 | $2.38\times10^5$ to $2.77\times10^7$ | Smooth to 0.0195 | | See Table 2 |
| Tate relined pipes | 3 | 13.1 to 23.43 | 2.825 to 5.160 | $2.38\times10^5$ to $8.30\times10^5$ | 0.0069 to 0.0195 | 0.0130 | 0.015 |

*Smooth pipes include smooth drawn non-ferrous pipes of aluminium, brass, copper, lead, etc. and non-metallic pipes of Alkathene, glass, Saran, etc.

0.35 and 2-inch. These curves, as well as several other irrelevant curves for diameters up to about six inches, should have been omitted in the redraft by the author; effects arising from differences in manufacture on roughness are not considered to be separable for larger sizes, but small sizes, particularly under 3-inches, are known to exhibit dissimilar characteristics. In terms of distribution design, any size smaller than 6-inches would be of little interest. (The curve well below the "smooth" curve is for an 11-inch "spun bitumen-lined" pipe). With the curves for the small sizes omitted, it is possibly reasonably to argue that "for (selected) new pipes as exponent m from 1.80 to 1.90 is common - - - - ." In Colebrook's[5] Fig. 2 (reproduced by Hinds[12] as his Fig. 8) which summarizes selected tests on sixteen new "centrifugally spun concrete" lined C. I. pipes 4-inch to 60-inch in diameter and on six new "centrifugally spun bitumen" lined pipes 11-inch to 46-inch in diameter, the divergence from a "smooth" pipe characteristic is slight. The same result is indicated in Table D-2 for spun linings (but it appears that much of the same data was probably reused by Lamont).

Although the selected data discussed above is reassuring, it is not necessarily representative of typical field conditions. In Table D-3 is presented a summary of results from field measurements on cleaned existing pipe with new cement linings obtained under the direction of Mr. Herbert Thamer, resident engineer in Philadelphia for the Pitometer Associates. Not many of

(Disc. of 1962)

TABLE D-3

Recent Resistance Tests on Cleaned and Cement Lined Philsdelphia Water Department Mains

NEW LININGS

| Internal Diameter, Inches, Di | Average Velocity, fps, for Di | Length Used in Test, Ft. | Head Loss per 1000', Ft. | Reynolds Number @ 60° F x10$^{-5}$ | Friction Factor f | Equiv. Sand Rough., $\epsilon$ Ft. | Hazen-Williams C for Di |
|---|---|---|---|---|---|---|---|
| 47.5 | 3.47 | 11,040 | 0.663 | 11.0 | .0140 | .0006 | 138 |
| 35.3 | 4.02 | 2,780 | 1.251 | 9.9 | .0147 | .0006 | 138 |
| 29.8 | 2.31 | 1,270 | 0.475 | 4.8 | .0142 | .0002 | 147 |
| 29.4 | 3.51 | 10,190 | 1.047 | 7.2 | .0134 | .0002 | 148 |
| 29.8 | 2.87 | 3,690 | 0.885 | 5.9 | .0172 | .0011 | 131 |
| 23.6 | 3.37 | 5,950 | 1.500 | 5.5 | .0168 | .0007 | 134 |
| 23.6 | 3.91 | 3,500 | 2.01 | 6.4 | .0167 | .0007 | 132 |
| 23.6 | 4.60 | 6,240 | 2.43 | 7.6 | .0146 | .0006 | 140 |
| 23.6 | 5.15 | 1,770 | 3.13 | 8.5 | .0150 | .0004 | 137 |
| 19.8 | 2.68 | 8,565 | 1.195 | 3.7 | .0176 | .0007 | 134 |
| 19.5 | 3.45 | 7,500 | 1.777 | 4.7 | .0156 | .0003 | 141 |
| 19.3 | 2.19 | 9,500 | 0.793 | 2.9 | .0171 | .0005 | 140 |
| 19.5 | 2.71 | 6,470 | 1.14 | 3.7 | .0163 | .0004 | 141 |
| 19.5 | 3.45 | 7,460 | 1.945 | 4.7 | .0171 | .0007 | 135 |
| 19.3 | 2.69 | 375 | 1.191 | 3.6 | .0170 | .0006 | 143 |
| 19.4* | 4.19 | 4,365 | 2.92 | 5.7 | .0173 | .0007 | 132 |
| 19.4** | 2.41 | 2,710 | 1.18 | 3.3 | .0211 | .0015 | 124 |
| 11.4 | 3.45 | 2,400 | 4.60 | 2.7 | .0236 | .0017 | 118 |
| 8.0 | 1.91 | 940 | 1.96 | 1.1 | .0230 | .0006 | 130 |

*Including 6 bends and 4 reducers.

**Including 2 bends and 6 reducers.

these tests represent a near-"smooth" characteristic. There is considerable scatter in the values of e despite the possibly consistent 'statistical' roughness of a machine-applied lining. The scatter can be attributed to differences in local losses due to alignment of pipes and bends and fittings, assuming that the tests were of consistent accuracy.

The author's Fig. 3 is a redraft of Lamont's Fig. 4.(14) Colebrook and White(4) in 1937 had observed that "old pipes - - - - obey the square law," and that their graphs included rather flat curves in the transition region (same data as used by Lamont?). In preceding comments it was argued that the anticipated field roughness characteristics for "new" commercial pipe are necessarily inexact, (viz: results to be expected from cleaning and lining). To plot "old" pipe friction factors on a general resistance diagram is to suggest that the increase in roughness with age indigenous to a given water system (i.e. incrustation due to a variety of local causes) is as generally applicable as the somewhat inexact case of new commercial pipe. It is difficult to believe that incrustations are necessarily of the same pattern and form, or yield equivalent friction results from one system to another for chemically different waters. Details on the data plotted in Fig. 3 are lacking in reference (14). The evidence presented by the author does not provide the reader with an adequate basis for concluding with any assurance that "for old pipes an exponent of nearly 2.0 is common." A partial basis for this argument is given by the author by means of the m-values of his Table III, in which the Hazen-Williams C turns out to be only 89 for a 3-year old, and 100 for a 5-year old cement-lined 24-inch pipe. In both instances it would appear that the lining work was substandard, or a number of bends and fittings were included, or that tuberculation in Austin is extremely rapid, or that the measurements were not very accurate, or some combination of these factors. For comparison, data from the Pitometer Company for some "old" cement-lined pipes in Philadelphia are presented in Table D-4. It is hoped that the author will supply similar details for the pipes listed in Table III.

## CONCLUSIONS

Continued use of the Hazen-Williams formula in the analysis of water distribution networks will persist until such time as the accuracy in appraising the several major assumptions affecting design is substantially improved. Consideration of detailed refinements for only one factor, pipe resistance, may create the illusion that by default the other variables are associated with a small margin of error. For estimating head losses for future new pipes or linings in a network, the Hazen-Williams formula is of the same order of reliability as the general resistance diagram when all other factors affecting the design are considered. The convenience in network analysis afforded by a relation with a single exponent (relaxation procedures are made feasible; tables and other computational aids are available) outweighs the probable greater accuracy of the diagram for existing pipes in good condition which have been field calibrated at one or more rates of flow. When "old" pipes comprise part of an existing network, the expediency of a constant m-value for flows in all pipes appears to be justified since arterial mains in poor condition must often be cleaned and lined to meet expanding demands for the future; if rehabilitation is not indicated it follows that the line will not carry an important amount of flow and hence it's contribution to the system head

(Disc. of 1962)

TABLE D-4

Recent Resistance Tests on Cleaned and Cement Lined Philadelphia Water Department Mains.

"OLD" LININGS

| Internal Diameter, Inches, Di | Age, Years | Average Velocity, fps, for Di | Length Used in Test, Ft. | Head Loss per 1000', Ft. | Reynolds Number @ 60° F x10$^{-5}$ | Friction Factor, f | Equiv. Sand Rough., e, Ft. | Hazen-Williams C for Di |
|---|---|---|---|---|---|---|---|---|
| 54. | 12 | 3.71 | 3,900 | 0.813 | 14.0 | .0171 | .0023 | 122 |
| 54. | 10 | 3.78 | 6,075 | 0.755 | 14.0 | .0153 | .0014 | 129 |
| 46.8 | 12 | 4.69 | 9,450 | 1.447 | 15.0 | .0165 | .0016 | 124 |
| 47.5 | 11 | 3.75 | 5,265 | 1.010 | 12.0 | .0183 | .0027 | 119 |
| 47.8 | 11 | 3.62 | 4,750 | 0.952 | 12.0 | .0186 | .0029 | 118 |
| 47.5 | 10 | 3.77 | 6,045 | 0.895 | 13.0 | .0160 | .0014 | 128 |
| 47.8 | 10 | 5.62 | 6,085 | 1.740 | 19.0 | .0142 | .0008 | 132 |
| 23.6 | 12 | 2.49 | 10,700 | 1.275 | 4.1 | .0261 | .0055 | 110 |
| 23.6 | 5 | 2.58 | 3,400 | 0.796 | 4.2 | .0151 | .0003 | 145 |
| 19.4 | 6 | 2.70 | 440 | 1.530 | 3.6 | .0218 | .0023 | 124 |
| 19.3 | 5 | 2.57 | 4,160 | 1.280 | 3.4 | .0200 | .0014 | 126 |
| 19.3 | 5 | 3.41 | 6,030 | 2.310 | 4.6 | .0205 | .0016 | 122 |
| 15.6 | 14 | 2.04 | 12,060 | 0.976 | 2.2 | .0195 | .0009 | 133 |
| 15.3 | 14 | 1.81 | 6,400 | 0.980 | 1.9 | .0245 | .0026 | 119 |
| 15.4 | 7 | 2.20 | 10,625 | 1.200 | 2.4 | .0205 | .0012 | 132 |
| 15.4 | 7 | 2.31 | 5,700 | 1.192 | 2.5 | .0185 | .0006 | 136 |
| 15.4 | 5 | 2.75 | 4,550 | 1.570 | 2.9 | .0171 | .0004 | 140 |
| 11.4 | 13 | 2.03 | 10,350 | 1.265 | 1.6 | .0188 | .0004 | 140 |
| 11.3 | 13 | 2.48 | 5,370 | 2.250 | 1.9 | .0221 | .0012 | 126 |
| 11.6 | 10 | 3.95 | 5,415 | 5.010 | 3.2 | .0200 | .0009 | 128 |
| 11.6 | 8 | 2.07 | 2,225 | 1.770 | 1.7 | .0257 | .0021 | 118 |
| 11.6 | 2 | 4.35 | 3,725 | 5.065 | 3.5 | .0166 | .0003 | 140 |

loss will be relatively minor. At the present time there is insufficient evidence available to warrant adoption of further design complications through use of a mixed set of m-values for analysis when a network includes "old" pipes.

In the design of non-network ('express,' 'pumping,' 'feeder,' etc.) the empirical curve-fitting technique offered by the author is a poor and unnecessary substitute for the general resistance diagram itself. The author disdains the use of empirical formulae, yet proposes a system of infinite approximation formulae which he purports to be "correct" and "proper" because one value for a given pipe is made to coincide with the diagram. The author treats only the case where a precise value of e is known in advance, a rather atypical design situation.

It is quite evident that there is much remaining to be investigated from the standpoint of theory and basic experiment if a higher degree of precision in design calculations is to be achieved. Periodic shuffling of warmed-over data is not a very satisfactory substitute for fundamental investigation. It is sincerely hoped that the ASCE Hydraulics Division "Task Force on Flow in Large Conduits" will stimulate interest in further basic research on pipe friction characteristics.

REFERENCES

1 - 17. (See Proc. Paper 1962 by Moore).

18. "Engineering Hydraulics," Edited by Hunter Rouse, Wiley, p. 405, (1950).

19. "Fluid Mechanics," Victor L. Streeter, McGraw-Hill, pp. 207-208, (1951).

20. "Fluid Mechanics for Hydraulic Engineers," Hunter Rouse, McGraw-Hill, pp. 251 to 255, (1938).

21. "The Turbulent Velocity Distribution in Rough Pipe," James M. Robertson, Fifth Midwestern Conference on Fluid Mechanics, p. 67, (1957).

22. "Elementary Fluid Mechanics," John K. Vennard, Wiley, pp. 206 to 208, (1954).

23. "Friction Factors for Large Conduits Flowing Full," by J. N. Bradley and L. R. Thompson, U.S.B.R. Engineering Monograph No. 7, Denver, (March, 1951).

24. "Direct-Reading Electric Analyzer for Pipeline Networks," by Malcolm S. McIlroy, Jour. A.W.W.A., Vol. 42, No. 4, pp. 347-365, (April, 1950).

25. Discussion of "Paper No. 1608, Digital Computers for Pipeline Network Analysis, by Graves and Branscome," by John W. Hamblen, ASCE Proc. Paper No. 1855, pp. 11 to 16, (November, 1958).

26. Unpublished doctorate thesis, Malcolm S. McIlroy, Mass. Institute of Technology, Cambridge, Mass. (1946).

27. Discussion of "Relative Pipe Roughness, by Chenoweth and Leaver," by Malcolm S. McIlroy, Journ. AWWA, Vol. 43, No. 3, pp. 224-226, (March, 1951).

28. "Experiments with Fluid Friction in Roughened Pipes," C. F. Colebrook and C. M. White, Proc. Royal Society London (A), Vol. 161, pp. 367, 381, (1937).

NICHOLAS BILONOK.[1]—The improved knowledge incorporated in the authors general pipe resistance diagram shows the effect of the various factors entering into the problem, which is of great importance to the civil engineers. Valuable experimental data regarding resistance in existing water mains are recorded in this paper.

The general pipe resistance diagram has not received wide usage among practicing engineers due to its inconvenience as compared with similar exponential formulas for water flow where viscosity has little effect and restricted range of Reynolds number, and the velocity of flow, also the diagram in its common form, trial-and-error solution is required for finding the rate of flow or pipe diameter; and for given boundary material the pipe diameter must be known before the relative roughness may be evaluated.

The diagram is based on the Prandtl-Karman formula for pipe resistance relations which are improved by the experiments of Nikuradse, Colebrook,

1. Civ. Engr., Eng. Civ., Corps of Engrs., U.S. Army, Philadelphia, Pa.

and White in form (authors Table I)

$$\frac{1}{\sqrt{f}} = -2\log\left(\frac{2.51}{N_R\sqrt{f}} + \frac{e}{3.7\,D}\right) \qquad (1)$$

The friction factor f expressed in Equation (1) is a combination of variables, which are evidently applicable to the problem, in very complicated form where f is dependable from itself, or friction factor must be known before the friction factor may be evaluated.

It is evident that aging of the pipe under varying conditions of use will result a varying of absolute roughness which at present are not easily predicted. The experiments show that the surface of the pipe is changing with the age increasing the value of f. The factor e expressed in inches is a complete measure of the size, shape, and distribution of individual roughness element.

The pipes that are rough in practice generally have no uniformity of the roughness element as assumed these by the authors of the equation. As there is at present no method for measuring or defining distribution of roughness element, the value of e is hypothetical.(1) In author's examples illustrate the steps in obtaining an exponential equation with the aid of the modified di-diagram

$$h_f = f\,\frac{1}{D}\,\frac{V^2}{2g} = \frac{0.155\,(1000)\,(4.5)^2}{(1)\,2g} = 4.88 \text{ ft}$$

instead $h_f = 5.84$ ft

$$K_Q = \frac{h_f}{Q^m} = \frac{4.88}{3.53^{1.88}} = 0.456$$

$$h_f = 0.456\,Q^{1.88}$$

Recommended use of Fig. 1 to find exponent in example 2 m = 1.95 is not in agreement with f and e/D. It would be helpful to show symbols how to find numerical variables entering problem in examples.

The pipe resistance relations listed in the Table I as well as many other equations known by the writer, were based on experimental data with the flow of water, therefore, in common language, in development of pipe resistance relations, must be used term water or liquid versus fluid.(2)

"A liquid is a body in that state in which the particles move freely among themselves, but remain in one mass, keeping the same volume but taking always the form of the containing vessel; a liquid is an inelastic fluid; a gas is an elastic fluid that tends to expend to the utmost limits of the containing space. All liquids are fluids, but not all fluids are liquids; air and all the gases are fluids, but they are not liquids under ordinary circumstances, tho capable of being reduced to a liquid form by special means, as by cold and pressure. Water at the ordinary temperature is once a fluid and a liquid."

The values of e, f, and exponents from the modified diagram in the Darcy-Weisbach equation are important for designers to know these values properly

and apply it intelligently. It is probable that, if accuracy alone were the deciding factor, any of the values given from the modified diagram, as well as C, f, n, and exponents in other suggested formulas which are in general use, if properly applied would be equally satisfactory.

## REFERENCES

1. Victor Streeter. "Frictional Resistance in Artificially Roughened Pipes." Trans. ASCE, Vol. 101 pp 682-704, 1936.

2. Funk and Wagnells. "New Standard Dictionary of the English Language," p 948, Ed. 1942.

J. V. DAWSEY,[1] M. ASCE.—Professor Moore has collected information which was heretofore scattered in many parts of the literature. Research to determine methods for predicting or computing resistance encountered by fluids flowing through a pipe is of interest in various fields of engineering and industry.

Numerous experiments to determine the relative roughness of a pipe, $\frac{e}{D}$, have been completed throughout the world in recent years. Some of these tests were made for the purpose of correlating the general resistance equations with friction and roughness data collected in model and prototype tests. The late Andre Jorissen(1) of Belgium experimented with relative roughness measurements on large conduits by forcing air at high velocities through concrete-lined and unlined rock tunnels. Viparelli(2) of Italy recently has experimented with a photographic determination of roughness.

The Waterways Experiment Station is using a method devised by Mr. Frank B. Campbell,(3) F. ASCE, to determine the equivalent sand roughness of conduit linings. Two-in.-square plaster cast impressions are made at selected locations in the conduit that represent the roughness of some percentage of the total conduit lining. Vertical-displacement measurements of the cast surface profile yield an average surface roughness of the conduit lining represented by the cast.

An Ames dial is presently used for surface-profile measurements on the plaster casts after an initial attempt to measure profiles electrically. The point of contact on the shaft of an electrical contour analyzer was modified by using the point from a ball-point pen. This pen point indented the surface of the soft plaster casts under force of the analyzer probe. The Ames dial shaft was also modified by the addition of a similar pen point, but did not indent the cast surface during measurements. For profile measurements, the casts are firmly anchored in a mechanical vise and traversed under the shaft of the Ames dial. If the root-mean-square deviation of the surface-profile measurements is interpreted as the equivalent sand-grain roughness $\epsilon$ (one-half the diameter of the sand grain k in inches), then the friction factor f, at the Reynolds number of the test, can be computed by using the general pipe resistance equations.

Roughness casts of representative areas inside the 20-ft-diameter

1. Hydr. Engr. (Research), Prototype Section, Hydr. Analysis Branch, Hydraulics Div., U. S. Army Engr., Waterways Experiment Station, Vicksburg, Miss.

flood-control conduit No. 6, Denison Dam,(4) were obtained by making two-inch-square impressions of the conduit lining with elastic dental-impression material. Plaster casts were then reproduced from the impression material negative. Equivalent roughness $\epsilon$ for the conduit lining was determined from root-mean-square deviations of the surface profile measurements on the casts. This value of $\epsilon$ was then used in the Colebrook-White equation, which includes the effect of Reynolds number, to compute the Darcy-Weisbach friction factor, f. The value of f computed in this manner was about 35 per cent greater than the value of f computed from pressure measurements with piezometers installed in the conduit during construction. Similar prototype pressure measurements and roughness casts were recently completed at Enid Dam.(5) The value of f determined from the casts was only 15 per cent less than the value computed from the slope of the friction gradient.

Although there was considerable difference between the measured and computed values of roughness, $\epsilon$, the corresponding friction factors differ much less because of the exponential-logarithmic relationship between f and $\epsilon$. With some additional refinment in sampling the conduit surface and analyzing the plaster casts, it should be possible to determine conduit roughness accurately from plaster casts alone, including conduits where different types of forms and construction techniques are used.

Additional plaster-cast roughness data are needed to aid in the analysis and interpretation of the equivalent sand-grain roughness relationship in turbulent flow. Information from anyone making casts in conduits where the hydraulic friction gradient is known or can be measured would be appreciated.

It appears that parentheses were inadvertently omitted in the Colebrook-White equation in Table I of Professor Moore's paper. The equation should read:

$$\frac{1}{\sqrt{f}} = -2 \log \left( \frac{2.51}{N_R \sqrt{f}} + \frac{e}{3.7D} \right)$$

## REFERENCES

1. Jorissen, Andre, Contribution a L'Etude des Pertes de Charge Continues dans les Conduites Circulaire, Bull. Contre Etude Constr. Genie Civil Hydr. Fluviale, pp. 288-291, 1949.

2. Viparelli, M., Relevement Photographique Des Rugosites (Photographic Determination of Roughness), Universita di Napoli, Recherches Hydrauliques, 1957, p. 250, No. 15.

3. Campbell, Frank B., Chief, Hydraulic Analysis Branch, Hydraulics Division, U. S. Army Engineer Waterways Experiment Station, Vicksburg, Mississippi.

4. "Pressure and Air Demand Tests in Flood-Control Conduit, Denison Dam, Red River, Oklahoma and Texas." MP No. 2-31, April 1953, B. Guyton, U. S. Army Engineer Waterways Experiment Station, Vicksburg, Mississippi.

5. "Prototype Hydraulic Tests of Flood-Control Conduit, Enid Dam, Yocona River, Mississippi." TR No. 2-510, June 1959, C. J. Huval, U. S. Army Engineer Waterways Experiment Station, Vicksburg, Mississippi.

# HYDRAULIC ANALYSIS OF SURGE TANKS BY DIGITAL COMPUTER[a]

## Discussion by Charles Jaeger

CHARLES JAEGER[1].—The paper of Mr. Barbarossa deals with two most important problems.

### The use of digital computers

The use of digital computers for advanced research on surges in complex systems of surge tanks is clearly demonstrated by the author. Digital computers have been used in hydraulic research by several authors especially for solving problems of water hammer.

The paper by McCaig and Jonker, is a typical example of what can be achieved with this new tool. The writer too has used a digital computer for solving a simple but tedious problem. It was suggested that a small hydro power station could be provided with a surge tank too narrow to cope with large surges, provided the power sets were hand operated and put slowly on the line, the operator observing very definite rules concerning the turbine gates opening times. There was no turbine governor and the load on the station was supposed to remain constant for long periods.

When a large number of possible load combinations and possible errors by the operator were considered and their effect on surges analysed, the proposal was abandoned.

The approach by digital computer can be compared with more conventional graphic methods: For example the paper by McCaig and Jonker, can be compared with graphical computations carried out by Bouvard and Molbert of Electricité de France. The precision given by a direct calculation on the digital computer goes far beyond of what can be achieved with a graphic diagram. In the case described by McCaig and Yonker such high precision was required for comparison of cost estimates for several design alternatives.

Paynter has been using the electric analog method for research on surges and on water hammer. His methods are highly suitable for very general research.

When problems concerning concentrated pressure and head losses (losses occurring at this junction of a surge tank with the pressure tunnel) have to be analysed or when turbulence is involved, experiments on model tests is often the best approach.

### The Thoma condition for surge stability

The author correctly remarks that the whole surge stability theory established during the past 40 years by Thoma, Calame and Gaden, Escande and

a. Proc. Paper 1996, April, 1959, by Mr. Nicholas Barbarossa.
1. English Electric Co., Ltd., Rugby, England.

others is based on the assumption that the demand for power varies abruptly, then stays absolutely constant for the period under observation and that the governor is able to correctly adjust the power generation to the demand.

The paper shows how trial calculations on the digital computer prove this basic assumption to be over-simplifying. According to Fig. 10, 11, and 12 of the paper, the gates continue to open to "full gate opening" beyond the point where better stability could be expected.*

It should be remarked here that the points on Fig. 10 and 11 on which the discussion is based correspond to the very beginning of the surge: time about 1 second, whereas the surge period is about 200 seconds (Fig. 7.). There is no precise indications given in the paper why a variable surge with constant power generation could not be established during the rest of the period. Depressed water levels will raise again. In addition, the governing equation relating speed variations to the moment of inertia of the rotating masses could possibly be introduced as an additional condition to the computation: it may show how the governor tends to stabilise the power output and additional research is suggested. The main point to be stressed here is the authors belief shared by the writer, that further research on surge stability is definitely wanted. A first phase of research has been concluded: simplified mathematical theories expanding Thoma's stability creterion to all types of surge tanks and systems of surge tanks have been worked out. The Routh-Hurwitz mathematical stability criterion and the Liapunoff theorem have been used successfully by skilled mathematicians. All this approach work is based on the same basic assumption of abrupt change in the load demand, which then remains constant.

How does this basic assumption fit in with the behaviour of real electric systems? This is the question facing us for the second phase of the research. A certain amount of preparatory work has already been done:

Chevalier and Hug (Electricité de France) have tested the Cordéac surge tank: They found that the governor was reacting correctly to the power demand but with a time lag of about 10 seconds. This time lag was found to dampen the surges quite efficiently.

Cuénod and Gardel (Lausanne) have tested the differential surge tank of Oelberg (Switzerland). By modifying the actual surge tank they caused it to become unstable. They tested different types of feed back linking surge levels and line voltage to the frequency in order to re-establish the stability of the surges.

Finally Aillert (Electricité de France) has designed and built several surge tanks, which are definitely unstable but where the surges are controlled otherwise.

These are definite efforts to approach the stability problem from a completely new angle. More light could be thrown on the way governors react and surges can be controlled. Possible savings on the tank volume could be achieved thanks to a closer analysis of the physical conditions in large electric systems.

It is suggested that a comprehensive paper summarising all these new efforts should analyse the up to date position of the problem and show the way to further research.

*Similar effects have been observed on large tanks. Too little is known for any explanation to be suggested.

The author has to be warmly congratulated for his successful use of a new tool in surge computation and for his criticism of the assumptions on which the present surge stability theory is based.

## ADDITIONAL BIBLIOGRAPHY

1. McCaig, I. W. and Jenker, F. Applications of computer and model studies to problems involving hydraulic transients. A.S.M.E. Paper No. 58 - A.101, 1958/59.

2. Jaeger, C. Present trend in surge tank design. Proc. Inst. Mech. Eng., Vol. 168, No. 2, 1954.

3. Jaeger, C. The double surge tank systems. Water Power, Vol. 9, No. 7/8, July/August 1957, and La Houille Blanche No. 4, September 1957.

4. Jaeger, C. Contribution to the stability theory of systems of surge tanks. A.S.M.E. Paper No. 51 - A.65; Trans. A.S.M.E. Vol. 80, No. 7, October 1958.

5. Chevalier, J. and Hug, M. Tests on the Cordeac surge tank, concerning Thoma's condition. La Houille Blanche, Vol. 12, No. 6, December 1957.

6. Cuénod, M. and Gardel, A. Communication du Laboratoire d'Hydraulique, Ecole Polytechnique, Université de Lausanne, 1953, and La Houille Blanche No. 3, June 1954.

7. Bouvard and Molbert. La Houille Blanche, Vol. 8, No. 2, May 1953.

# TWO METHODS TO COMPUTE WATER SURFACE PROFILES[a]

Discussion by R. Silvester

R. SILVESTER[1].—In their use of Manning's formula the authors have bulked area, hydraulic radius and the roughness coefficient "n" into the conveyance factor $K_d$. There seems little to gain from including Manning's coefficient in order to determine some nebulous quantity of conveyance which is of little use in itself. The writer discarded this concept some time ago(1,2) with the result that $K(=1.486\ A\ R^{2/3})$ is determined solely by the geometry of the channel cross-section and the stage. Such values when graphed on a logarithmic scale resulted in straight lines and slight curves depending upon the shape of the channel. Graphs were supplied for trapezoidal, parabolic, rectangular, circular and U shaped channels. Once K has been so determined the discharge is given by $Q = \frac{K}{n}\sqrt{S_f}$ ; for the solution of this a nomograph was included.

## REFERENCES

1. R. Silvester "Flow in Open Channels" J. Inst. Engrs Aust. Vol. 25, 1953, p. 155.
2. R. Silvester "New Graphs Aid Open Channel Calculations" Water Power, 1954, p. 339.

a. Proc. Paper 1997, April, 1959, by J. M. Lara and K. B. Schroeder.
1. R. Silvester, Senior Lecturer in Civ. Eng. (Hydraulics), University of Western Australia, Nedlands, Australia.